SHRP-A-400

# Low-Temperature Cracking: Test Selection

D.H. Jung
T.S. Vinson

Department of Civil Engineering
Oregon State University

**Strategic Highway Research Program**
National Research Council
Washington, DC 1994

SHRP-A-400
Contract A-003A
ISBN: 0-309-05807-4
Product No.: 1021, 1022

Program Manager: *Edward T. Harrigan*
Project Manager: *Rita Leahy*
Program Area Secretary: *Juliet Narsiah*

June 1994

key words:
asphalt concrete
asphalt
cold climates
cracking
low-temperature cracking
pavements
temperatures
thermal cracking

Strategic Highway Research Program
National Research Council
2101 Constitution Avenue N.W.
Washington, DC 20418

(202) 334-3774



1500/NAP/694

# Acknowledgments

The research described herein was supported by the Strategic Highway Research Program (SHRP). SHRP is a unit of the National Research Council that was authorized by section 128 of the Surface Transportation and Uniform Relocation Assistance Act of 1987.

This project, entitled "Performance Related Testing and Measuring of Asphalt-Aggregate Interactions and Mixtures," was conducted at the Institute of Transportation Studies, University of California at Berkeley, with Carl L. Monismith as Principal Investigator.

The work reported herein was conducted as a part of project A-003A of the Strategic Highway Research Program (SHRP). The support and encouragement of R. Gary Hicks, co-principal investigator of the C.3 Low-Temperature Cracking subtask, is gratefully acknowledged. In addition, the authors express their appreciation to Professor Wolfgang Arand, Braunschweig University, Germany, and Dr. Vincent Janoo, United States Army Corps of Engineers Cold Regions Research and Engineering Laboratory (CRREL), for their encouragement and willingness to share their ideas regarding the thermal stress restrained specimen test. Finally, special appreciation is extended to Marco Fellin, of Oregon State University, who prepared the test samples, Andrew Brickman, of Oregon State University, who assisted in the fabrication of the test equipment, Greg Paulsen of Austin Research Engineers who documented a test protocol and prepared a videotape of the test procedure, and Teresa Culver who typed this report.

# Contents

# List of Figures

# List of Tables

# Abstract

The thermal stress restrained specimen test (TSRST) was selected to evaluate the low-temperature cracking resistance of asphalt concrete mixtures. The TSRST system includes a load frame, step-motor-driven load ram, data acquisition hardware and software, temperature controller, and specimen alignment stand. The overall system is controlled by a personal computer.

TSRST is conducted by cooling an asphalt concrete specimen at a specified rate while maintaining the specimen at constant length. A typical thermally induced stress curve obtained in TSRST is divided into two parts: relaxation and nonrelaxation. The temperature at which the curve is divided into two parts is termed the transition temperature. The temperature at fracture is termed the fracture temperature, and the maximum stress is the fracture strength.

An experiment design that considered a range of mixture and test condition variables was developed to evaluate the suitability of TSRST for characterizing low-temperature cracking resistance of asphalt concrete mixtures. Four asphalts and two aggregates were selected for the experiment. The mixture variables included asphalt type, aggregate type, and air voids content; the test condition variables included specimen size, stress relaxation, aging, and cooling rate.

# Executive Summary

Low-temperature cracking of asphalt concrete pavements is a serious problem in the northern tier of the United States, as well as in Alaska, Canada, and other countries at extreme northern and southern latitudes. Low-temperature cracking occurs when tensile stresses develop in an asphalt concrete pavement as the temperature drops to an extremely low value. When the tensile stress equals the strength of the asphalt concrete mixture at that temperature, a microcrack develops at the surface and edge of the pavement structure. At colder temperatures or repeated temperature cycles, the crack penetrates the full depth and width of the asphalt concrete layer. The primary pattern of low-temperature cracking is transverse to the direction of traffic. Thermal cracks are regularly spaced at intervals of 30 m (100 ft) for new pavement to less than 3 m (10 ft) for old pavement.

To better understand low-temperature cracking, a research program was undertaken under the Strategic Highway Research Program (SHRP) contract A-003A with the following objectives:

1. To identify and develop a test system to evaluate the low-temperature cracking resistance of an asphalt concrete mixture.

2. To execute an experimental program with the thermal stress restrained specimen test (TSRST) system to investigate low-temperature cracking of asphalt concrete mixtures.

3. To correlate fundamental properties of asphalt cements and air void contents of asphalt concrete mixtures with the mixtures' TSRST low-temperature cracking characteristics.

TSRST was identified to evaluate the low-temperature cracking resistance of asphalt concrete mixtures. The TSRST system includes a loading and data acquisition system, temperature controller, and specimen alignment stand. The overall system is controlled with a personal computer.

TSRST is conducted by cooling an asphalt concrete specimen at a specified rate while maintaining the specimen at constant length. A typical stress-temperature curve obtained in TSRST is divided into two parts: relaxation and nonrelaxation. The temperature at which the curve is divided into two parts is termed the transition temperature. The temperature at fracture is termed the fracture temperature, and the maximum stress is the fracture strength.

Based on the results presented in this report, the following conclusions can be made:

- The repeatability of TSRST based on the coefficient of variation is estimated as excellent for fracture and transition temperatures and good for fracture strength and slope.

- TSRST results provide an excellent indication of the low-temperature cracking resistance of asphalt concrete mixtures. A ranking of this resistance based on TSRST results is in good agreement with a ranking based on the physical properties of the asphalt cements used in the mixtures.

- All the variables considered in the experiment designs are significant factors in the TSRST results. Variables include asphalt type, aggregate type, air voids content, specimen size, degree of aging, stress relaxation, and cooling rate. The interactions among variables are not significant except for the interaction between asphalt type and stress relaxation.

- Fracture and transition temperatures are most sensitive to asphalt type. They are also affected by aggregate type, specimen size, degree of aging, and cooling rate. Fracture strength and slope are most sensitive to air voids content followed by aggregate type. They are also affected by asphalt type, stress relaxation, and cooling rate.

# 1

# Introduction

## 1.1 Background

Thermal or low-temperature cracking of asphalt concrete pavements is a serious problem in many regions of the United States. Low-temperature cracking is attributed to tensile stresses induced in asphalt concrete pavement by temperature drops to extremely low levels. If the pavement is cooled to a low-temperature, tensile stresses develop as the pavement contracts. The friction between the pavement and the base layer resists the contraction. When the tensile stress induced in the pavement equals the strength of the asphalt concrete mixture at that temperature, a microcrack develops at the edge and surface of the pavement. At colder temperatures or repeated temperature cycles, the crack penetrates the full depth and width of the asphalt concrete layer (Figure 1.1).

Sugawara et al. (1982) reported that a typical microcrack initiates at the center or side lines, the edges of core sampling, and the corners of ditches, which are considered weak points in the pavement structure. The primary pattern of low-temperature cracking is transverse to the direction of traffic and is fairly regularly spaced at intervals of 30 m (100 ft) for new pavements to less than 3 m (10 ft) for older pavements. If the transverse crack spacing is less than the width of the pavement, longitudinal cracking may occur and a block pattern can develop (Figure 1.2).

Low-temperature cracks through the pavement structure create a conduit for the migration of water and fines into and out of the pavement. During the winter, the intrusion of deicing solutions into the base through the crack can lead to localized thawing of the base and a depression at the crack. Water entering the crack also freezes and forms ice lenses, which can produce upward lipping at the crack edge. Pumping fine materials through the crack will produce voids under the pavement and a depression at the crack upon loading. All of these effects result in poor ride quality and reduced pavement service life.

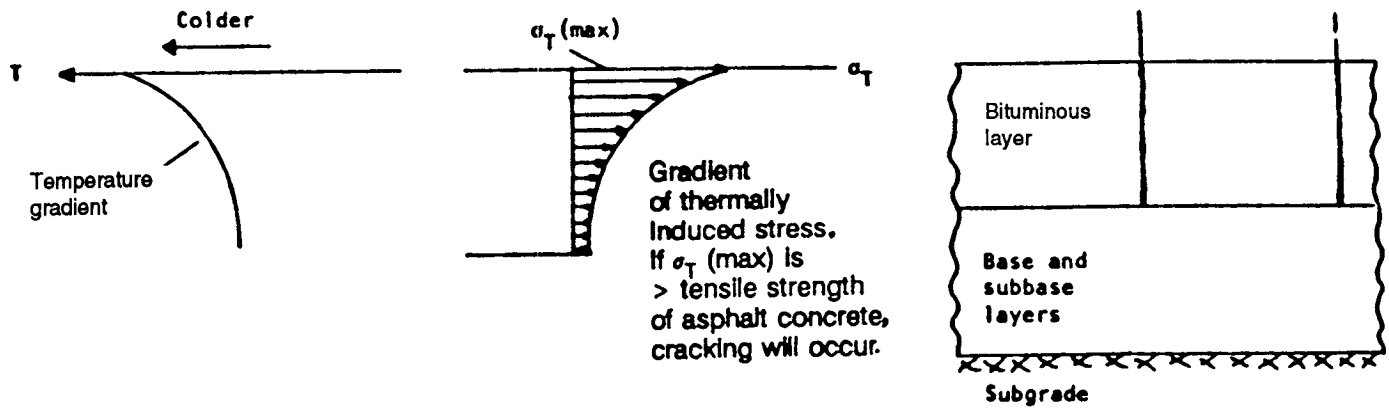


**Figure 1.1. Cross section of cold pavement showing temperature and thermal stress gradients (after Haas et al. 1987)**

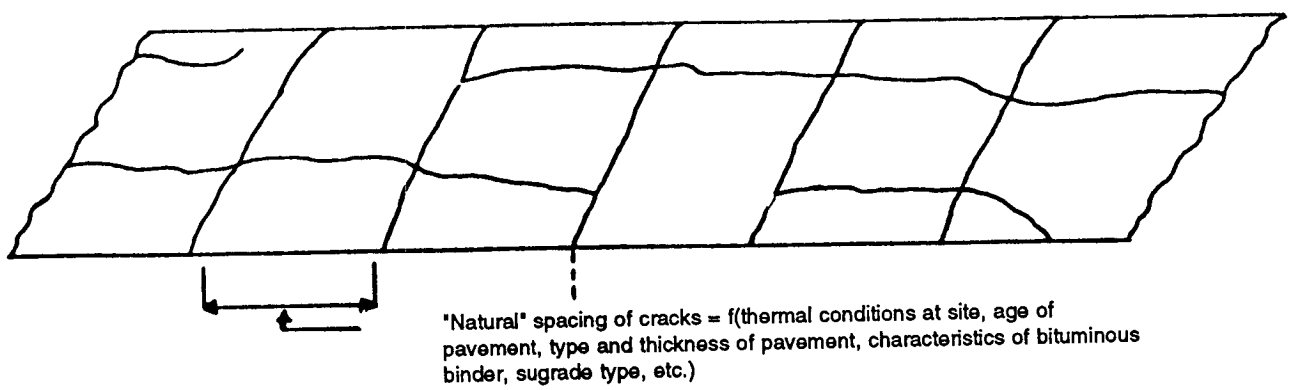


**Figure 1.2. Plan view of runway with schematic illustration of typical thermal cracking pattern (after Haas et al. 1987)**

Factors that influence low-temperature cracking in asphalt concrete pavements may be broadly categorized as (1) material, (2) environmental, and (3) pavement structure geometry.

**Material Factors**

Several material factors can affect the thermal behavior of asphalt-aggregate mixtures. These factors include the following:

1. Asphalt Cement. The temperature-stiffness relationship of the asphalt cement is generally accepted as the single most important factor affecting the degree of low-temperature cracking in an asphalt concrete mix. The stiffness or consistency (i.e., viscosity or penetration) at a cold temperature and the temperature susceptibility (i.e., the range in consistency with temperature) are the most important considerations. A lower viscosity (or higher penetration) grade of asphalt cement will produce a lower rate of increase in stiffness with decreasing temperature and thus reduces the potential for low-temperature cracking. Anderson et al. (1989), the Committee on Characteristics of Bituminous Materials (1988), and Carpenter and VanDam (1985) have conducted comprehensive studies on the relationship of asphalt cement to low-temperature cracking. An annotated bibliography on the temperature susceptibility of asphalt cements has been published by the Transportation Research Board (1989).

2. Aggregate Type and Gradation. Maximum resistance to transverse cracking is associated with aggregates that have high abrasion resistance, low freeze-thaw loss, and low absorption. Aggregates that possess these characteristics show little variation in low-temperature strengths. Absorptive aggregates reduce low-temperature strength because the asphalt cement remaining in the mixture for bonding is less than it would be in a mixture with a nonabsorptive aggregate. The gradation of the aggregate used in the mix apparently has little influence on low-temperature strength, assuming the mix is designed to provide reasonable resistance to rutting.

3. Asphalt Cement Content. Changes in asphalt cement content, within a reasonable range of optimum, do not have a significant influence on a mix's low-temperature cracking performance. Increasing the asphalt cement content increases the coefficient of thermal contraction but lowers the stiffness. The apparent net effect is that the thermal stress that develops is similar to the stress developed before the asphalt cement content was changed.

4. Air Void Content. The degree of compaction and related air void content and permeability do not, by themselves, significantly influence the low-temperature cracking characteristics of the mix.

**Environmental Factors**

Several environmental factors can affect low-temperature cracking. These factors include the following:

1. Temperature. For a given mix, the colder the pavement surface temperature, the greater the incidence of thermal cracking. The pavement surface temperature is related to the ambient air temperature and wind speed. The majority of low-temperature cracks apparently are initiated when the temperature decreases to a level below the glass transition temperature and is maintained at this level for a period of time.

2. Rate of Cooling. The faster the rate of cooling, the greater the tendency for thermal cracking.

3. Pavement Age. The older the pavement, the greater the incidence of thermal cracking. This situation is associated with the increase in stiffness of aging asphalt cement. The mix's air void content may influence its aging characteristics. Also, as the pavement's time in service increases, the probability that more extreme low-temperatures will occur increases as well. Benson (1976), in a study of low-temperature pavement cracking in Texas, proposed a generalized model for predicting the hardening of asphalt as a function of time.

**Pavement Structure Geometry**

Several pavement structure geometry factors can affect thermal cracking response. These factors include the following:

1. Pavement Width. Field evidence suggests that thermal cracks are more closely spaced in narrow pavements than in wide pavements. Initial crack spacing for secondary roads 7.3 m (24 ft) in width is approximately 30 m (100 ft), whereas for general aviation airports, with pavements 15 m to 30 m (50 ft to 100 ft) wide, the initial spacing can be greater than 45 m (150 ft). As the pavement ages, secondary and tertiary cracks develop and the differences in crack spacing are not apparent.

2. Pavement Thickness. In general, the thicker the asphalt concrete layer, the lower the incidence of thermal cracking. At the St. Anne Test Road, increasing the thickness of the ACL from 10 cm to 25 cm (4 in. to 10 in.) resulted in one-half the cracking frequency when all other variables were the same.

3. Friction Coefficient Between the Asphalt Concrete Layer and Base Course. A prime coat on an untreated aggregate base course layer apparently reduces the incidence of low-temperature cracking. This result may be due to the fact that an asphalt concrete layer bonded perfectly to an underlying granular base has a

reduced thermal contraction coefficient because the granular base has a lower thermal contraction coefficient. The gradation of the base course, particularly the percentage of material finer than the No. 200 sieve, may have a minor influence on the incidence of low-temperature cracking.

4. Subgrade Type. The frequency of low-temperature cracks is usually greater for pavements on sand subgrades than on cohesive subgrades.

5. Construction Flaws. Steel roller compaction of asphalt layers at high temperatures and low mix stiffness creates transverse flaws. As the pavement cools, cracks may be initiated at these flaws, often at spacings closer than the width of a lane.

## 1.2 Objectives

Many investigators have attempted to evaluate low-temperature cracking in asphalt concrete pavement using analytical or experimental approaches and to relate their results to field performance. The objectives of this study are as follows:

1. To identify and develop a test system to evaluate the low-temperature cracking resistance of an asphalt concrete mixture.

2. To execute an experimental program with the thermal stress restrained specimen test (TSRST) system to investigate low-temperature cracking of asphalt concrete mixtures.

3. To correlate fundamental properties of asphalt cements and the air voids content of asphalt concrete mixtures with mixtures' TSRST low-temperature cracking characteristics.

The scope of work includes the following:

1. Review existing test methods/systems to evaluate thermal cracking of asphalt concrete mixtures.

2. Develop a test system and protocol to characterize low- temperature cracking of an asphalt concrete mixture.

3. Execute an experimental program to investigate low-temperature cracking of asphalt concrete mixtures.

4. Analyze test results to correlate fundamental properties of asphalt cement and the air voids content of mixtures to the fracture temperature and stress and the stress-temperature characteristics of asphalt concrete mixtures.

# 2

# Review of Test Systems and Methods to Evaluate Thermal Cracking of Asphalt concrete Mixtures

## 2.1 Evaluation of Test Method/System Associated with Thermal Cracking

A number of test methods have been used to evaluate thermal cracking in asphalt concrete mixtures. These test methods have also been used to provide input data for thermal cracking models such as *COLD* (Finn et al. 1986), University of Florida model (Ruth et al. 1982), the Texas A&M model (Lytton et al. 1983), and the University of Texas model (Shahin and McCullough 1972). The test methods that have been most widely employed to study the phenomenon of low-temperature cracking in asphalt concrete mixtures include (1) the indirect tension test (Hadipour and Anderson 1988, Anderson and Leung 1987); (2) the direct tension test (Haas 1973, Kallas 1982); (3) the direct tensile creep test (Haas 1973, Fromm and Phang 1972); (4) the flexural bending test (Busby and Rader 1972, Sugawara et al. 1982); (5) the thermal stress restrained specimen test (Monismith et al. 1965, Fabb 1974, Carpenter 1983, Sugawara and Moriyoshi 1984, Janoo 1989, Arand 1987); and (6) the coefficient of thermal expansion and contraction test (Jones et al. 1968, Osterkamp et al. 1986).

Vinson et al. (1990) evaluated these test methods based on the following criteria:

1. Simulation of field conditions.
2. Application of test results to mechanistic models.
3. Suitability for aging and moisture conditioning.
4. Potential to accommodate large stone mixes.
5. Ease of conduct.
6. Cost of equipment.

These criteria are given in their relative order of importance with respect to meeting the overall objectives of the Strategic Highway Research Program (SHRP) A-003A project. The most important objective of the project is to identify a test method that relates as closely as possible to the field conditions being simulated.

The evaluation of the test methods associated with low-temperature cracking is summarized in Table 2.1. The evaluation indicated that only two test methods actually simulate field conditions — the thermal stress restrained specimen test (TSRST) and the coefficient of expansion and contraction test. The remaining methods provide (1) low-temperature stress-strain characteristics of an asphalt concrete specimen when the specimen fails during loading, the tensile strength; or (2) an energy release rate fracture mechanics parameter. These properties are only indirect measures of the mix is response to cooling.

Results of the load deformation tests are indirectly applicable to mechanistic models. "Indirectly applicable" is used because the results from these tests often support the determination of the thermal stress/temperature relationship, but they are not a direct measure of this relationship. The coefficient of thermal contraction also is indirectly applicable since it is multiplied by the temperature change and stiffness modulus to arrive at the thermal stress relationship. In many of the models, the coefficient of thermal contraction is assumed. The results from the fracture mechanics tests (i.e., C*-line integral) also are indirectly applicable to a mechanistic model because fracture is induced by an applied load and not by a temperature drop or cycling.

The only results directly applicable to the existing mechanistic models are the thermal stress versus temperature relationship obtained in a thermal stress restrained specimen test. The thermal cracking models currently available do not allow this relationship to be input, because the algorithms developed to support the models calculate the relationship from indirect measurements of thermal response or properties of the asphalt cement.

The assessment of the suitability of the test method for aging and moisture conditioning is speculative. Those test methods that employ cylindrical specimens are believed to be moderately suitable for aging and moisture conditioning; the flexural bending test uses a rectangular beam specimen, which has low suitability for aging and moisture conditioning.

For all practical purposes, the tensile creep (direct or indirect) test and flexural bending tests are not currently used by practitioners or researchers to determine low-temperature tensile stress/strain and strength characteristics of asphalt concrete mixes.

The potential to accommodate large stone mixes (maximum aggregate particle size greater than 2.54 cm [1 in.] is considered because of the current trend to use these mixes to reduce rutting. All of the test methods identified can accommodate large stone mixes or could be easily modified to accommodate such mixes except for the fracture mechanics test methods. The three-point bend test is limited to specimens with fine aggregate, and the C*-line integral test is limited to a maximum aggregate size of 1.9 cm (3/4 in.).

**Table 2.1. Evaluation of thermal cracking test methodologies (after Vinson et al. 1990)**

| Test Method | Properties Measured | Simulation of Field Conditions | Ease of Use | Application of Test Results to Mechanistic Model | Suitability for Aging and Moisture Conditioning | Potential to Accommodate Large Stone Mixtures | Comments |
|---|---|---|---|---|---|---|---|
| Indirect tension | Low-temperature tensile stress/strain characteristics; tensile strength | No | Easy | Indirectly applicable | Moderate suitability | High | Well-documented procedure; significant prior use in profession |
| Direct tension constant rate of extension | tensile stress/strain characteristics; tensile strength | No | Easy | Indirectly applicable | Moderate suitability | High | Well-documented procedure; significant prior use in profession |
| Direct tensile creep | Tensile stress/strain characteristics; tensile strength | No | Easy | Indirectly applicable | Moderate suitability | High | No longer used in profession |
| Flexural bending | Stress/strain characteristics; tensile strength | No | Easy | Indirectly applicable | Low suitability | High | No longer used in profession |
| Thermal stress restrained specimen | Low-temperature thermal stress characteristics; tensile strength; fracture temperature | Yes | Easy | Directly applicable | Moderate suitability w/ beams or cylinders | High | Well-documented procedure; significant prior use in profession |
| Coefficient of thermal expansion and contraction | Thermal expansion/contraction coefficient | Yes | Easy | Indirectly applicable; used in conjunction with tensile stress/stress characteristics | Moderate suitability | High | Well-documented procedure |
| C*-line integral | Energy release rate line integral | No | Easy | Indirectly applicable | Moderate suitability | High | Well-documented procedure |

All of the tests are relatively easy to conduct, except the three-point bend and C*-line integral. These are identified as difficult and moderate, respectively, because they require that the specimen be notched and the rate of crack propagation be monitored. The procedures for the load deformation tests (i.e., indirect and direct tension, tensile creep, and flexural bending) are well established and documented. The equipment associated with the indirect and direct tension test methods is routinely used in many laboratories. The test equipment for tensile creep, flexural bending, thermal stress, and coefficient of expansion/contraction is not routinely used. The procedures for the three-point bend specimen tests are documented but are in first generation use.

## 2.2 Thermal Stress Restrained Specimen Test (TSRST) Systems

Based on the evaluation of the test methods by Vinson et al. (1990), TSRST was judged to have the greatest potential to evaluate the low-temperature cracking susceptibility of an asphalt concrete mixture. The test has been successfully used by several investigators to characterize the response of asphalt concrete mixtures at low-temperatures (Monismith et al. 1965, Fabb 1974, Carpenter 1983, Arand 1987, Sugawara et al. 1982, Janoo 1989).

The basic requirement for the TSRST test apparatus is that it must maintain the specimen at a constant length during a temperature cooling cycle. Initial efforts to meet this requirement involved the use of fixed frames constructed from invar steel (Monismith et al. 1965, Fabb 1974, Carpenter 1983, Janoo 1989). A summary of test systems associated with TSRST is presented in Table 2.2. In general, these devices were not satisfactory because as the temperature decreased, the load in the specimen caused the frame to deflect to a point at which the stresses relaxed and the specimen didn't fail. Fixed frames may also limit the length of the specimen. As indicated in Table 2.2, specimens of 305 mm in length were used for the systems employing fixed frames.

Arand (1987) substantially improved the test system by inserting a displacement feedback loop, which ensured that the stresses in the specimen would not relax because the specimen length was continuously corrected during the test. The major properties measured in TSRST are low-temperature thermal stress characteristics, tensile strength, and fracture temperature under one or more temperature cycles.

**Table 2.2. Summary of thermal stress restrained specimen test systems (after Janoo et al. 1990)**

| Investigators | Specimen Size W × D × L (mm) | Cooling Rate (°C/hr) | Cooling Fluid | Crack Observed |
|---|---|---|---|---|
| Monismith (1965) | 25 × 25 × 305 | 4 | Air | No |
| Fabb (1974) | 25 × 25 × 305 | 5, 10 | Methylated spirit | Yes |
| Sugawara et al. (1982) Sugawara and Moriysuhi (1984) | 25 × 25 × 305 | 3, 6, 12, 18, 24, 30 | Methanol | Yes |
| Carpenter (1983) | 25 × 25 × 305 | 5, 10, 20 | Air | Yes |
| Janoo et al. (1990) | 76 × 25 × 305<br>51 × 51 × 305<br>76 × 76 × 305 | 5, 10, 20 | Air | Yes |
| Arand (1987) | 40 × 40 × 160 | 10 | Liquid nitrogen | Yes |

# 3

# Development of a Thermal Stress Restrained Specimen Test System

The thermal stress restrained specimen test (TSRST) system developed in this study is an automated, closed-loop system specifically designed to measure the tensile stress in an asphalt concrete specimen that is cooled at a constant rate while restrained from contraction. The test system consists of a load system, data acquisition system, temperature control system, and specimen alignment stands. The load, data acquisition, and temperature control systems are controlled with a personal computer.

## 3.1 Load System

The load system includes a load frame, a step motor and two swivel jigs. The load frame consists of two aluminum base plates that are supported by four connecting circular rods. A step motor is mounted on the top base plate and a load cell is attached to the bottom base plate. The height of the load frame can be adjusted to accommodate various specimen lengths. Figure 3.1 shows the load system in detail.

The step motor keeps the specimen at constant length during the test by driving a threaded axial loading rod. The motor is controlled by a computer and operates in response to electric signals from the linear variable differential transformers (LVDTs). It pulls the test specimen whenever the specimen contracts by 0.00025 cm (0.0001 in.). Tensile stresses are induced in the specimen when it is restrained from contraction. The tensile force is measured with a load cell.

The motor can also be controlled manually. Two swivel assemblies are connected to the top and bottom of the specimen end platens. These enable the step motor to stretch the specimen concentrically. Both swivel assemblies link the specimen with the step motor and the load cell, respectively, through Micarta blocks. The Micarta blocks prevent heat conduction to the specimen from the outside environment.

## 3.2 Data Acquisition System

The data acquisition system (Figure 3.2) consists of a transducer signal conditioner, a data acquisition/control unit, and a personal computer. The change of specimen length caused by change temperature is measured with two LVDTs and two invar rods attached to the specimen end platens (Figure 3.1). Three thermistors are attached to their appropriate locations on the specimen to measure its surface temperature. The electric signals (voltages) from the load cell and LVDTs are sent to the data acquisition/control unit through the transducer signal conditioner. The electrical resistances from the thermistors are sent directly to the data acquisition/control unit. The data collected in the data acquisition/control unit are transmitted to the computer by way of an IEEE 488 bus driver. Finally, the computer collects all the required data according to a specified time interval.

The data acquisition system is controlled by a computer program that is written in Turbo Pascal. The program also operates the step motor via a PC21 indexer, that sends motor commands from a computer to a motor and reads position data from the LVDTs through an IEEE 488 driver. User-defined calibration constants are input to determine the position error relative to the initial position. The motor commands are then synthesized and ported to the motor via the PC21 indexer to correct position. The program is shown as a flow chart in Figure 3.3.

## 3.3 Temperature Control System

The temperature control system that controls the rate of cooling includes a liquid nitrogen (LN2) container, a temperature controller (ATHENA), and a resistance temperature device (RTD) (Figure 3.4). It is separated from the data acquisition system and operates independently.

The cooling process is performed by vaporizing the compressed liquid nitrogen into the environmental chamber through a solenoid valve. The cooled air is then circulated with a fan to provide a uniform temperature distribution in the chamber. The RTD connected to the temperature controller is placed in the chamber at a location that provides the most uniform temperature distribution. The temperature controller regulates the amount of nitrogen required to reach a specified temperature. The controller allows various cooling rates and temperature cycles to be easily programmed and monitored.

## 3.4 Specimen Alignment Stand

The alignment of the specimen is critical to obtaining meaningful test results. Poor alignment may cause bending stresses in the specimen. The stand provides concentric and perpendicular alignment between the platens and the specimen using an epoxy compound and will secure the specimen and platens while the epoxy sets. The stand is mounted vertically (Figure 3.5).

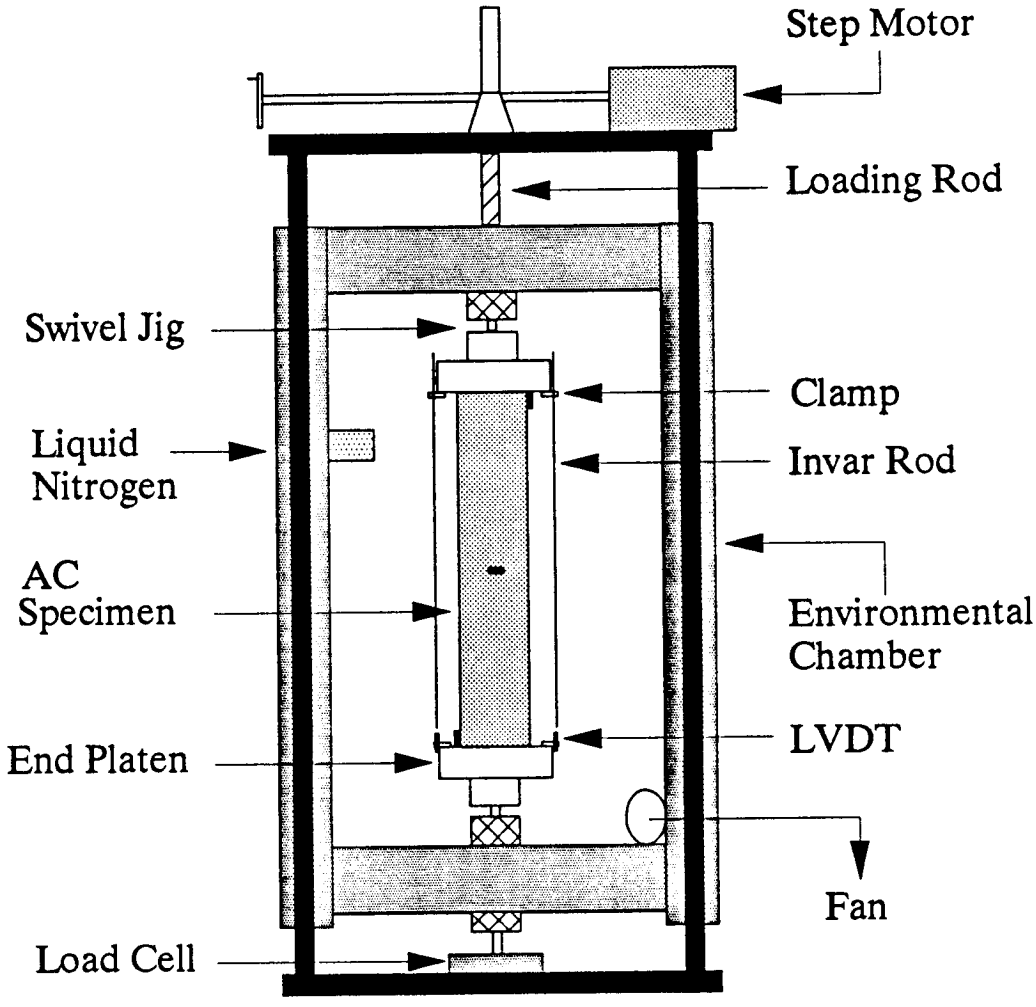


**Figure 3.1. Schematic of TSRST apparatus**

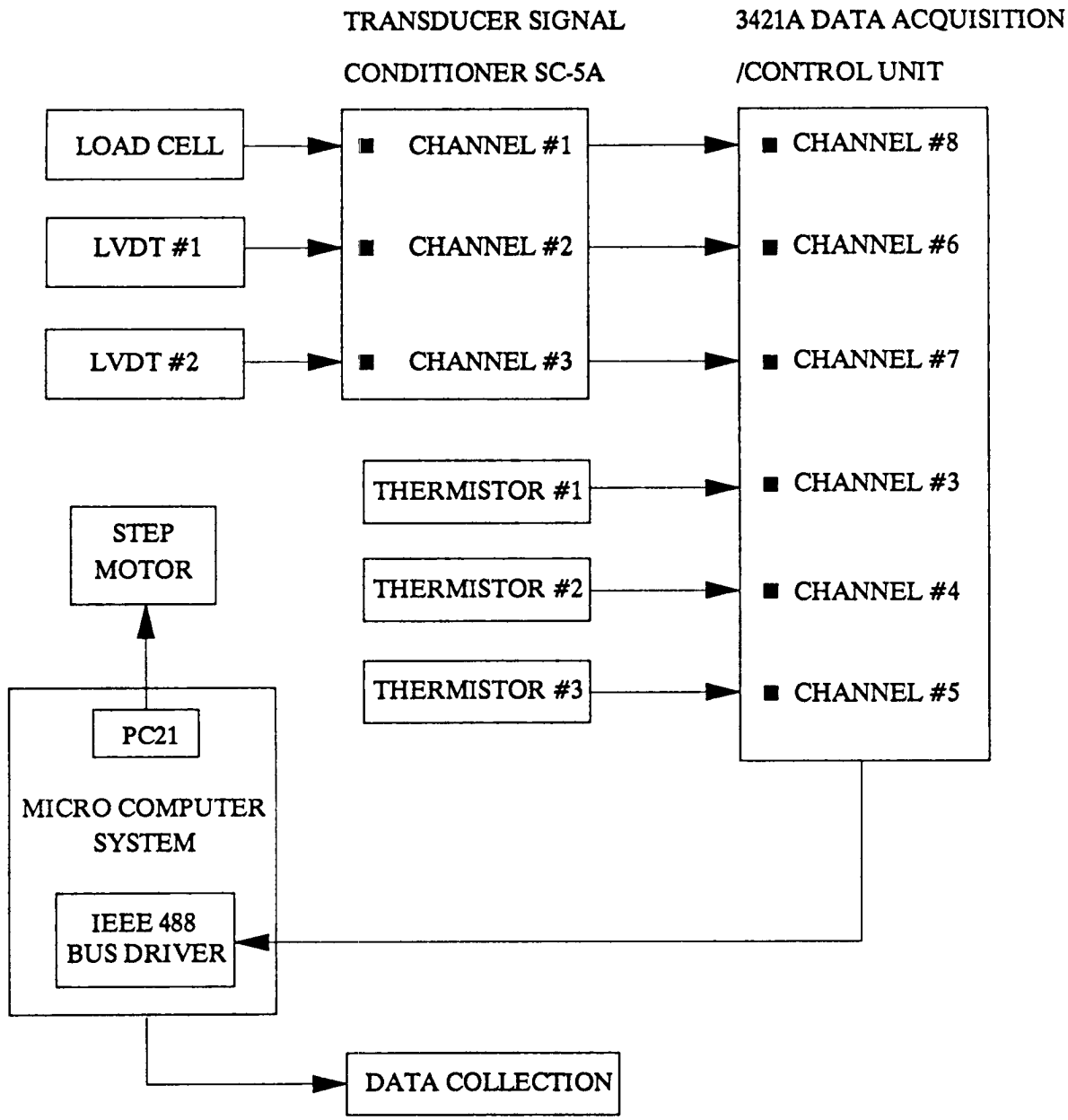


**Figure 3.2. Schematic of data acquisition system**

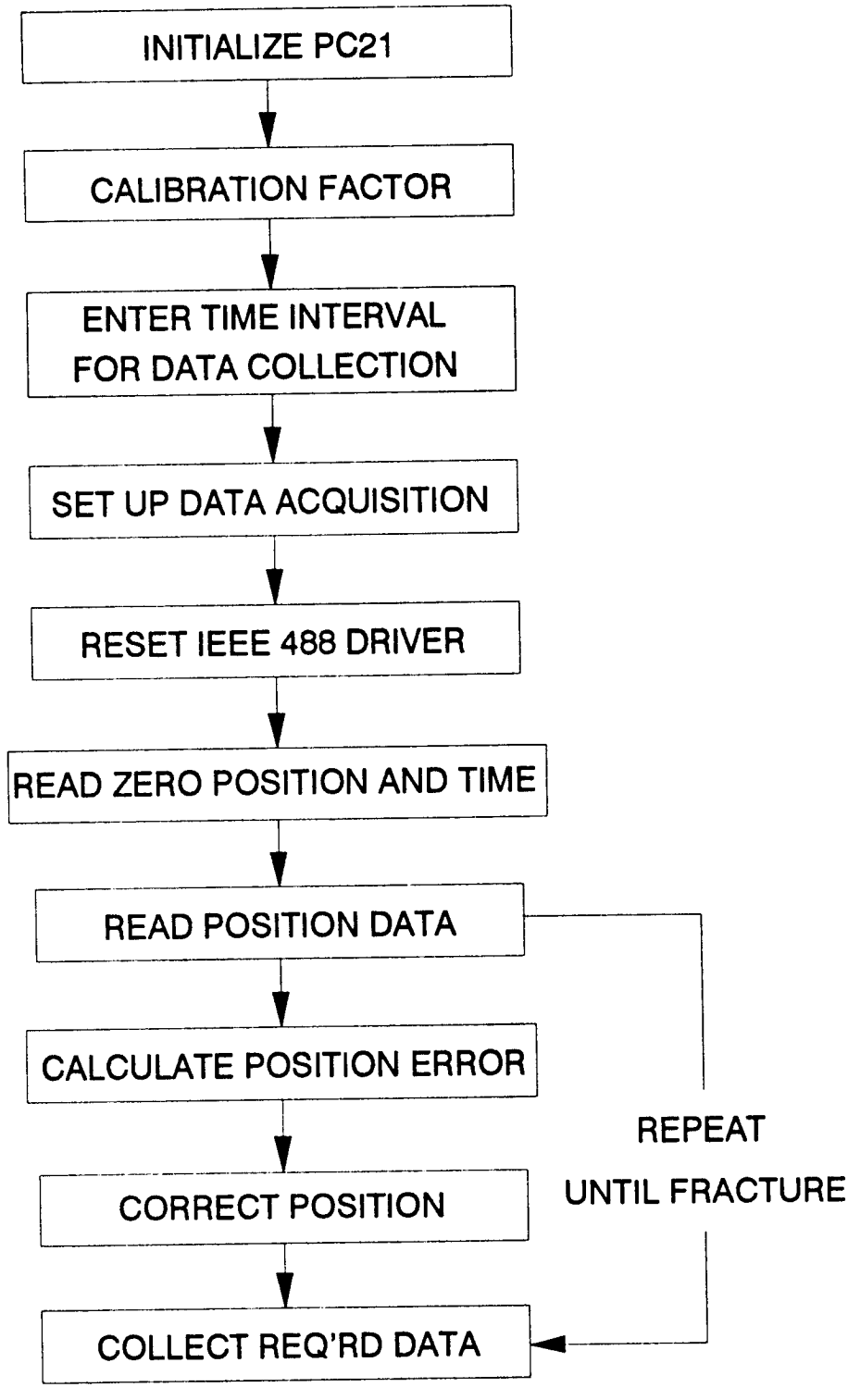


**Figure 3.3. Flow chart of control program**

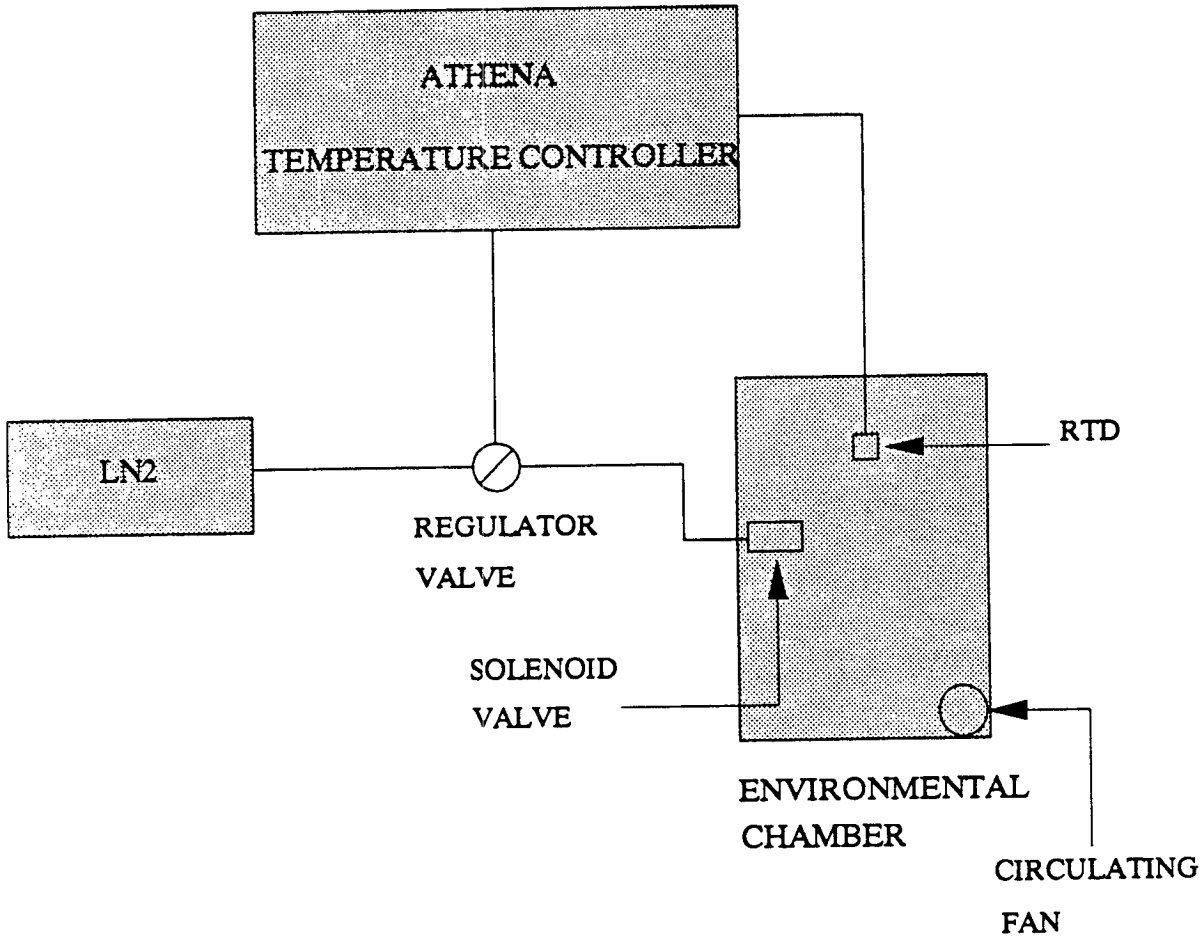


**Figure 3.4. Schematic of temperature control system**

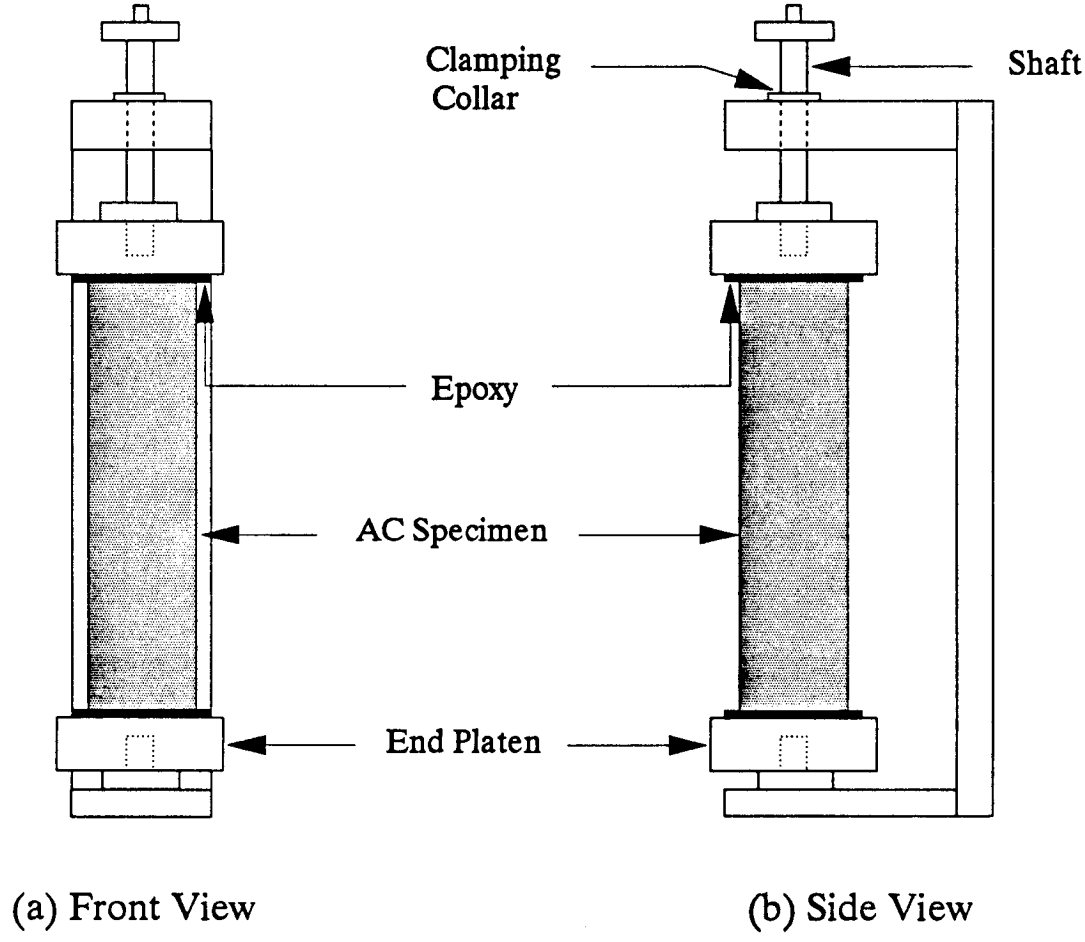


**Figure 3.5. Schematic of specimen alignment stand**

## 3.5 Test Procedure

The thermal stress restrained specimen test developed in this study is performed as follows:

1. **Prepare an asphalt concrete specimen (50 mm$^2$ square and 250 mm in length).** It takes approximately 2 hours to prepare four test specimens, excluding the time required for curing and measuring the air voids content. This step includes batching aggregate, mixing aggregate and asphalt, compacting and extruding a beam, and cutting a beam.

2. **Clean the specimen end platens with a suitable degreasing agent (to remove asphalts) and with a piece of sandpaper (to remove any remaining epoxy and to provide a rough surface).** Asphalt films, degreasing agents, or water should not remain on the platens. It takes 10 minutes to clean the end platens. It is recommended that the end platens be heated in the oven for about 30 minutes at 120°C prior to cleaning. The platens should not be overheated. Overheating will stiffen the epoxy.

3. **Prepare the epoxy according to manufacturer's instructions.** Typically, epoxy has two components: resin and hardener. The curing time and resulting maximum strength depend on the mix proportions of two components. (For example, the mix proportions (hardener:resin) used in this study were 1:1 [by weight] for DC-80 [Thermoplastic Inc.] and 1:9 [by weight] for Plastic Steel Putty [Devcon Co.]). It is recommended that the manufacturer's instructions be followed for handling and storage. Poor handling and storage can alter the chemical properties of the epoxy.

4. **Attach the end platens to the specimen alignment stand and secure with an adequate amount of epoxy (3 mm in thickness).**

5. **Place the specimen between the platens and align it. Build up a fillet of epoxy approximately 2 cm in height along the specimen's sides.** Take special care not to move the specimen. Misalignment will result in bending stresses in the specimen. It takes 30 minutes to accomplish steps 3, 4, and 5.

6. **Leave the specimen in the alignment stand until the epoxy has cured.** Be sure to allow enough time for the epoxy to set. Curing time depends on mix proportions and manufacturers. (Typically, curing took about 24 hours to ensure setting of DC-80 and 4 hours for Plastic Steel Putty.)

7. **Remove the specimen with the end platens from the alignment stand and store it at 5°C for 5 to 6 hours to allow the specimen to reach thermal equilibrium.** If air is circulated around the specimen during storage, the precooling time can be reduced to approximately 1 hour.

8. **Connect the specimen/platen assembly to the top U-joint and the bottom U-joint with the clevis pin.** Make sure the specimen is not loaded.

9. **Attach the two clamps used to secure the invar rods and the LVDTs to the top and bottom platens, respectively.** The clamps should be aligned so that the invar rods and the LVDTs can be aligned.

10. **Attach the thermistors to the specimen with modeling clay. Secure a thermistor to the bottom, the center, and the top of the specimen. Each thermistor should be attached to a different side of the specimen.**

11. **Attach the RTD cable to an appropriate location in the chamber.** The location of the RTD affects the temperature distribution in the chamber. Examine several locations to ensure a uniform temperature distribution. In the tests performed for this study, the RTD on the middle portion of the specimen's free side typically resulted in uniform temperature distribution.

12. **Attach the two invar rods and LVDTs to the clamps on the top and bottom platens, respectively.** Each invar rod and LVDT should be aligned properly. It takes 30 minutes to accomplish steps 7 through 11.

13. **Close the chamber.**

14. **Set the desired cooling rate with the temperature controller.** A variety of cooling rates can be used. Typical cooling rates used in this study were 1°, 2°, 5°, and 10°C/hr.

15. **Cool the chamber down to 5°C and then hold the temperature for 15 to 20 minutes until the specimen reaches thermal equilibrium.**

16. **Apply an initial tension load of approximately 44 N (10 lb) to the specimen by manually turning the hand crank on the step motor. Start cooling the cabinet at a desired rate.** Be very careful not to apply excessive load.

17. **Engage the computer to begin position correction and record all the required data until the specimen breaks.**

All the procedures discussed above can be accomplished by one person. If a high level of test production is required, two people — one for sample preparation and the other for conducting the test and data analysis — are recommended.

## 3.6 Selection of Cooling Rate and Specimen Size

The cooling rates for the low-temperature cracking test reported in the literature range from 3° to 30°C/hr. The majority of investigators have conducted their tests at a cooling rate of

10°C/hr. A summary of cooling rates used by various investigators was presented in Table 2.2. Fabb (1974) and Sugawara et al. (1982) confirmed with their test results that the cooling rate had little or no effect on the fracture temperature and tensile strength when the rate was equal to or greater than 5°C/hr.

Field cooling rates are much slower than 10°C/hr. Fromm and Phang (1972) reported that in Canada the cooling rate very seldom exceeded 2.7°C/hr. Preliminary results from a study on air cooling rates in the northern United States over the last 10 years indicate that the most frequently observed cooling rate is between 0.5° and 1.0°C/hr (Janoo et al. 1990). Therefore, laboratory tests should be conducted at a cooling rate slower than 2°C/hr if field cooling rates are to be simulated. However, this slow rate results in an extremely long test program. Thus, most investigators have conducted tests at a cooling rate of 10°C/hr (or greater) and have used their results only to provide a relative assessment of the temperature susceptibility of asphalt concrete mixtures.

The specimen cross-sectional areas used in the thermal stress restrained specimen tests ranged from 25 mm × 25 mm to 76 mm × 76 mm; the aspect (length/width) ratio ranged from 4 to 20. A summary of specimen sizes was also presented in Table 2.2.

Janoo et al. (1990) reported the effect of specimen size on fracture strength in terms of the cross-sectional area. The fracture strength decreases as the cross-sectional area increases (Figure 3.6). Similar results have been reported in the rock mechanics literature.

Based on results reported by Janoo et al. (1990), a minimum specimen size of 51 mm × 51 mm should be used. The main concerns with larger specimens are that a larger rigid frame will be required and that it will take the specimen longer to reach thermal equilibrium between its surface and its center. Monismith et al. (1965) reported results on the lag time of a 25 mm × 25 mm × 305 mm asphalt concrete specimen in reaching thermal equilibrium. As shown in Figure 3.7, the difference between the ambient and specimen temperature was initially about 10°F. As time elapses, this difference becomes small.

In this study, a cooling rate of 10°C/hr and two different specimen sizes (3.8 cm × 3.8 cm × 20.3 cm and 5 cm × 5 cm × 25 cm) were selected to investigate low-temperature cracking in asphalt concrete mixtures.

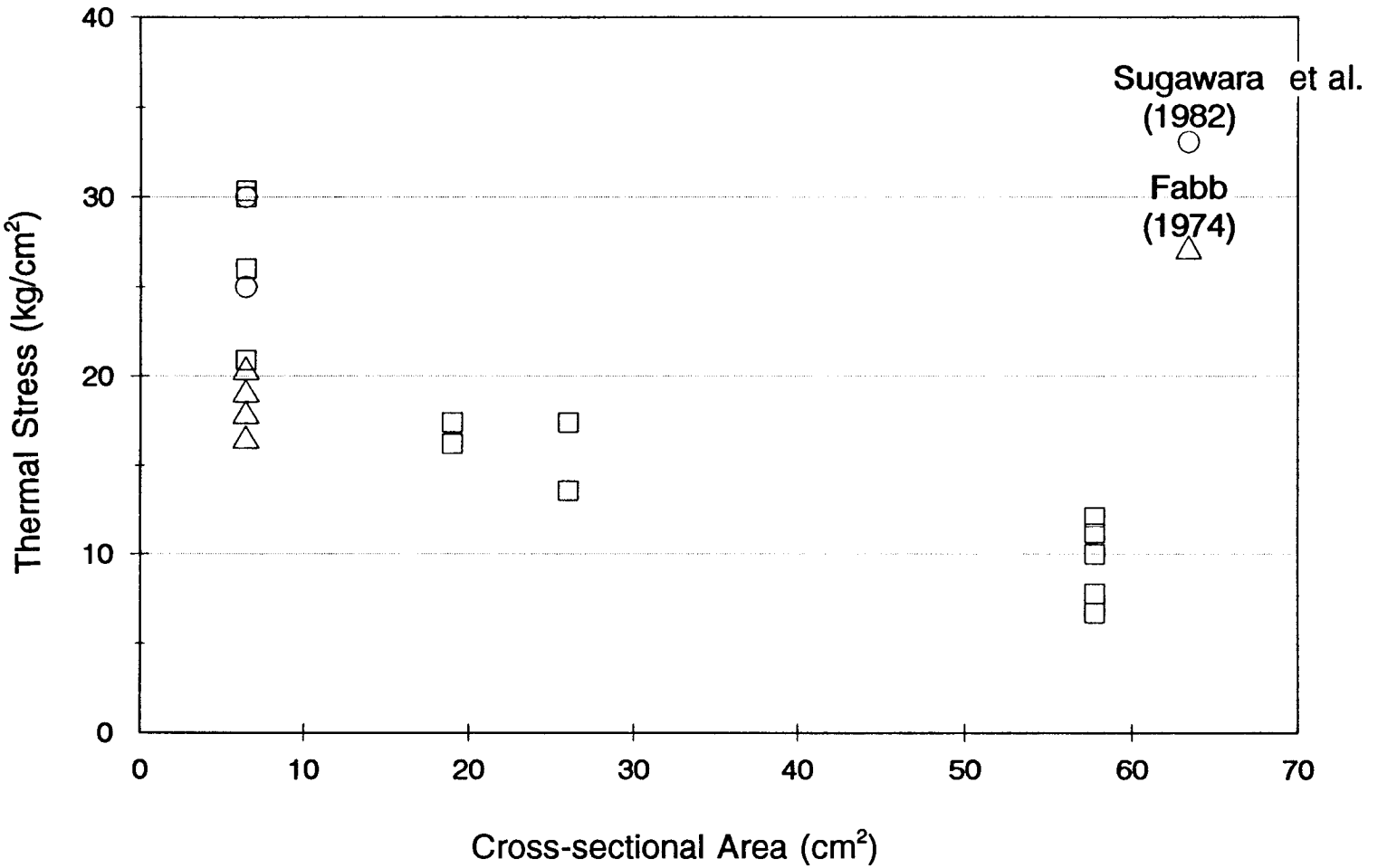


**Figure 3.6. Effect of specimen size on peak thermal stress (after Janoo 1989)**

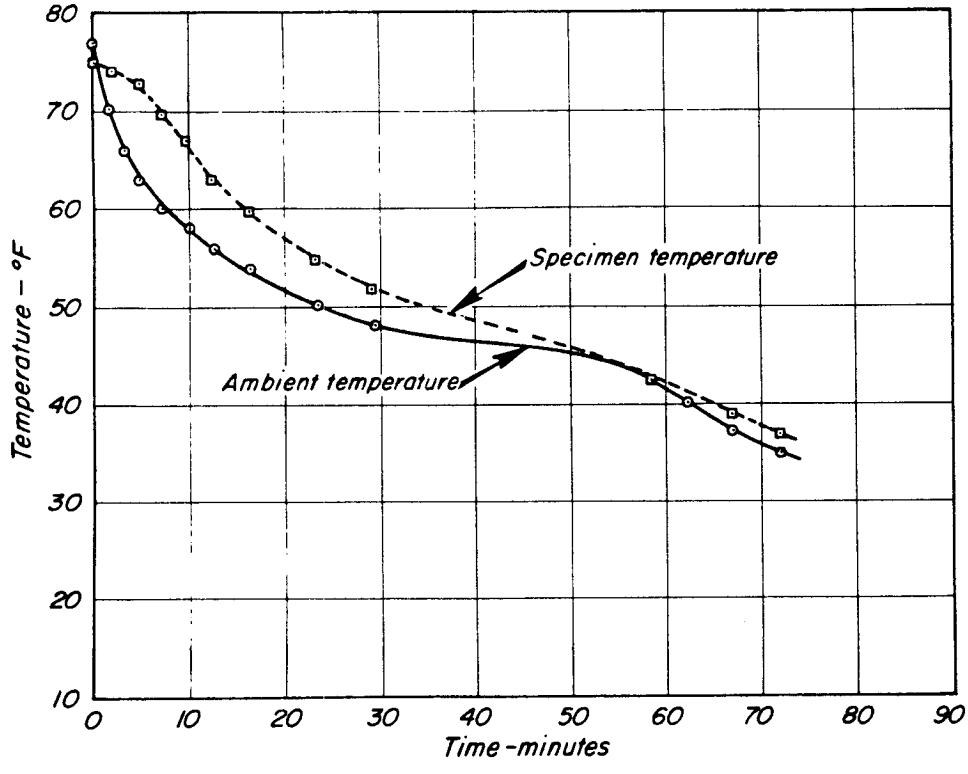


**Figure 3.7. Comparison of ambient and specimen temperatures in restrained beam experiment (after Monismith et al. 1965)**

# 4

# Experiment Design

The experiment design was developed with the following goals:

1. To evaluate the suitability of TSRST to characterize low-temperature cracking of asphalt concrete mixtures.

2. To evaluate the low-temperature cracking performance of asphalt concrete mixtures over a variety of conditions.

3. To relate test results to fundamental properties of asphalt cements.

The details of the experiment design are discussed in this section. Materials, sample preparation, and the test procedure are also discussed.

## 4.1 Experiment Design

The experiment design was divided into five phases each with a specific purpose. Each phase included different test variables, as follows:

**I. Initial Tests ($4 \times 2 \times 4 = 32$)**

| Variables | Levels |
|---|---|
| Asphalt Type | AAK-1, AAK-2, AAG-1, and AAG-2 |
| Aggregate Type | RB |
| Air Voids Content | 4% and 8% $\pm$ 1% |
| Specimen Size | 3.8 cm $\times$ 3.8 cm $\times$ 20.3 cm |
| Relaxation | No |
| Aging | No |
| Rate of Cooling | 10°C/hr |
| Replicates | 4 |

## II. Tests with Larger Specimen (4 × 2 × 2 × 4 = 64)

| Variables | Levels |
|---|---|
| Asphalt Type | AAK-1, AAK-2, AAG-1, and AAG-2 |
| Aggregate Type | RB and RL |
| Air Voids Content | 4% and 8% ± 1% |
| Relaxation | No |
| Aging | No |
| Specimen Size | 5.0 cm × 5.0 cm × 25.0 cm |
| Rate of Cooling | 10°C/hr |
| Replicates | 4 |

## III. Relaxation Tests (4 × 2 × 2 = 16)

| Variables | Levels |
|---|---|
| Asphalt Type | AAK-1, AAK-2, AAG-1, and AAG-2 |
| Aggregate Type | RB |
| Air Voids Content | 4% and 8% ± 1% |
| Relaxation | No |
| Aging | No |
| Specimen Size | 5.0 cm × 5.0 cm × 25.0 cm |
| Rate of Cooling | 10°C/hr |
| Replicates | 2 |

## IV. Effect of Various Cooling Rates (2 × 3 × 2 = 12)

| Variables | Levels |
|---|---|
| Asphalt Type | AAK-2 and AAG-1 |
| Aggregate Type | RB |
| Air Voids Content | 6% ± 1% |
| Specimen Size | 5.0 cm × 5.0 cm × 25.0 cm |
| Relaxation | No |
| Aging | No |
| Rate of Cooling | 1°, 2°, and 5°C/hr |
| Replicates | 2 |

**V. Effect of Aging (2 × 2 × 4 = 16)**

| Variables | Levels |
|---|---|
| Asphalt Type | AAK-2 and AAG-1 |
| Aggregate Type | RB |
| Air Voids Content | 6% ± 1% |
| Specimen Size | 5.0 cm × 5.0 cm × 25.0 cm |
| Relaxation | No |
| Aging | Long-term oven aging at 110° and 135°C for 4 days |
| Rate of Cooling | 10°C/hr |
| Replicates | 2 |

## 4.2 Materials Selected

The asphalts and aggregates used in the experiment were selected from the Strategic Highway Research Program (SHRP) Materials Reference Library (MRL). The four asphalt cements and two aggregates used in the experiment design are identified in Table 4.1. Considering the physical properties of the asphalt cement, the expected ranking of asphalts for resistance to low-temperature cracking is AAK-2 (greatest resistance)> AAK-1> AAG-2> AAG-1 (least resistance).

**Table 4.1. Materials involved in the experiment design**

| Materials | Type |
|---|---|
| Asphalt | AAG-1 and AAG-2<br>AAK-1 and AAK-2 |
| Aggregate | RB<br>RL |

The fundamental properties of the asphalt cements from the MRL are given with the asphalt grade in Table 4.2. Mineral aggregates from two sources were used in the experiment. The RB aggregate is a crushed granite that has a rough surface texture and angular shape; the RL aggregate is a chert that has a smooth surface texture and round shape.

## 4.3 Sample Preparation

Medium aggregate gradations for the two aggregates were used to prepare the asphalt concrete mixtures. Aggregate gradations for aggregates RB and RL are shown graphically in

**Table 4.2. Properties of asphalt cements (from the MRL)**

| Asphalt Type | AAG-1 | AAG-2 | AAK-1 | AAK-2 |
|---|---|---|---|---|
| Asphalt Grade | AR-4000 | AR-2000 | AC-30 | AC-10 |
| **Original Asphalt** | | | | |
| Viscosity | | | | |
| @ 60°C, poise | 1862 | 1056 | 3256 | 996 |
| @ 135°C, cSt | 243 | 170 | 562 | 320 |
| Penetration, dmm | | | | |
| @ 25°C, 100g, 5s | 53 | 76 | 70 | 154 |
| @ 4°C, 100g, 5s | 2 | | 2 | 12 |
| Ductility, cm | | | | |
| (4°C, 1 cm/min) | 0.0 | 150+ | 27.8 | 150+ |
| Softening point (R&B), °F | 120 | 111 | 121 | 108 |
| **Aged Asphalt (Thin Film Oven Test)** | | | | |
| Mass change, % | -.1799 | -.0190 | -.5483 | -1.2305 |
| Viscosity @ 60°C, poise | 3,253 | 1,781 | 9,708 | 3,098 |
| Viscosity @ 135°C, cSt | 304 | 216 | 930 | 533 |
| Viscosity ratio (60°C) | 1.75 | 1.69 | 2.98 | 3.11 |

Figure 4.1. The asphalt cement contents used with aggregates RB and RL are given in Table 4.3.

**Mixing.** Both the aggregate and asphalt to be mixed were preheated to a specified mixing temperature depending on asphalt type. The mixing temperature for each asphalt was selected from a Bitumen Test Data Chart (BTDC) and is presented with the compaction temperature in Table 4.4. The mixing temperature corresponds to a viscosity of 170±20 cSt (approximately 160 poise ± 20 poise). After mixing, the loose mixture was cured in an oven at 60°C (140°F) for 15 hours. The curing time allows the asphalt cement to be absorbed into the aggregate before compaction.

**Compaction.** Two different sizes of beam samples were prepared using a kneading compactor. Beam samples of 7.6 cm × 7.6 cm × 40.6 cm were prepared for 3.8 cm × 3.8 cm × 20.3 cm specimens, and 11.4 cm × 11.4 cm × 40.6 cm beam samples were prepared for 5.0 cm × 5.0 cm × 25.0 cm specimens. The compaction tools, compaction equipment, and mixture were preheated to the compaction temperature. The compaction temperature for each asphalt type appears in Table 4.4. The compaction temperature corresponds to a viscosity of 280 cSt ± 30 cSt (approximately 265 poise ± 30 poise).

Beam samples were compacted with two lifts and each lift was compacted at three different levels of pressure with several passes. Compaction pressure and number of passes varied depending on target air void content, beam size, asphalt type, and aggregate type. The compaction schedules are presented in Tables 4.5 through 4.7.

**Sawing.** After the beam sample cooled and the mold was removed, the sample was sawed into four test specimens (3.8 cm × 3.8 cm × 20.3 cm or 5.0 cm × 5.0 cm × 25.0 cm). The sawed specimens were washed with water and then air dried. After drying, the specimens were labeled and their bulk specific gravity was measured. The measurement of bulk specific gravity was performed according to the method developed by the Chevron Research Company (American Society of Testing Materials [ASTM] D 1188 with parafilm).

**Aging.** The specimens were aged in a forced-draft oven for 4 days at 110°C or 135°C. Specimens with asphalt AAK-2 were aged at 110°C and 135°C. Specimens with asphalt AAG-1 were aged at 135°C. After aging, the specimens were stored in a cold room at 5°C prior to testing.

## 4.4 Test Procedure

The test specimen was aligned using an alignment stand and glued to end platens with the epoxy compound DC-80 (Thermoset Plastics, Inc.). The specimen was left in the alignment stand for 24 hours to ensure curing of the epoxy.

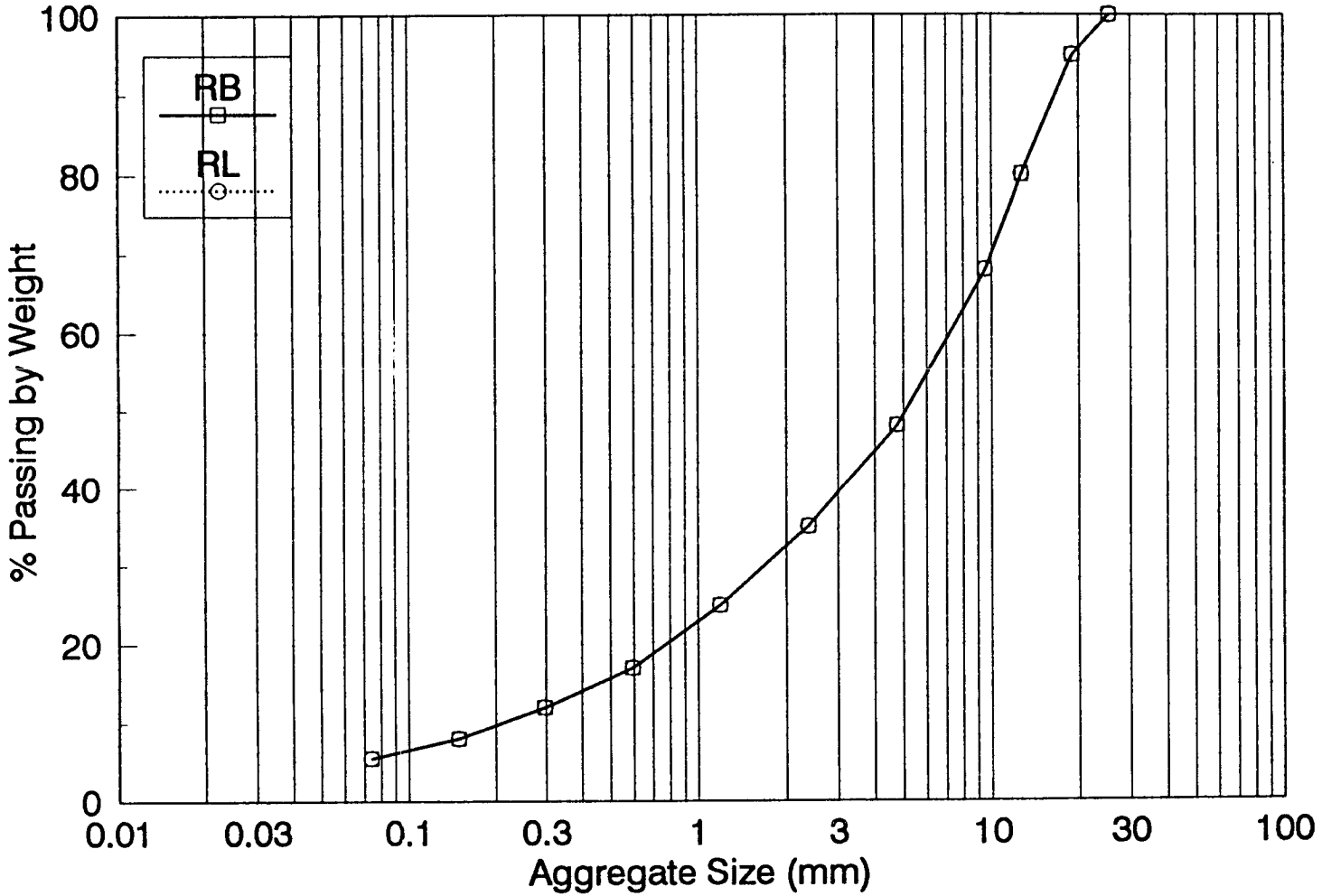


**Figure 4.1. Aggregate gradations**

**Table 4.3. Asphalt cement contents used with RB and RL aggregates**

| Aggregate Type | Asphalt Type | Asphalt-content %* |
|---|---|---|
| RB | AAK-1 and AAK-2 | 5.1 |
| | AAG-1 and AAG-2 | 4.9 |
| RL | AAK-1 and AAK-2 | 4.3 |
| | AAG-1 and AAG-2 | 4.1 |

*Percent by dry weight of aggregate

**Table 4.4. Mixing and compaction temperatures**

| Asphalt Type | Mixing Temperature (°C) | Compaction Temperature (°C) |
|---|---|---|
| AAG-1 | 142 ± 2 | 133 ± 2 |
| AAG-2 | 135 ± 2 | 126 ± 2 |
| AAK-1 | 160 ± 2 | 148 ± 2 |
| AAK-2 | 148 ± 2 | 138 ± 2 |

**Table 4.5. Compaction schedule for 7.6 cm × 7.6 cm × 40.6 cm beam (RB)**

| Asphalt | Target Air Voids Content (%) | Leveling Load (N) | Lift No. | No. of Passes | | |
|---|---|---|---|---|---|---|
| AAG-1 | 8 (High) | 35,600 | 1 | 3 | 4 | 5 |
| | | | 2 | 3 | 5 | 6 |
| | | | Press. (kPa) | 517 | 1,035 | 2,415 |
| | 4 (Low) | 267,000 | 1 | 2 | 14 | 18 |
| | | | 2 | 2 | 16 | 24 |
| | | | Press. (kPa) | 517 | 1,035 | 2,415 |
| AAG-2 | 8 (High) | 35,600 | 1 | 2 | 6 | 8 |
| | | | 2 | 2 | 8 | 10 |
| | | | Press. (kPa) | 517 | 1,035 | 2,415 |
| | 4 (Low) | 267,000 | 1 | 3 | 12 | 16 |
| | | | 2 | 3 | 14 | 18 |
| | | | Press. (kPa) | 517 | 1,035 | 2,415 |
| AAK-1 | 8 (High) | 35,600 | 1 | 2 | 3 | 3 |
| | | | 2 | 2 | 4 | 5 |
| | | | Press. (kPa) | 517 | 1,035 | 1,887 |
| | 4 (Low) | 311,500 | 1 | 3 | 14 | 18 |
| | | | 2 | 3 | 16 | 20 |
| | | | Press. (kPa) | 517 | 1,035 | 1,725 |
| AAK-2 | 8 (High) | 35,600 | 1 | 2 | 3 | 3 |
| | | | 2 | 2 | 4 | 5 |
| | | | Press. (kPa) | 517 | 1,035 | 1,725 |
| | 4 (Low) | 222,500 | 1 | 2 | 13 | 17 |
| | | | 2 | 2 | 15 | 19 |
| | | | Press. (kPa) | 517 | 1,035 | 2,415 |

1 lb = 4.45 N
1 psi = 6.9 kPa

**Table 4.6. Compaction schedule for 11.4 cm × 11.4 cm × 40.6 cm beam (RB)**

| Asphalt | Target Air Voids Content (%) | Leveling Load (N) | Lift No. | No. of Passes | | |
|---|---|---|---|---|---|---|
| AAG-1 | 8 (High) | 12,000 | 1 | 2 | 3 | 4 |
| | | | Press. (psi) | 517 | 759 | 1,035 |
| | | | 2 | 2 | 6 | 8 |
| | | | Press. (psi) | 517 | 1,035 | 1,898 |
| | 4 (Low) | 60,000 | 1 | 2 | 6 | 7 |
| | | | Press. (psi) | 517 | 863 | 1,553 |
| | | | 2 | 2 | 10 | 14 |
| | | | Press. (psi) | 517 | 1,553 | 2,415 |
| AAG-2 | 8 (High) | 8,000 | 1 | 2 | 2 | 2 |
| | | | Press. (psi) | 517 | 690 | 863 |
| | | | 2 | 2 | 3 | 4 |
| | | | Press. (psi) | 517 | 863 | 1,898 |
| | 4 (Low) | 60,000 | 1 | 2 | 3 | 5 |
| | | | Press. (psi) | 517 | 863 | 1,553 |
| | | | 2 | 2 | 10 | 12 |
| | | | Press. (psi) | 517 | 1,553 | 2,415 |
| AAK-1 | 8 (High) | 10,000 | 1 | 2 | 3 | 3 |
| | | | Press. (psi) | 517 | 1,035 | 1,553 |
| | | | 2 | 2 | 8 | 12 |
| | | | Press. (psi) | 517 | 1,553 | 2,415 |
| | 4 (Low) | 70,000 | 1 | 2 | 6 | 8 |
| | | | Press (psi) | 517 | 1,035 | 1,553 |
| | | | 2 | 2 | 12 | 20 |
| | | | Press. (psi) | 517 | 1,553 | 2,415 |
| AAK-2 | 8 (High) | 5,000 | 1 | 2 | 2 | 2 |
| | | | Press. (psi) | 345 | 517 | 690 |
| | | | 2 | 2 | 3 | 3 |
| | | | Press. (psi) | 517 | 932 | 1,380 |
| | 4 (Low) | 50,000 | 1 | 2 | 3 | 3 |
| | | | Press. (psi) | 517 | 1,035 | 1,725 |
| | | | 2 | 2 | 8 | 12 |
| | | | Press. (psi) | 517 | 1,553 | 2,415 |

Table 4.7. Compaction schedule for 11.4 cm × 11.4 cm × 40.6 cm beam (RL)

| Asphalt | Target Air Voids Content (%) | Leveling Load (N) | Lift No. | No. of Passes | | |
|---|---|---|---|---|---|---|
| AAG-1 | 8 (High) | 10,000 | 1 | 2 | 3 | 5 |
| | | | Press. (psi) | 517 | 690 | 1,035 |
| | | | 2 | 2 | 6 | 8 |
| | | | Press. (psi) | 517 | 863 | 1,553 |
| | 4 (Low) | 75,000 | 1 | 2 | 10 | 12 |
| | | | Press. (psi) | 517 | 690 | 1,035 |
| | | | 2 | 2 | 14 | 20 |
| | | | Press. (psi) | 517 | 1,035 | 2,415 |
| AAG-2 | 8 (High) | 10,000 | 1 | 2 | 4 | 6 |
| | | | Press. (psi) | 517 | 690 | 1,035 |
| | | | 2 | 4 | 6 | 10 |
| | | | Press. (psi) | 690 | 863 | 1,553 |
| | 4 (Low) | 70,000 | 1 | 4 | 10 | 14 |
| | | | Press. (psi) | 517 | 690 | 1,035 |
| | | | 2 | 4 | 14 | 22 |
| | | | Press. (psi) | 517 | 1,035 | 2,415 |
| AAK-1 | 8 (High) | 10,000 | 1 | 2 | 3 | 5 |
| | | | Press. (psi) | 517 | 690 | 1,035 |
| | | | 2 | 2 | 6 | 8 |
| | | | Press. (psi) | 517 | 863 | 1,553 |
| | 4 (Low) | 70,000 | 1 | 4 | 10 | 14 |
| | | | Press (psi) | 517 | 690 | 1,035 |
| | | | 2 | 4 | 14 | 22 |
| | | | Press. (psi) | 517 | 1,035 | 2,415 |
| AAK-2 | 8 (High) | 11,000 | 1 | 2 | 5 | 9 |
| | | | Press. (psi) | 517 | 690 | 1,035 |
| | | | 2 | 2 | 7 | 9 |
| | | | Press. (psi) | 517 | 863 | 1,380 |
| | 4 (Low) | 50,000 | 1 | 2 | 8 | 12 |
| | | | Press. (psi) | 517 | 690 | 1,035 |
| | | | 2 | 2 | 14 | 20 |
| | | | Press. (psi) | 517 | 1,035 | 2,415 |

After the epoxy cured, the specimen end platens was placed in the environmental cabinet (Figure 3.1). Three thermistors were secured to the specimen using modeling clay to measure the surface temperature of the specimen. A resistance temperature device (RTD) was placed in the cabinet to provide feedback to the temperature control system. The LVDTs and the invar rods were inserted into the bottom and the top clamps, respectively.

The test specimen with end platens was cooled to a temperature of 5°C for 1 hour to establish thermal equilibrium prior to testing. Finally, the computer was engaged to initiate position correction and collect all the required data. TSRST was performed at a specified cooling rate until fracture. The protocol for TSRST is described in SHRP test method M-010 (Harrigan et al. 1994).

Typical TSRST results are shown in Figure 4.2. The thermally induced stress gradually increases as temperature is lowered until the specimen breaks. At the break point, the stress reaches its highest value, which is referred to as the fracture strength. The slope of the stress-temperature curve, dS/dT, increases gradually until the temperature reaches a certain value and becomes constant, and the stress-temperature curve is linear. The slope tends to decrease again when the specimen is close to the break point. This decrease may be due to the formation of microcracks.

The temperature at which the curve is divided into two parts, relaxation and nonrelaxation, is termed the transition temperature. As the temperature approaches the transition temperature, the asphalt cement becomes stiffer and the thermally induced stresses do not relax beyond this temperature. The transition temperature and dS/dT may play an important role in characterizing the rheological behavior of asphalt concrete mixtures at cold temperatures.

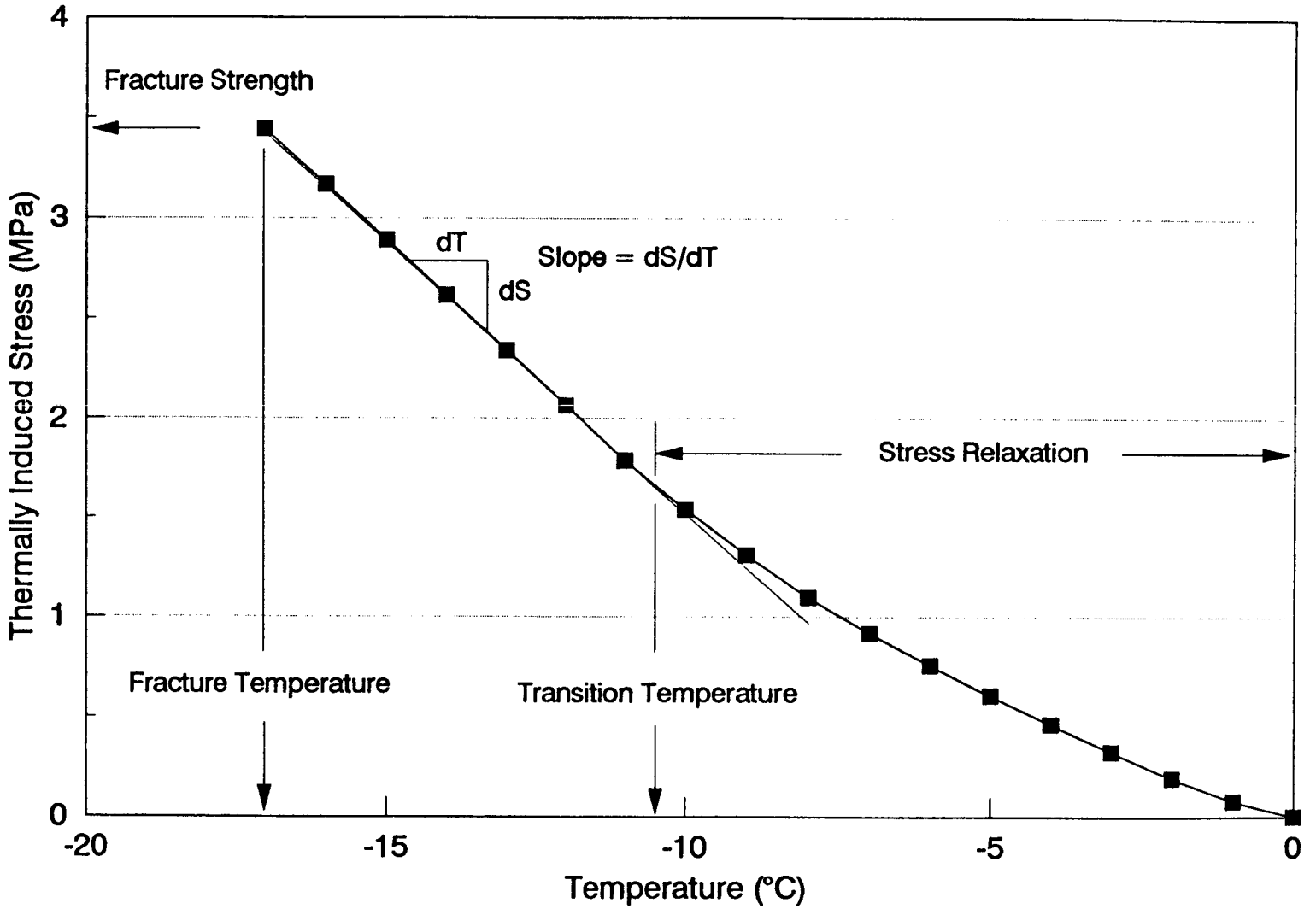


**Figure 4.2 Typical results from TSRST**

# 5

# Test Results

The thermal stress restrained specimen test (TSRST) device was used to evaluate asphalt concrete mixes under a range of conditions. The five experiment designs used four asphalt cements (AAK-1, AAK-2, AAG-1, and AAG-2) and two aggregates (RB and RL) at three levels of air voids content (4 percent, 6 percent, and 8 percent). The rates of cooling employed were 1°, 2°, 5°, and 10°C/hr. Mean values and standard deviations of the test results are presented in this section; the results appear in their entirety in Appendix A.

## 5.1 Test Results with 3.8 cm × 3.8 cm × 20.3 cm Specimens (Designation: 20.3/3.8 RB)

Specimens were made with four asphalt cements and one aggregate (RB) at two levels of air void content (4 percent and 8 percent ± 1 percent). Tests were performed at a monotonic cooling rate of 10°C/hr. The experiment design included a total of 32 (4 × 2 × 4) tests, but the actual data set consists of 31 test results.

Typical thermally induced stress curves observed for two asphalts (AAG-1 and AAK-2) showing extreme fracture temperatures are compared in Figure 5.1. AAG-1H and AAK-2H indicate higher air void contents, and AAG-1L and AAK-2L indicate lower air voids content. Thermally induced stresses develop more rapidly, and stress relaxation ceases at warmer temperatures in specimens with stiffer asphalt. Thus, stresses in specimens with stiffer asphalt will exceed the strengths of specimens at warmer temperatures and result in fracture. In addition, as shown in Figure 5.1, the slope (dS/dT) of specimens with lower air voids contents tends to be greater than that of specimens with higher air voids contents. Specimens with lower air voids contents fracture at higher stress levels.

Summary statistics of test results are presented for the specific aggregate type in Table 5.1. Fracture and transition temperature tend to be slightly warmer for specimens with lower air voids contents. Fracture strength and slope are greater for specimens with lower air voids contents.

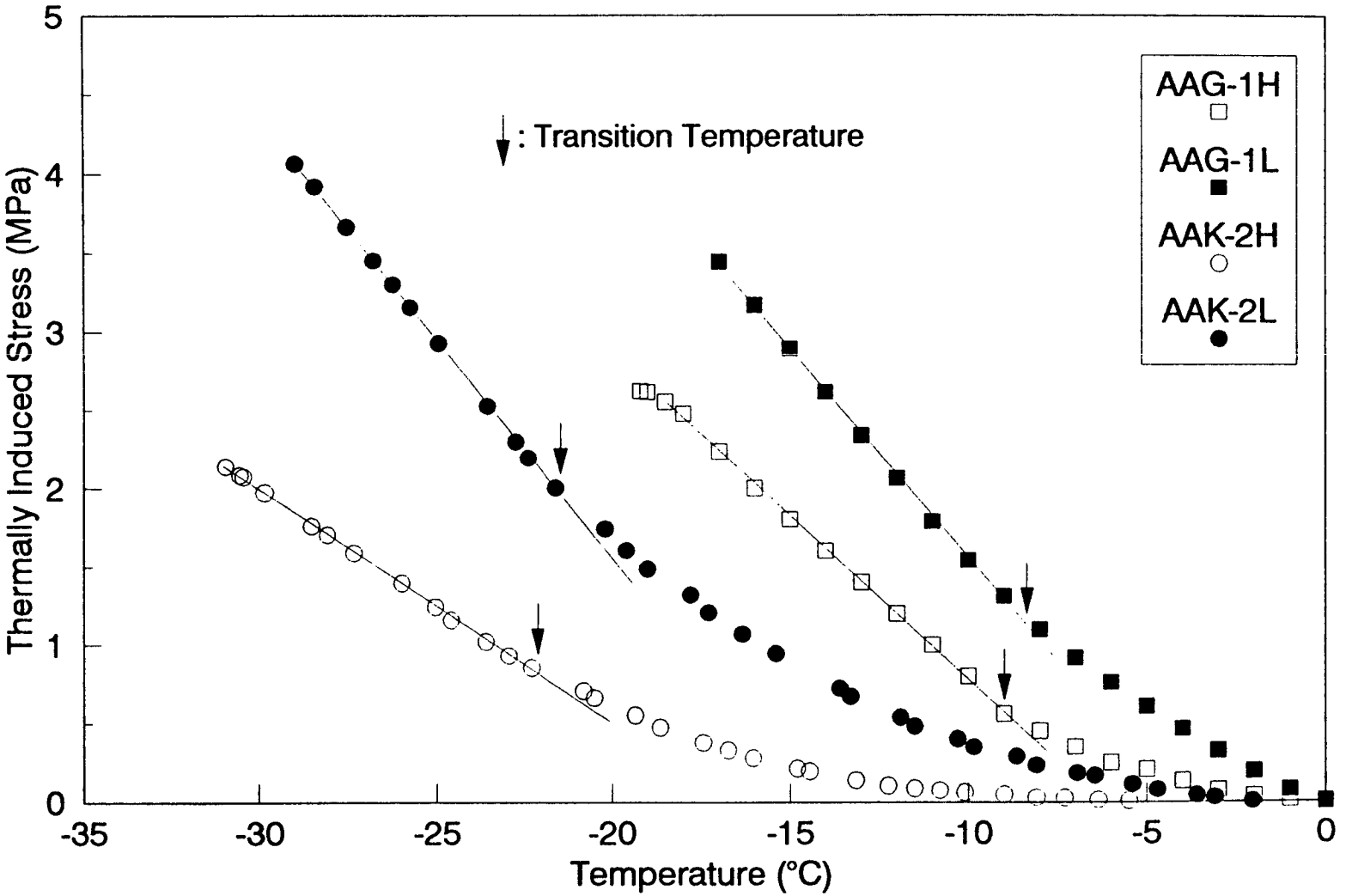


**Figure 5.1. Typical stress-temperature curves (20.3/3.8 RB)**

**Table 5.1. Summary statistics of test results (3.8 cm × 3.8 cm × 20.3 cm specimens with RB)**

| Asphalt | Target Air Void Content (%) | Air Void Content (%) | | Fracture Temperature (°C) | | Fracture Strength (MPa) | | Slope (dS/dT) (MPa/°C) | | Transition Temperature (°C) | |
|---|---|---|---|---|---|---|---|---|---|---|---|
| | | Mean | Std. Dev. | Mean | Std. Dev. | Mean | Std. Dev. | Mean | Std. Dev. | Mean | Std. Dev. |
| AAG-1 | 8 | 8.2 | 0.56 | -17.8 | 0.15 | 2.472 | 0.713 | 0.218 | 0.014 | -10.0 | 0.55 |
| | 4 | 4.3 | 0.74 | -16.6 | 1.23 | 3.146 | 0.193 | 0.264 | 0.022 | -9.1 | 0.10 |
| AAG-2 | 8 | 8.4 | 1.34 | -18.8 | 0.89 | 2.481 | 0.267 | 0.226 | 0.013 | -12.1 | 0.62 |
| | 4 | 5.2 | 0.76 | -17.6 | 0.43 | 3.012 | 0.406 | 0.274 | 0.025 | -11.1 | 0.10 |
| AAK-1 | 8 | 7.9 | 1.29 | -25.2 | 1.72 | 2.270 | 0.400 | 0.151 | 0.033 | -16.0 | 0.69 |
| | 4 | 3.5 | 0.66 | -23.7 | 0.95 | 3.021 | 0.465 | 0.190 | 0.020 | -13.8 | 0.37 |
| AAK-2 | 8 | 7.6 | 0.86 | -30.9 | 0.29 | 2.389 | 0.167 | 0.145 | 0.013 | -21.4 | 0.67 |
| | 4 | 3.9 | 0.31 | -29.7 | 0.61 | 4.039 | 0.102 | 0.269 | 0.012 | -20.8 | 0.61 |

## 5.2 Test Results with 5.0 cm × 5.0 cm × 25.0 cm Specimens (Designation: 25/5 RB and 25/5 RL)

Tests were performed to determine the effect of aggregate type on the low-temperature cracking characteristics of asphalt concrete mixtures. A monotonic cooling rate of 10°C/hr was used. The experiment design consisted of 64 (4 × 2 × 2 × 4) tests, but only two replicates were obtained for specimens with RL aggregate because of compaction difficulties. The actual data set includes 41 test results.

Typical stress-temperature curves observed for specimens with two asphalts (AAG-1 and AAK-2) with different aggregates are compared in Figure 5.2. Specimens with RL aggregate tend to fracture at warmer temperatures and lower stress levels. This situation may be due to the smooth surface texture and round shape of RL aggregate. The smooth surface and round shape provide less bonding and interlock forces between the asphalt cement and aggregate, consequently, mixtures with RL aggregate will have lower strength and be more susceptible to fracture.

Summary statistics of test results with RB and RL aggregates are presented for a specific aggregate type in Tables 5.2 and 5.3, respectively. No significant difference in fracture and transition temperature (depending on target air voids content) can be observed. Fracture strength and slope (dS/dT) are greater for specimens with lower air voids content.

## 5.3 Test Results with Stress Relaxation

Stress relaxation tests in TSRST were performed to evaluate the effect of stress relaxation on the low-temperature cracking characteristics of asphalt concrete mixtures.

Specimens (5.0 × 5.0 × 25.0 cm) were made with four asphalt cements and one aggregate (RB) at two levels of air voids content (4 percent and 8 percent). Stresses were relaxed for 6 hours at -22°C for asphalts AAK-1 and AAK-2 and at -14°C for asphalts AAG-1 and AAG-2 while the specimen was cooled at 10°C/hr.

Figure 5.3 shows typical cooling schedules used in the stress relaxation test. Typical thermally induced stress curves observed in the tests are shown in Figure 5.4. Initially, stresses in the specimen increase as temperature is lowered. When the temperature is held constant, stresses are relaxed. After the relaxation period, stresses increase again upon cooling.

Summary statistics of results from the stress relaxation test are presented in Table 5.4. No significant difference in fracture temperature was observed as a function of target air voids content. Fracture strength is greater for lower air voids content.

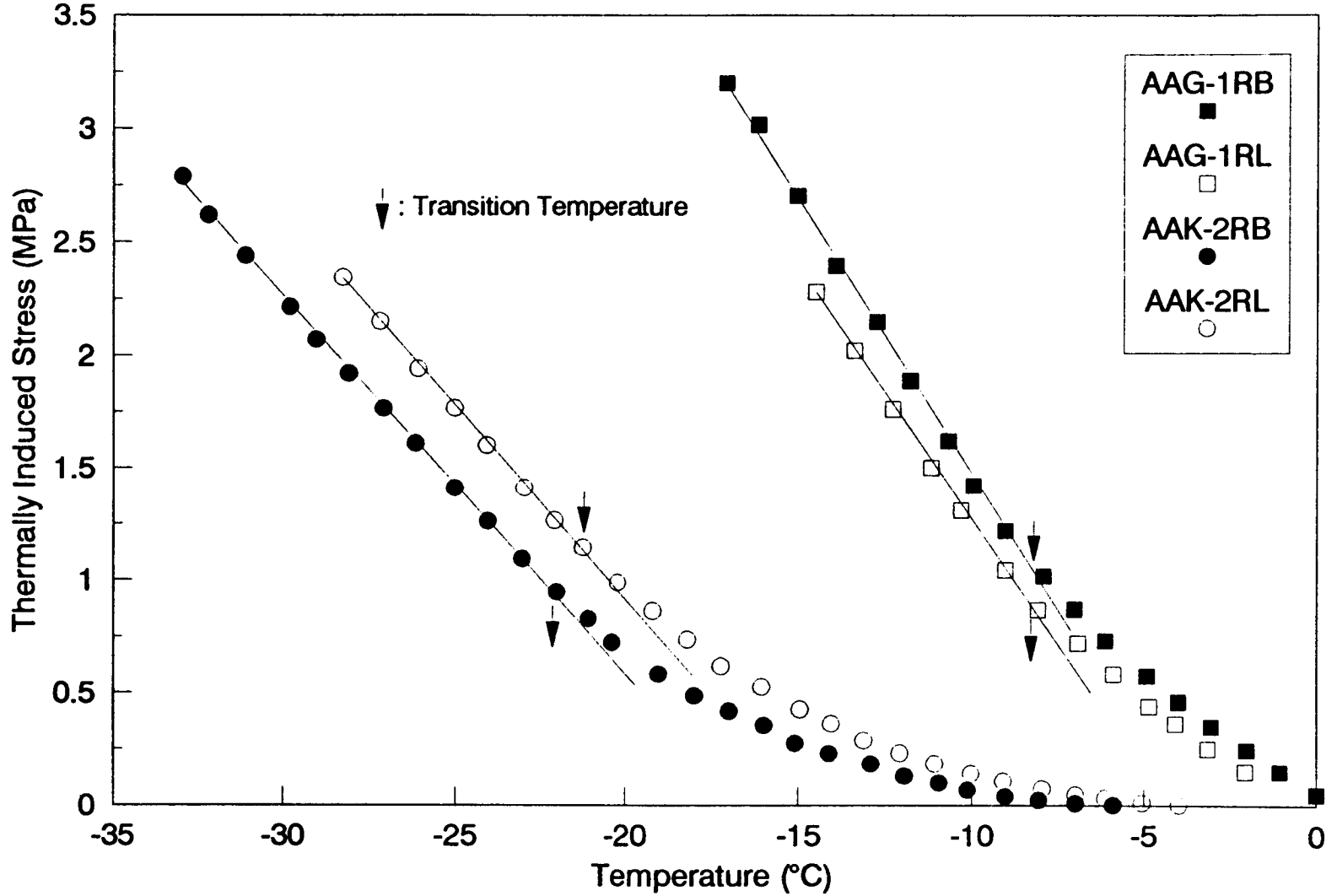


**Figure 5.2. Typical stress-temperature curves (25/5 RB and RL)**

**Table 5.2. Summary statistics of test results (5.0 cm × 5.0 cm × 25.0 cm specimens with RB)**

| Asphalt | Target Air Void Content (%) | Air Void Content (%) | | Fracture Temperature (°C) | | Fracture Strength (MPa) | | Slope (dS/dT) (MPa/°C) | | Transition Temperature (°C) | |
|---|---|---|---|---|---|---|---|---|---|---|---|
| | | Mean | Std. Dev. | Mean | Std. Dev. | Mean | Std. Dev. | Mean | Std. Dev. | Mean | Std. Dev. |
| AAG-1 | 8 | 7.2 | 0.35 | -18.4 | 0.31 | 2.629 | 0.454 | 0.235 | 0.057 | -11.9 | 1.69 |
| | 4 | 4.3 | 0.29 | -17.3 | 0.59 | 3.257 | 0.369 | 0.274 | 0.028 | -11.5 | 0.69 |
| AAG-2 | 8 | 7.2 | 0.38 | -19.4 | 1.56 | 2.146 | 0.042 | 0.194 | 0.023 | -12.9 | 0.10 |
| | 4 | 3.5 | 0.17 | -18.6 | 1.90 | 2.983 | 0.761 | 0.263 | 0.044 | -13.1 | 1.37 |
| AAK-1 | 8 | 7.5 | 0.30 | -26.2 | 0.42 | 2.751 | 0.152 | 0.201 | 0.012 | -19.4 | 0.25 |
| | 4 | 3.7 | 0.35 | -26.4 | 0.84 | 3.743 | 0.310 | 0.268 | 0.020 | -19.6 | 1.01 |
| AAK-2 | 8 | 7.6 | 0.25 | -32.6 | 0.76 | 2.289 | 0.470 | 0.157 | 0.022 | -23.0 | 0.79 |
| | 4 | 3.8 | 0.21 | -31.6 | 0.28 | 3.802 | 0.244 | 0.246 | 0.037 | -22.4 | 0.14 |

**Table 5.3. Summary statistics of test results (5.0 cm × 5.0 cm × 25.0 cm specimens with RL)**

| Asphalt | Target Air Void Content (%) | Air Void Content (%) | | Fracture Temperature (°C) | | Fracture Strength (MPa) | | Slope (dS/dT) (MPa/°C) | | Transition Temperature (°C) | |
|---|---|---|---|---|---|---|---|---|---|---|---|
| | | Mean | Std. Dev. | Mean | Std. Dev. | Mean | Std. Dev. | Mean | Std. Dev. | Mean | Std. Dev. |
| AAG-1 | 8 | 9.5 | 0.35 | -15.3 | 0.14 | 1.483 | 0.009 | 0.154 | 0.006 | -9.7 | 0.14 |
| | 4 | 5.4 | 0.21 | -14.2 | 0.42 | 2.050 | 0.322 | 0.234 | 0.013 | -9.8 | 0.85 |
| AAG-2 | 8 | 7.6 | 0.28 | -17.8 | 0.85 | 1.622 | 0.204 | 0.175 | 0.030 | -13.2 | 0.35 |
| | 4 | 6.6 | 0.14 | -17.3 | 0.07 | 1.791 | 0.239 | 0.185 | 0.026 | -12.1 | 0.14 |
| AAK-1 | 8 | 7.3 | 0.07 | -23.9 | 0.71 | 2.250 | 0.039 | 0.168 | 0.003 | -15.4 | 0.14 |
| | 4 | 6.0 | 0.64 | -24.3 | 0.21 | 2.291 | 0.127 | 0.176 | 0.007 | -15.6 | 0.78 |
| AAK-2 | 8 | 6.9 | 0.07 | -28.9 | 0.78 | 2.556 | 0.297 | 0.217 | 0.023 | -22.7 | 0.56 |
| | 4 | 4.1 | 0.21 | -28.7 | 0.35 | 2.985 | 0.561 | 0.230 | 0.004 | -21.8 | 1.84 |

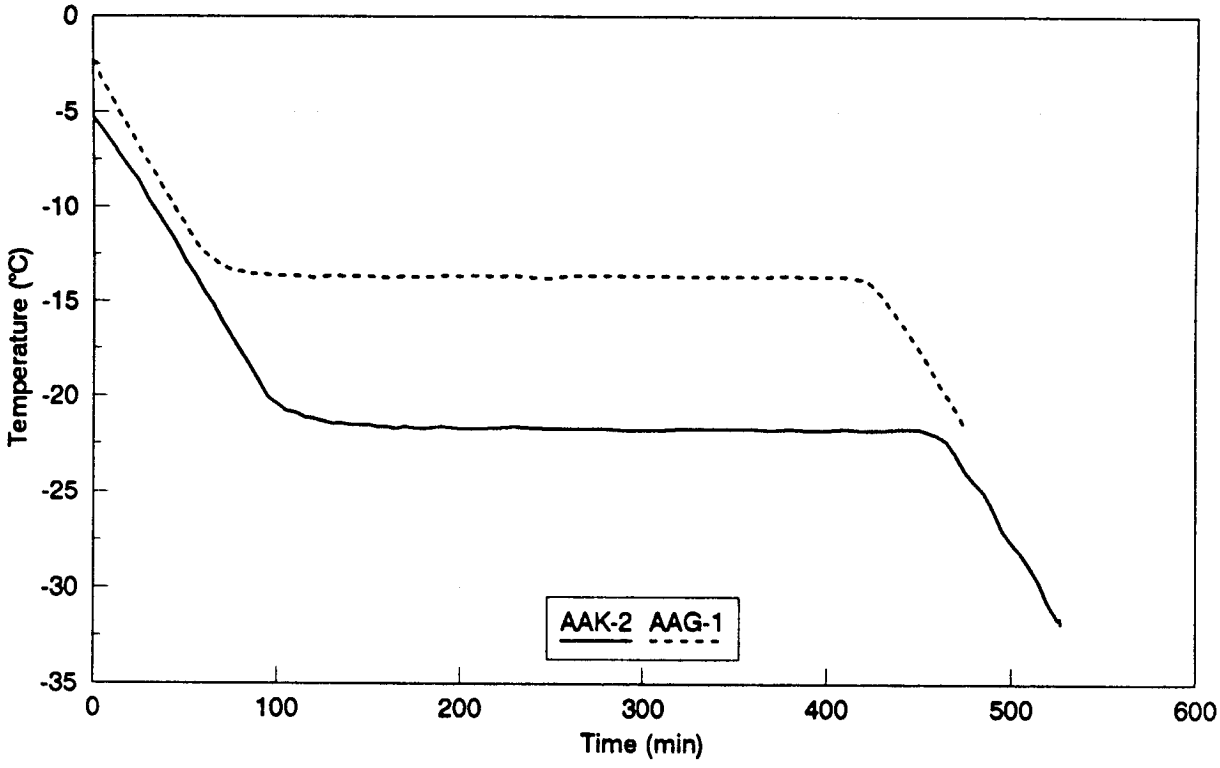


**Figure 5.3. Typical cooling schedules for stress relaxation**

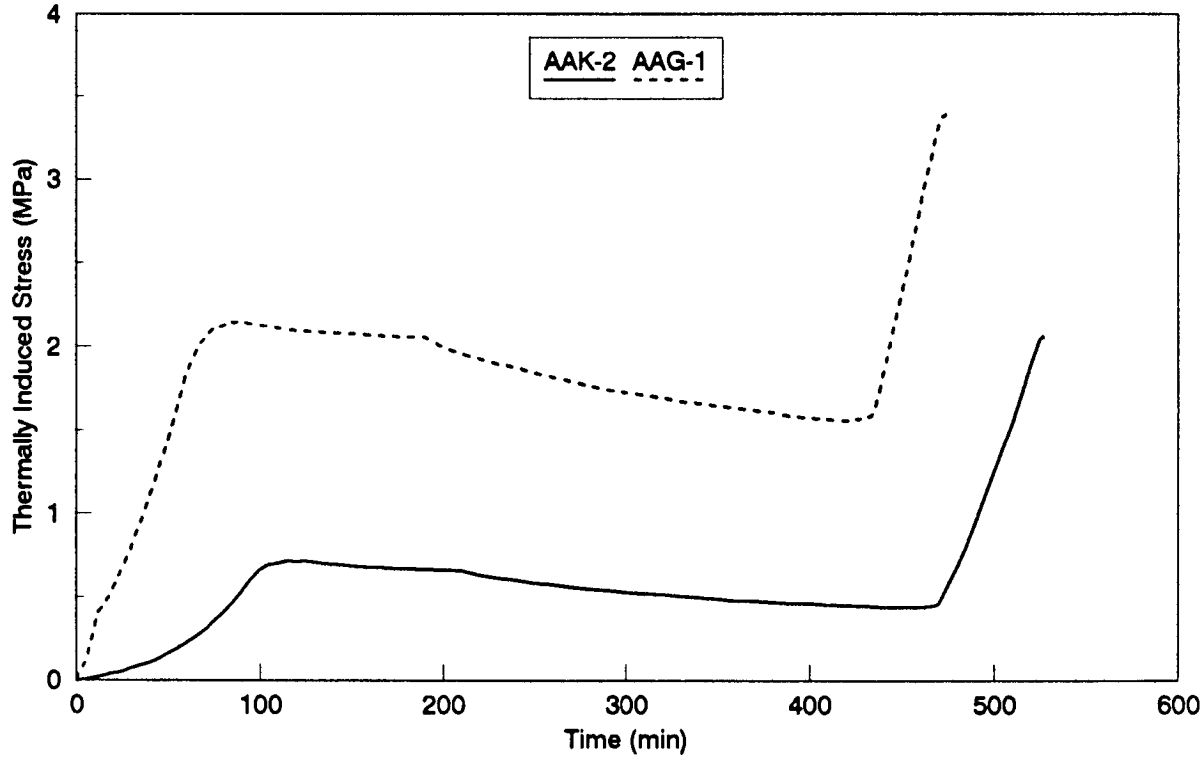


**Figure 5.4. Stress variation with time in relaxation test**

**Table 5.4. Summary statistics of stress relaxation test results (RB aggregate)**

| Asphalt | Target Air Void Content (%) | Air Void Content (%) | | Fracture Temperature (°C) | | Fracture Strength (MPa) | |
|---|---|---|---|---|---|---|---|
| | | Mean | Std. Dev. | Mean | Std. Dev. | Mean | Std. Dev. |
| AAG-1 | 8 | 8.4 | 0.00 | -19.5 | 0.64 | 1.477 | 0.283 |
| | 4 | 4.4 | 0.78 | -19.7 | 1.98 | 3.185 | 0.298 |
| AAG-2 | 8 | 8.1 | 1.13 | -21.4 | 1.41 | 2.122 | 0.385 |
| | 4 | 4.1 | 0.99 | -20.4 | 0.14 | 3.077 | 0.293 |
| AAK-1 | 8 | 8.5 | 0.35 | -27.2 | 0.49 | 1.877 | 0.048 |
| | 4 | 3.9 | 0.85 | -27.1 | 0.56 | 3.226 | 0.385 |
| AAK-2 | 8 | 7.2 | 0.21 | -30.9 | 1.25 | 2.022 | 0.049 |
| | 4 | 3.1 | 0.0 | -30.7 | 0.28 | 2.843 | 0.615 |

## 5.4 Test Results with Various Cooling Rates

Specimens (5.0 cm × 5.0 cm × 25.0 cm) were made with two asphalt cements (AAG-1 and AAK-2) and one aggregate (RB). The air voids content was fixed at 6 percent. Tests were performed at monotonic cooling rates of 1°, 2°, 5°, and 10°C/hr to determine the effect of cooling rate on the low-temperature cracking of mixtures.

Typical thermally induced stress curves for cooling rates of 1°, 2°, 5°, and 10°C/hr are compared in Figure 5.5. Thermally induced stresses tend to accumulate faster at a faster cooling rate. Specimens tend to fracture at a higher stress level with a faster cooling rate.

Summary statistics of test results with various cooling rates are presented in Table 5.5. Fracture and transition temperatures tend to be lower for slower cooling rates. Specimens with AAG-1 asphalt exhibit no significant difference in fracture strength and slope (dS/dT) regardless of the cooling rate. In the case of specimens with AAK-2 asphalt, fracture strength and slope are greater at faster cooling rates.

## 5.5 Test Results with Aged Specimens

To study the effect of aging, 5.0 cm × 5.0 cm × 25.0 cm specimens were fabricated with two asphalt cements (AAG-1 and AAK-2) and one aggregate (RB). Specimens were aged in a forced-draft oven at two different temperatures (110° and 135°C) for 4 days. A significant number of microcracks were observed at the surface of the aged specimens. Tests were performed at a monotonic cooling rate of 10°C/hr.

Thermally induced stress curves for aged specimens are compared with those for unaged specimens in Figure 5.6. As a mixture is aged, the asphalt cement becomes stiffer, and stress relaxation is substantially reduced at warmer temperatures. Therefore, the aged mixture will be more susceptible to cracking and fracture at warmer temperatures.

Summary statistics of test results with aged specimens are presented in Table 5.6. The results indicate that asphalt concrete mixtures are more susceptible to low-temperature cracking as the degree of aging increases. Fracture and transition temperatures for specimens with asphalt AAK-2 aged at 135°C are significantly warmer compared with specimens aged at 110°C. Fracture strength is lower for specimens aged at 135°C.

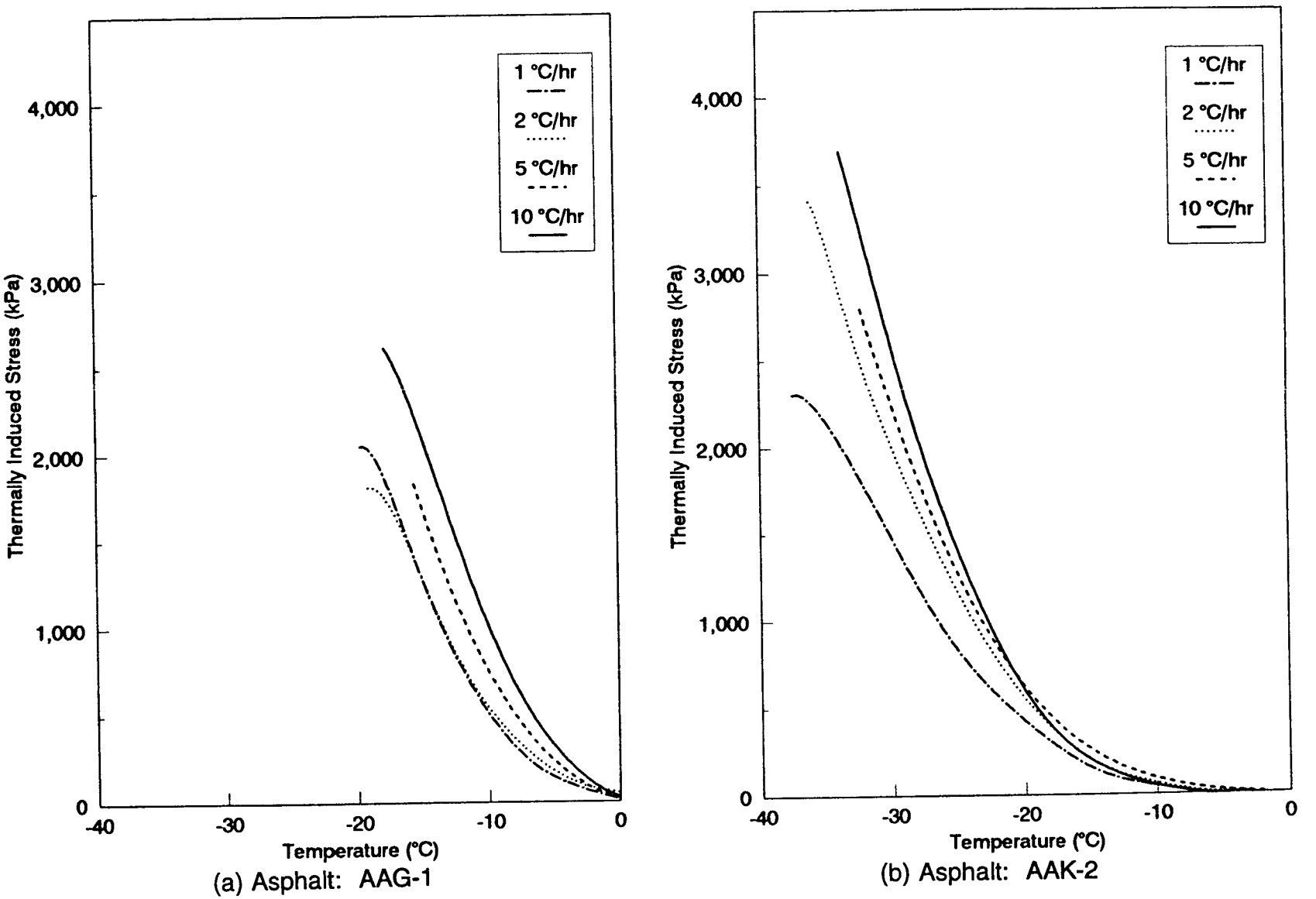


**Figure 5.5. Thermally induced stress for various cooling rates**

## Table 5.5. Summary statistics of test results with various cooling rates

| Asphalt | Cooling Rate (°C/hr) | Target Air Void Content (%) | Air Void Content (%) | | Fracture Temperature (°C) | | Fracture Strength (MPa) | | Slope (dS/dT) (MPa/°C) | | Transition Temperature (°C) | |
|---|---|---|---|---|---|---|---|---|---|---|---|---|
| | | | Mean | Std. Dev. | Mean | Std. Dev. | Mean | Std. Dev. | Mean | Std. Dev. | Mean | Std. Dev. |
| AAG-1 | 1 | 6 | 7.0 | 0.42 | -19.7 | 0.00 | 2.218 | 0.249 | 0.221 | 0.028 | -14.7 | 1.56 |
| | 2 | 6 | 6.9 | 0.21 | -18.9 | 0.28 | 2.187 | 0.390 | 0.220 | 0.066 | -13.9 | 1.56 |
| | 5 | 6 | 6.8 | 0.14 | -15.6 | 0.00 | 2.036 | 0.274 | 0.226 | 0.043 | -12.1 | 0.14 |
| AAK-2 | 1 | 6 | 6.2 | 0.42 | -36.6 | 0.64 | 2.253 | 0.288 | 0.162 | 0.012 | -27.7 | 0.64 |
| | 2 | 6 | 5.5 | 0.00 | -34.5 | 0.49 | 2.491 | 0.185 | 0.195 | 0.002 | -27.2 | 0.64 |
| | 5 | 6 | 5.4 | 0.42 | -31.4 | 0.92 | 2.867 | 0.024 | 0.220 | 0.038 | -25.5 | 0.71 |

## Table 5.6. Summary statistics of test results with aged specimens

| Asphalt | Aging Temp. (°C) | Target Air Void Content (%) | Air Void Content (%) | | Fracture Temperature (°C) | | Fracture Strength (MPa) | | Slope (dS/dT) (MPa/°C) | | Transition Temperature (°C) | |
|---|---|---|---|---|---|---|---|---|---|---|---|---|
| | | | Mean | Std. Dev. | Mean | Std. Dev. | Mean | Std. Dev. | Mean | Std. Dev. | Mean | Std. Dev. |
| AAG-1 | 110 | 4 | 6.0 | 0.78 | -13.6 | 1.13 | 2.560 | 0.312 | 0.213 | 0.021 | -7.7 | 0.19 |
| | 135 | 8 | 9.5 | 1.34 | -14.0 | 0.82 | 1.906 | 0.273 | 0.157 | 0.016 | -7.7 | 0.34 |
| AAK-2 | 110 | 8 | 7.70 | 0.74 | -25.2 | 0.85 | 2.158 | 0.523 | 0.117 | 0.036 | -17.3 | 2.03 |
| | 135 | 4 | 4.73 | 0.47 | -20.7 | 0.55 | 1.714 | 0.482 | 0.101 | 0.020 | -7.4 | 1.18 |

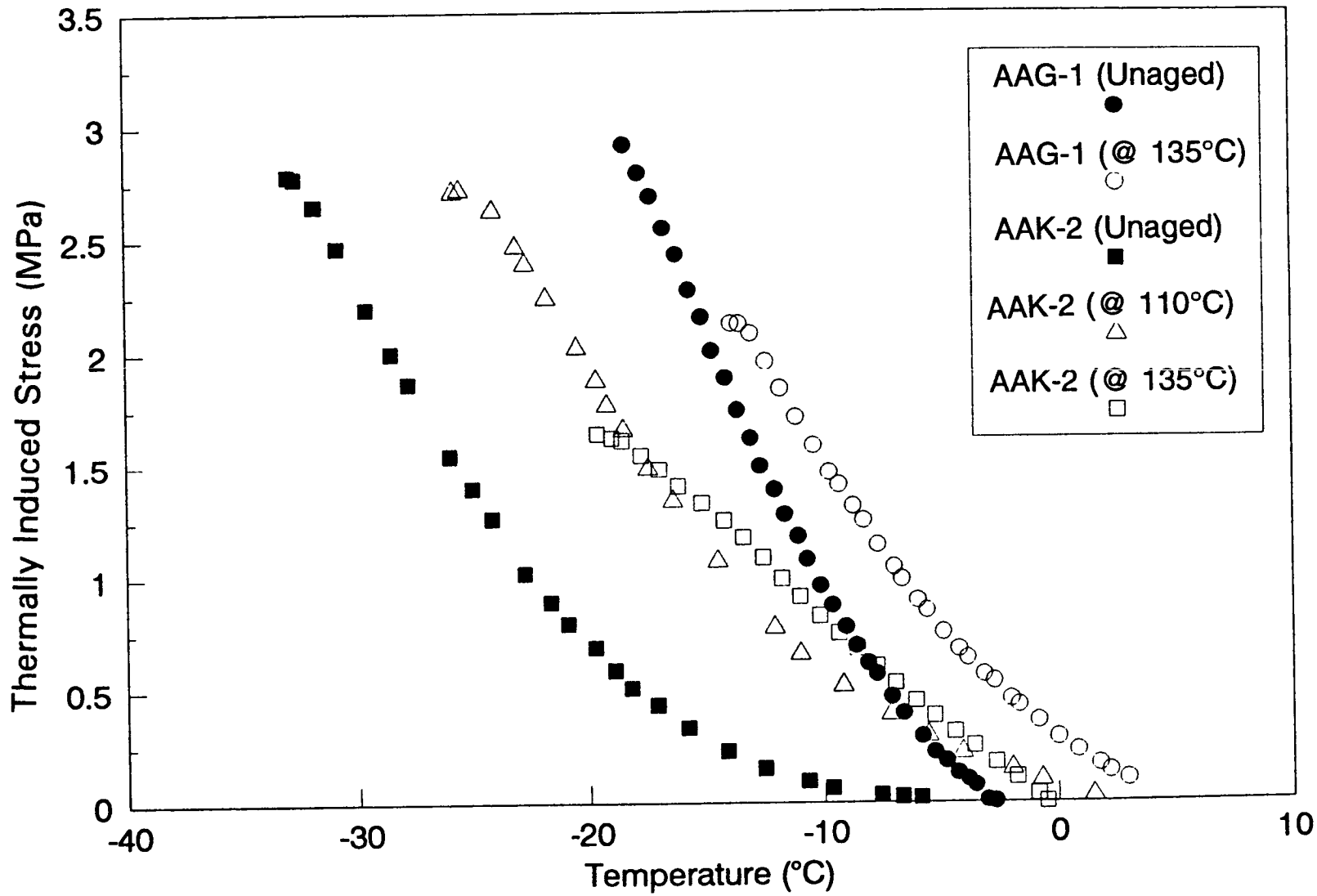


**Figure 5.6. Thermally induced stress for aged specimens**

# 6

# Analysis of Test Results

Statistical analyses were performed to evaluate the effects of test variables on the test results using a statistical analysis system (SAS). The analyses were carried out according to a general linear model (GLM) procedure. Least-square means (LSMEAN) of test results were also obtained during the analyses. The GLM procedure provides a Type III hypothesis test at a significance level of 0.05. If the Type III $P_r > F$ value of a factor is less than 0.05, the factor is considered to be significant. The Type III mean squares indicate the influence of that factor after the effects of all the other factors in the model have been removed. LSMEAN are mean values of test results adjusted for an average value of air voids content considered in the analysis.

## 6.1 Repeatability of Thermal Stress Restrained Specimen Test

The thermal stress restrained specimen test (TSRST) was evaluated based on the 95 percent repeatability limit (American Society of Testing Materials [ASTM] C 670-90a and E 177-90a) for each property measured. The evaluations were performed for the test results from 3.8 cm × 3.8 cm × 20.3 cm specimens with aggregate RB (20.3/3.8 RB) and 5.0 cm × 5.0 cm × 25.0 cm specimens with aggregates RB and RL (25/5 RB and 25/5 RL) at a monotonic cooling rate of 10°C/hr. Since the test results presented in the previous section exhibited fracture and transition temperatures that were not sensitive to air void content, these temperatures were only evaluated for a specific asphalt cement. Fracture strength and slope were evaluated for a target air void content and a specific asphalt cement. The results are summarized in Table 6.1.

As indicated in sections (a) and (b) of Table 6.1, 95 percent repeatability limits for fracture and transition temperatures are less than 40 percent. The 95 percent repeatability limit ranged from 2.2 percent to 20.5 percent for fracture temperature and from 3.0 percent to 39.3 percent for transition temperature.

## Table 6.1. Summary statistics showing the repeatability of TSRST

(a) Fracture temperature

| Data Set | Asphalt | Target Voids (%) | Fracture Temperature (°C) | | | | |
|---|---|---|---|---|---|---|---|
| | | | No. of Obs. | Mean | Std. Dev. | C.V. (%) | 95% Repeat. Limit (%) |
| 20.3/3.8 (RB) | AAG-1 | 8 | 3 | -17.8 | 0.15 | 0.8 | 2.2 |
| | | 4 | 4 | -16.6 | 1.23 | 7.4 | 20.5 |
| | AAG-2 | 8 | 4 | -18.8 | 0.89 | 4.7 | 13.0 |
| | | 4 | 4 | -17.6 | 0.43 | 2.4 | 6.6 |
| | AAK-1 | 8 | 4 | -25.2 | 1.72 | 6.8 | 18.8 |
| | | 4 | 4 | -23.7 | 0.95 | 0.4 | 1.1 |
| | AAK-2 | 8 | 5 | -30.9 | 0.29 | 0.9 | 19.4 |
| | | 4 | 3 | -29.7 | 0.61 | 2.1 | 5.8 |
| 25/5 (RB) | AAG-1 | 8 | 3 | -18.4 | 0.35 | 1.9 | 5.3 |
| | | 4 | 3 | -17.3 | 0.29 | 1.7 | 4.7 |
| | AAG-2 | 8 | 3 | -19.4 | 0.38 | 2.0 | 5.5 |
| | | 4 | 3 | -18.6 | 0.17 | 0.9 | 2.5 |
| | AAK-1 | 8 | 3 | -26.2 | 0.30 | 1.1 | 3.0 |
| | | 4 | 5 | -26.4 | 0.35 | 1.3 | 3.6 |
| | AAK-2 | 8 | 3 | -32.6 | 0.25 | 0.8 | 2.2 |
| | | 4 | 2 | -31.6 | 0.21 | 0.7 | 1.9 |
| 25/5 (RL) | AAG-1 | 8 | 2 | -15.3 | 0.14 | 0.9 | 2.5 |
| | | 4 | 2 | -14.2 | 0.42 | 3.0 | 8.3 |
| | AAG-2 | 8 | 2 | -17.8 | 0.85 | 4.8 | 13.3 |
| | | 4 | 2 | -17.3 | 0.07 | 0.4 | 1.1 |
| | AAK-1 | 8 | 2 | -23.9 | 0.71 | 3.0 | 8.3 |
| | | 4 | 2 | -24.3 | 0.21 | 0.9 | 2.5 |
| | AAK-2 | 8 | 2 | -28.9 | 0.78 | 2.7 | 7.5 |
| | | 4 | 2 | -28.7 | 0.35 | 1.2 | 3.3 |

Continued on next page

**Table 6.1 (continued). Summary statistics showing the repeatability of TSRST**

(b) Transition temperature

| Data Set | Asphalt | Target Voids (%) | Transition Temperature (°C) | | | | |
|---|---|---|---|---|---|---|---|
| | | | No. of Obs. | Mean | Std. Dev. | C.V. (%) | 95% Repeat. Limit (%) |
| 20.3/3.8 (RB) | AAG-1 | 8 | 3 | -10.0 | 0.55 | 5.5 | 15.2 |
| | | 4 | 4 | -9.1 | 0.10 | 1.1 | 3.0 |
| | AAG-2 | 8 | 4 | -12.1 | 0.62 | 5.1 | 14.2 |
| | | 4 | 4 | -11.1 | 0.10 | 0.9 | 2.5 |
| | AAK-1 | 8 | 4 | -16.0 | 0.69 | 4.3 | 11.9 |
| | | 4 | 4 | -13.8 | 0.37 | 2.7 | 7.4 |
| | AAK-2 | 8 | 5 | -21.4 | 0.67 | 3.1 | 8.7 |
| | | 4 | 3 | -20.8 | 0.61 | 2.9 | 8.1 |
| 25/5 (RB) | AAG-1 | 8 | 3 | -11.9 | 1.69 | 14.2 | 39.3 |
| | | 4 | 3 | -11.5 | 0.69 | 6.0 | 16.6 |
| | AAG-2 | 8 | 3 | -12.9 | 0.10 | 0.8 | 2.1 |
| | | 4 | 3 | -13.1 | 1.37 | 10.5 | 29.0 |
| | AAK-1 | 8 | 3 | -19.4 | 0.25 | 1.3 | 3.6 |
| | | 4 | 5 | -19.6 | 1.01 | 5.2 | 14.3 |
| | AAK-2 | 8 | 3 | -23.0 | 0.79 | 3.4 | 9.5 |
| | | 4 | 2 | -22.4 | 0.14 | 0.6 | 1.7 |
| 25/5 (RL) | AAG-1 | 8 | 2 | -9.7 | 0.14 | 1.4 | 4.0 |
| | | 4 | 2 | -9.8 | 0.85 | 8.6 | 24.0 |
| | AAG-2 | 8 | 2 | -13.2 | 0.35 | 2.7 | 7.3 |
| | | 4 | 2 | -12.1 | 0.14 | 1.2 | 3.2 |
| | AAK-1 | 8 | 2 | -15.4 | 0.14 | 0.9 | 2.5 |
| | | 4 | 2 | -15.6 | 0.78 | 5.0 | 13.9 |
| | AAK-2 | 8 | 2 | -22.7 | 0.56 | 2.5 | 6.8 |
| | | 4 | 2 | -21.8 | 1.84 | 8.4 | 23.3 |

Continued on next page

**Table 6.1 (continued). Summary statistics showing the repeatability of TSRST**

(c) Fracture strength

| Data Set | Asphalt | Target Voids (%) | Fracture Strength (MPa) | | | | |
|---|---|---|---|---|---|---|---|
| | | | No. of obs. | Mean | Std. Dev. | C.V. (%) | 95% Repeat. Limit (%) |
| 20.3/3.8 (RB) | AAG-1 | 8 | 3 | 2.472 | 13.49 | 7.0 | 19.4 |
| | | 4 | 4 | 3.416 | 0.193 | 5.7 | 16.6 |
| | AAG-2 | 8 | 4 | 2.481 | 0.267 | 10.8 | 29.9 |
| | | 4 | 4 | 3.012 | 0.406 | 13.5 | 37.4 |
| | AAK-1 | 8 | 4 | 2.420 | 0.320 | 13.2 | 36.6 |
| | | 4 | 4 | 3.238 | 0.349 | 10.8 | 29.9 |
| | AAK-2 | 8 | 5 | 2.389 | 0.167 | 7.0 | 19.4 |
| | | 4 | 3 | 4.039 | 0.102 | 2.5 | 7.0 |
| 25/5 (RB) | AAG-1 | 8 | 3 | 2.629 | 0.454 | 17.3 | 47.9 |
| | | 4 | 3 | 3.257 | 0.369 | 11.3 | 31.4 |
| | AAG-2 | 8 | 3 | 2.146 | 0.042 | 2.0 | 5.5 |
| | | 4 | 3 | 2.983 | 0.760 | 25.5 | 70.6 |
| | AAK-1 | 8 | 3 | 2.751 | 0.152 | 5.5 | 15.3 |
| | | 4 | 5 | 3.743 | 0.310 | 8.3 | 23.0 |
| | AAK-2 | 8 | 3 | 2.289 | 0.470 | 20.5 | 56.8 |
| | | 4 | 2 | 3.802 | 0.244 | 6.4 | 17.8 |
| 25/5 (RL) | AAG-1 | 8 | 2 | 1.483 | 0.009 | 0.6 | 1.7 |
| | | 4 | 2 | 2.050 | 0.322 | 15.7 | 43.5 |
| | AAG-2 | 8 | 2 | 1.622 | 0.204 | 12.6 | 34.9 |
| | | 4 | 2 | 1.791 | 0.239 | 13.4 | 37.0 |
| | AAK-1 | 8 | 2 | 2.250 | 0.039 | 1.7 | 4.8 |
| | | 4 | 2 | 2.291 | 0.127 | 5.6 | 15.4 |
| | AAK-2 | 8 | 2 | 2.556 | 0.297 | 11.6 | 32.2 |
| | | 4 | 2 | 2.985 | 0.561 | 18.8 | 52.0 |

Continued on next page

**Table 6.1 (continued). Summary statistics showing the repeatability of TSRST**

(d) Slope (dS/dT)

| Data Set | Asphalt | Target Voids (%) | Slope (MPa/°C) | | | | |
|---|---|---|---|---|---|---|---|
| | | | No. of Obs. | Mean | Std. Dev. | C.V. (%) | 95% Repeat. Limit (%) |
| 20.3/3.8 (RB) | AAG-1 | 8 | 3 | 0.218 | 0.014 | 6.4 | 17.8 |
| | | 4 | 4 | 0.264 | 0.022 | 8.2 | 22.8 |
| | AAG-2 | 8 | 4 | 0.226 | 0.013 | 5.9 | 16.3 |
| | | 4 | 4 | 0.274 | 0.025 | 9.1 | 25.1 |
| | AAK-1 | 8 | 4 | 0.154 | 0.030 | 19.8 | 54.9 |
| | | 4 | 4 | 0.196 | 0.013 | 6.8 | 18.7 |
| | AAK-2 | 8 | 5 | 0.145 | 0.013 | 9.0 | 28.4 |
| | | 4 | 3 | 0.269 | 0.012 | 4.5 | 12.4 |
| 25/5 (RB) | AAG-1 | 8 | 3 | 0.235 | 0.057 | 24.2 | 67.0 |
| | | 4 | 3 | 0.274 | 0.028 | 10.2 | 28.3 |
| | AAG-2 | 8 | 3 | 0.194 | 0.023 | 12.1 | 33.6 |
| | | 4 | 3 | 0.263 | 0.044 | 16.7 | 46.3 |
| | AAK-1 | 8 | 3 | 0.201 | 0.012 | 6.0 | 16.6 |
| | | 4 | 5 | 0.268 | 0.020 | 7.4 | 20.5 |
| | AAK-2 | 8 | 3 | 0.157 | 0.022 | 14.0 | 38.7 |
| | | 4 | 2 | 0.246 | 0.037 | 15.1 | 41.8 |
| 25/5 (RL) | AAG-1 | 8 | 2 | 0.154 | 0.006 | 4.1 | 11.4 |
| | | 4 | 2 | 0.234 | 0.013 | 5.4 | 15.0 |
| | AAG-2 | 8 | 2 | 0.175 | 0.030 | 17.3 | 47.8 |
| | | 4 | 2 | 0.185 | 0.026 | 14.0 | 38.8 |
| | AAK-1 | 8 | 2 | 0.168 | 0.003 | 1.8 | 4.8 |
| | | 4 | 2 | 0.176 | 0.007 | 4.2 | 11.6 |
| | AAK-2 | 8 | 2 | 0.217 | 0.023 | 11.0 | 30.5 |
| | | 4 | 2 | 0.230 | 0.066 | 28.6 | 79.3 |

As indicated in sections (c) and (d) of Table 6.1 and, 95 percent repeatability limits for fracture strength and slope are less than or close to 50 percent in most cases. The 95 percent repeatability limit for fracture strength ranged from 1.7 percent to 52 percent, except for AAG-2 and AAK-2 (25/5 RB). The 95 percent repeatability limit for slope ranged from 4.8 percent to 54.9 percent, except for AAG-1 (25/5 RB) and AAK-2 (25/5 RL).

## 6.2 Effect of Specimen Size

Statistical analyses were performed on test results for two different specimen sizes — 3.8 cm × 3.8 cm × 20.3 cm and 5.0 cm × 5.0 cm × 25.0 cm. Their aspect ratios (length/width) were 5.3 and 5.0, respectively. Summary statistics of the analyses and the effects of variables are presented in Table 6.2.

From the Type III $P_r > F$ values, both asphalt type and specimen size are identified as significant factors for fracture temperature and transition temperature. Based on the Type III mean squares, fracture and transition temperatures are most affected by asphalt type followed by specimen size. As presented in Table 6.2, variations of fracture and transition temperature are greater than those related to specimen size. LSMEAN of fracture temperature and transition temperature for 20.3/3.8 (RB) and 25/5 (RB) are compared in Figures 6.1 and 6.2. Fracture and transition temperatures for 25/5 (RB) are colder than that for 20.3/3.8 (RB). This difference may be due to the greater time required for a larger specimen to reach thermal equilibrium.

From both the Type III $P_r > F$ values and mean squares, air voids content is identified as the most significant factor in fracture strength. Asphalt type and specimen size are not significant. The Type III mean squares for air voids content is extremely high compared with asphalt type and specimen size. LSMEAN of fracture strength for 25/5 (RB) and 20.3/3.8 (RB) are compared depending on asphalt type in Figure 6.3. Fracture strengths of 20.3/3.8 (RB) are greater than 25/5 (RB) except for asphalt AAK-1. This difference may be due to the nonuniformity of some specimens with the smaller cross section that resulted from poor compaction. Little or no breakage of aggregate was observed in the fracture surface of those specimens. Fracture at the interface between aggregate and asphalt was dominant. The overall fracture strength for 20.3/3.8 (RB) is slightly greater than for 25/5 (RB).

Slope (dS/dT) is also most affected by air void content, followed by asphalt type to a much lesser degree. The effect of specimen size is not consistent, as shown in Figure 6.4. No significant difference in the overall slope between 25/5 (RB) and 20.3/3.8 (RB) was observed.

Specimen size has a substantial effect on fracture and transition temperature but does not have a significant effect on fracture strength and slope. Fracture and transition temperatures are colder for mixtures of larger specimens. This situation may be attributed to the fact that larger specimens require a longer time to reach thermal equilibrium. Since the aspect ratios (length/width) of two specimen sizes are not substantially different, the resulting fracture strength and slope will not be significantly different. Tests with specimens having various

**Table 6.2. Summary statistics of test results for asphalt type and specimen size**

| Asphalt | Fracture Temperature (°C) | | Fracture Strength (MPa) | | Slope (MPa/°C) | | Transition Temperature (°C) | |
|---|---|---|---|---|---|---|---|---|
| | 25.0/5.0(RB) | 20.3/3.8(RB) | 25.0/5.0(RB) | 20.3/3.8(RB) | 25.0/5.0(RB) | 20.3/3.8(RB) | 25.0/5.0(RB) | 20.3/3.8(RB) |
| AAG-1 | -17.92 | -17.09 | 2.901 | 3.019 | 0.251 | 0.245 | -11.72 | -9.46 |
| AAG-2 | -19.54 | -17.99 | 2.589 | 2.966 | 0.228 | 0.263 | -13.32 | -11.42 |
| AAK-1 | -26.54 | -24.46 | 3.172 | 2.777 | 0.231 | 0.177 | -19.70 | -14.91 |
| AAK-2 | -32.19 | -30.34 | 2.932 | 3.081 | 0.195 | 0.206 | -22.72 | -21.12 |
| Range (max. - min.) | 14.27 | 13.25 | 0.583 | 0.304 | 0.056 | 0.086 | 11.00 | 11.66 |

| Specimen Size | Overall Fracture Temperature (°C) | Overall Fracture Strength (MPa) | Overall Slope (MPa/°C) | Overall Transition Temperature (°C) |
|---|---|---|---|---|
| 25/5(RB) | -24.04 | 2.899 | 0.226 | -16.86 |
| 20.3/3.8(RB) | -22.47 | 2.960 | 0.222 | -14.23 |
| Range (max. - min.) | 1.57 | 0.061 | 0.004 | 2.63 |

| Variables | Fracture Temperature | Fracture Strength | Slope | Transition Temperature |
|---|---|---|---|---|
| Asphalt type | HS | NS | S | HS |
| Size | S | NS | NS | S |
| Void | NS | HS | HS | NS |
| Interaction between asphalt and size | NS | NS | NS | NS |

HS = highly significant; S = significant; NS = not significant.

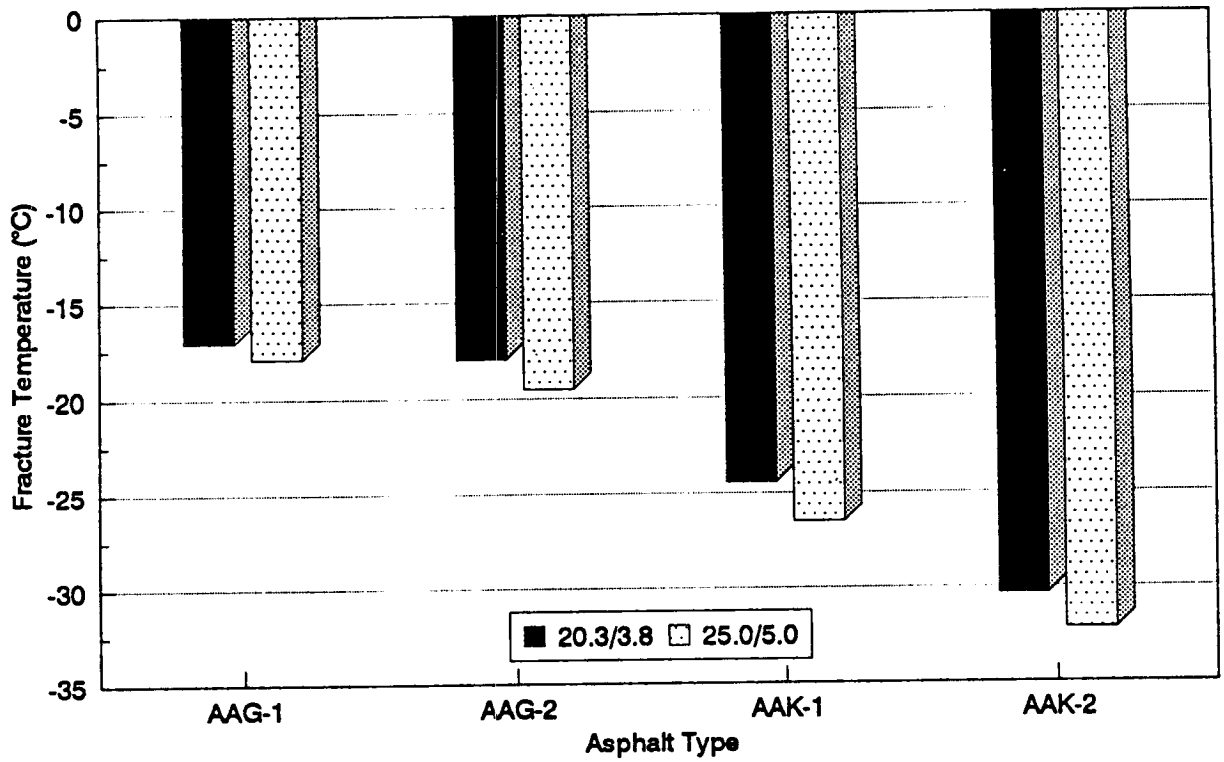


**Figure 6.1. Effect of specimen size on fracture temperature**

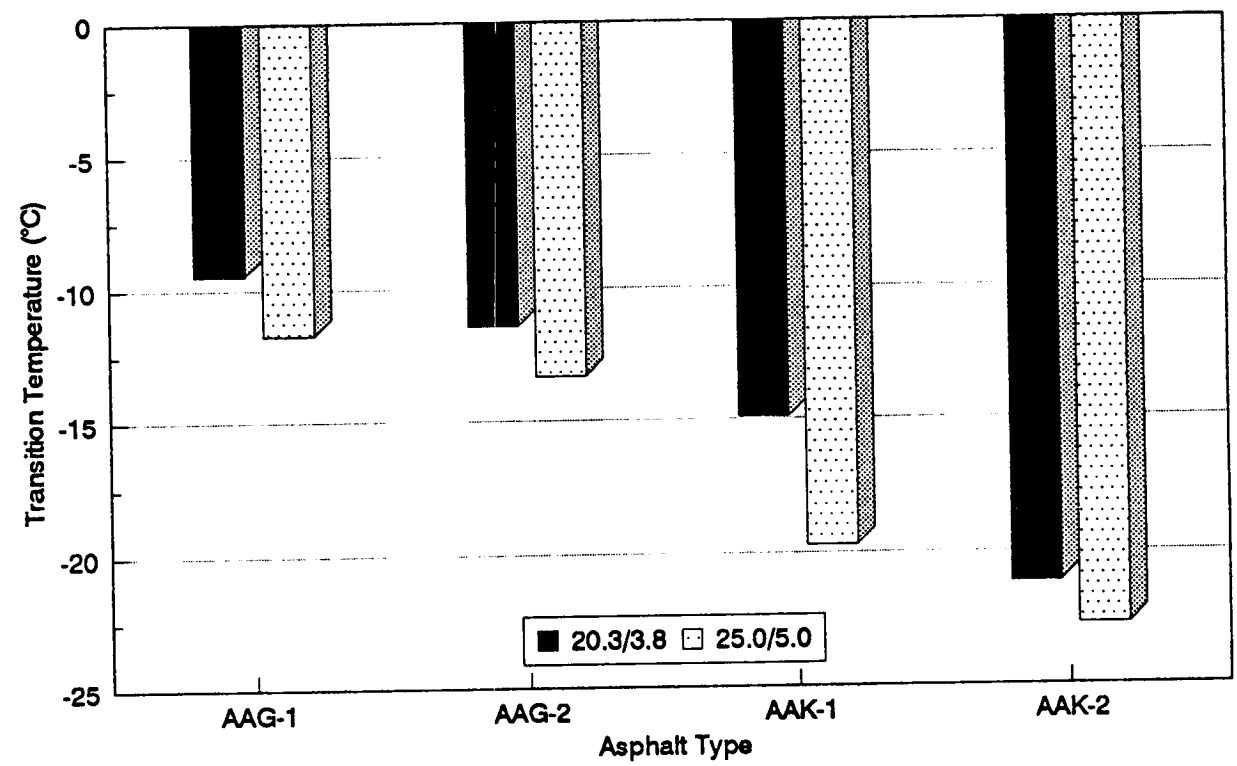


**Figure 6.2. Effect of specimen size on transition temperature**

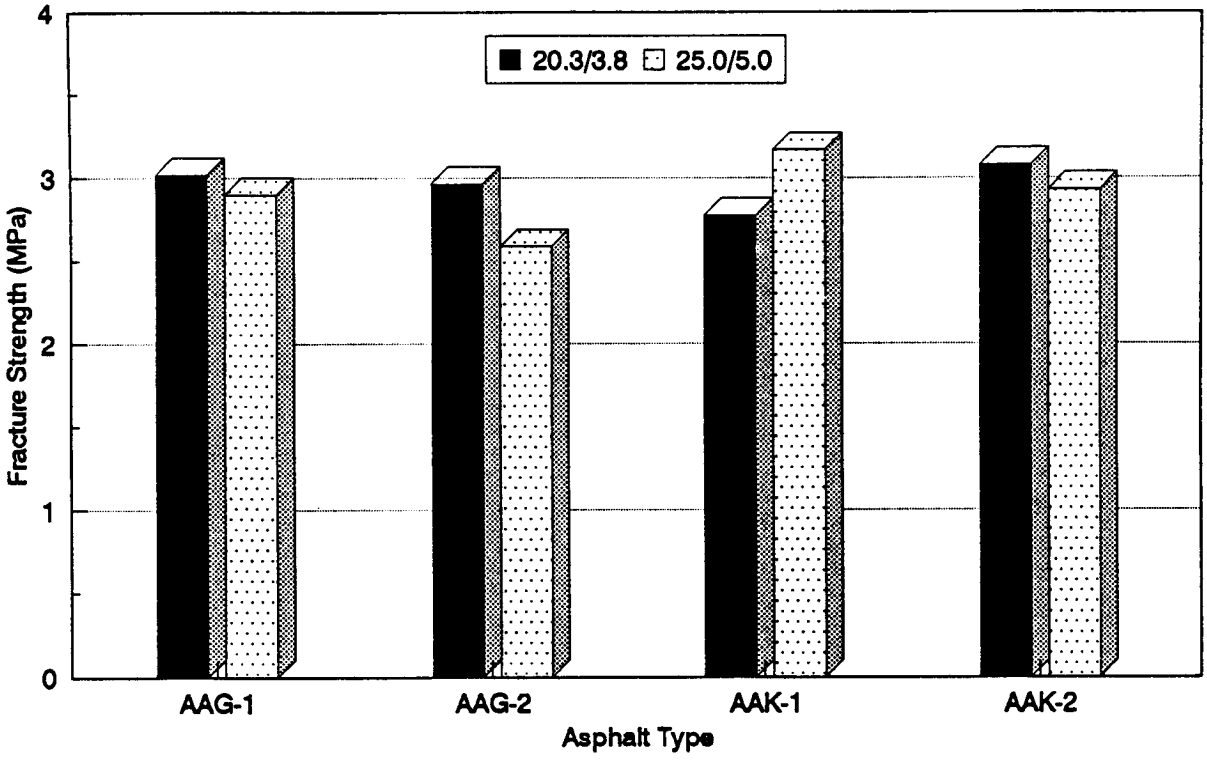


**Figure 6.3. Effect of specimen size on fracture strength**

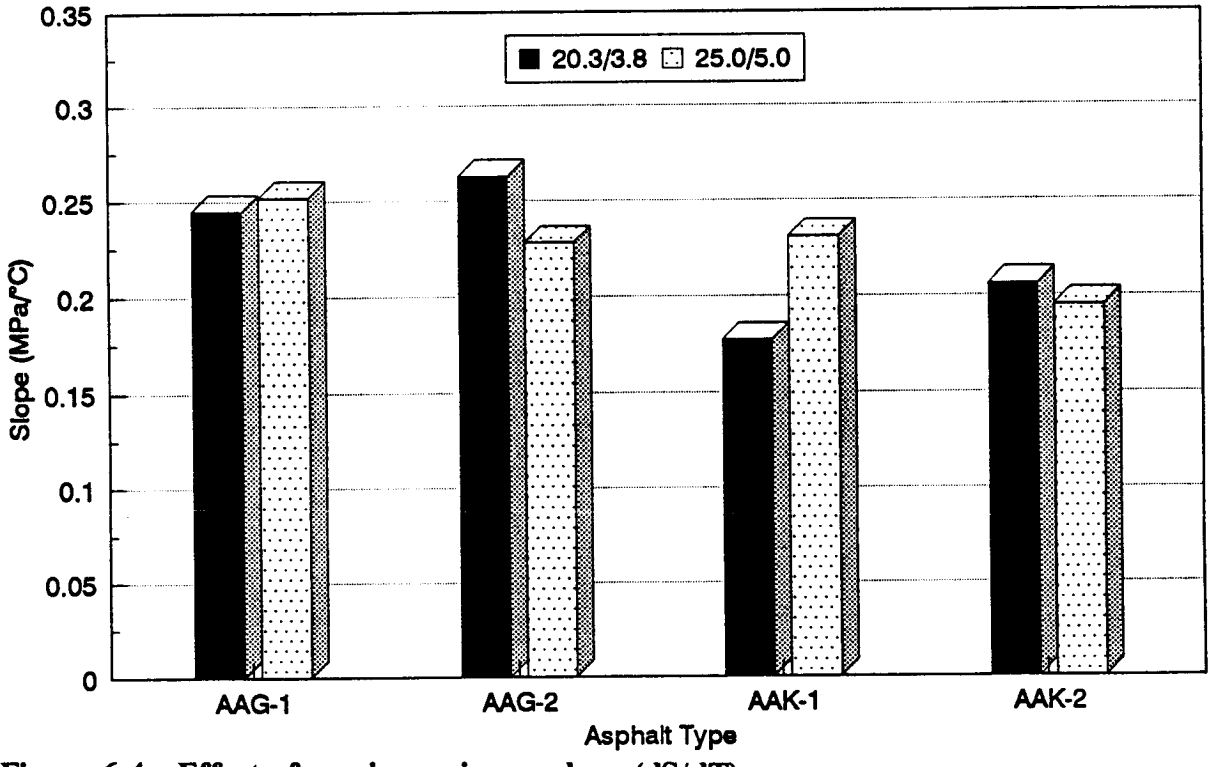


**Figure 6.4. Effect of specimen size on slope (dS/dT)**

aspect ratios may be required to obtain a better estimate of the effect of specimen size on test results.

## 6.3 Effect of Aggregate Type

Statistical analyses were performed on test results for 5.0 cm × 5.0 cm × 25.0 cm specimens with RL aggregate and for 5.0 cm × 5.0 cm × 25.0 cm specimens with RB aggregate. Summary statistics of the analyses and the effects of variables are presented in Table 6.3.

The Type III $P_r > F$ values indicate that asphalt type and aggregate type are significant factors in fracture and transition temperatures. The Type III mean squares indicate that fracture and transition temperatures are most affected by asphalt type followed by aggregate type. As presented in Table 6.3, variations in fracture and transition temperatures depending on asphalt type are greater than those depending on aggregate type. Figures 6.5 and 6.6 compare the LSMEAN of fracture and transition temperature for aggregates RB and RL depending on asphalt type, respectively. Both fracture and transition temperatures are warmer for RL aggregate than for RB aggregate. The overall fracture and transition temperatures for RL aggregate are 2.84°C and 1.86°C warmer than for RB aggregate, respectively.

Aggregate type has a substantial effect on all properties measured in TSRST. Fracture and transition temperatures are colder and fracture strength and slope are greater for mixtures with RB aggregate. This situation may be attributed to the surface texture and the shape of aggregate. The RB aggregate with rough surface texture and angular shape can provide more bonding and interlock forces between asphalt binder and aggregate, therefore resulting in better resistance to cracking.

The Type III $P_r > F$ values indicate that air voids content and aggregate type are significant factors for fracture strength and slope. The Type III mean squares indicate that fracture strength and slope are most influenced by air voids content followed by aggregate type. Figures 6.7 and 6.8 show LSMEAN of fracture strength and slope depending on asphalt type and aggregate type, respectively. As shown in Figure 6.7, fracture strengths for RL aggregate are lower than for RB aggregate. The overall fracture strength for RB aggregate is approximately 0.6 MPa greater than RL aggregate. As shown in Figure 6.8, slopes for RB aggregate are slightly greater than for RL aggregate except for asphalt AAK-2. The overall slope for RB aggregate is 0.02 MPa/°C greater than for RL aggregate.

## 6.4 Effect of Stress Relaxation

Test results with stress relaxation were analyzed together with test results without stress relaxation. Summary statistics from the analyses, including the effects of variables, are presented in Table 6.4.

**Table 6.3. Summary of the results from the statistical analysis of test results depending on asphalt type and aggregate type**

| | Fracture Temperature (°C) | | Fracture Strength (MPa) | | Slope (MPa/°C) | | Transition Temperature (°C) | |
|---|---|---|---|---|---|---|---|---|
| Asphalt | RB | RL | RB | RL | RB | RL | RB | RL |
| AAG-1 | -17.91 | -14.57 | 2.880 | 2.110 | 0.250 | 0.218 | -11.74 | -9.69 |
| AAG-2 | -19.53 | -17.38 | 2.568 | 1.975 | 0.226 | 0.199 | -13.30 | -12.55 |
| AAK-1 | -26.48 | -24.00 | 3.155 | 2.414 | 0.228 | 0.182 | -19.60 | -15.45 |
| AAK-2 | -32.21 | -28.82 | 2.909 | 2.629 | 0.194 | 0.213 | -22.76 | -22.28 |
| Range (max. - min.) | 14.30 | 14.25 | 0.587 | 0.654 | 0.056 | 0.036 | 11.02 | 12.59 |

| Specimen Size | Overall Fracture Temperature (°C) | Overall Fracture Strength (MPa) | Overall Slope (MPa/°C) | Overall Transition Temperature (°C) |
|---|---|---|---|---|
| RB | -24.03 | 2.878 | 0.224 | -16.85 |
| RL | -21.19 | 2.282 | 0.203 | -14.99 |
| Range (max. - min.) | 2.84 | 0.596 | 0.021 | 1.86 |

| Variables | Fracture Temperature | Fracture Strength | Slope | Transition Temperature |
|---|---|---|---|---|
| Asphalt type | HS | NS | S | HS |
| Aggregate type | S | HS | S | S |
| Void | NS | HS | HS | NS |
| Interaction between asphalt and aggregate | NS | NS | NS | NS |

HS = highly significant (Type III $P_r > F$ value is less than 0.05 and Type III mean square is significant).
S = significant (Type III $P_r > F$ value is less than 0.05 but Type III mean square is not significant).
NS = not significant (Type III $P_r > F$ value is greater than 0.05 and Type III mean square is not significant).

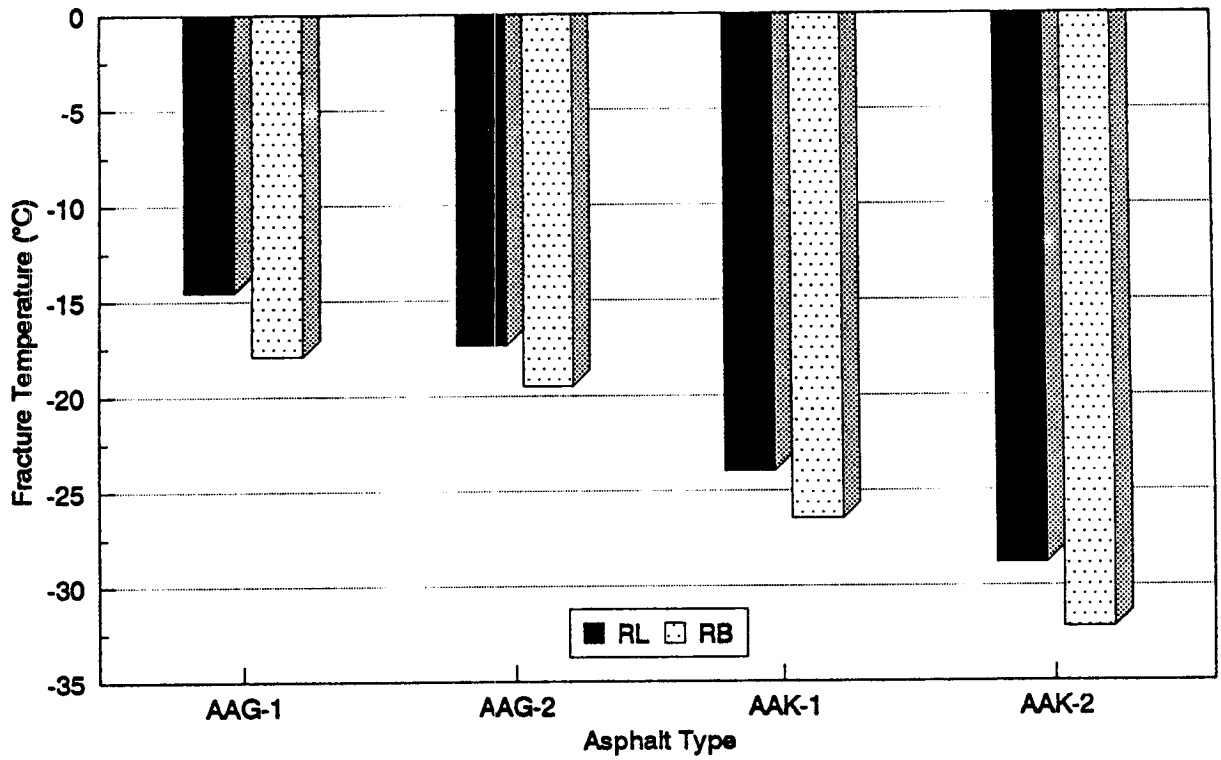


**Figure 6.5. Effect of aggregate type on fracture temperature**

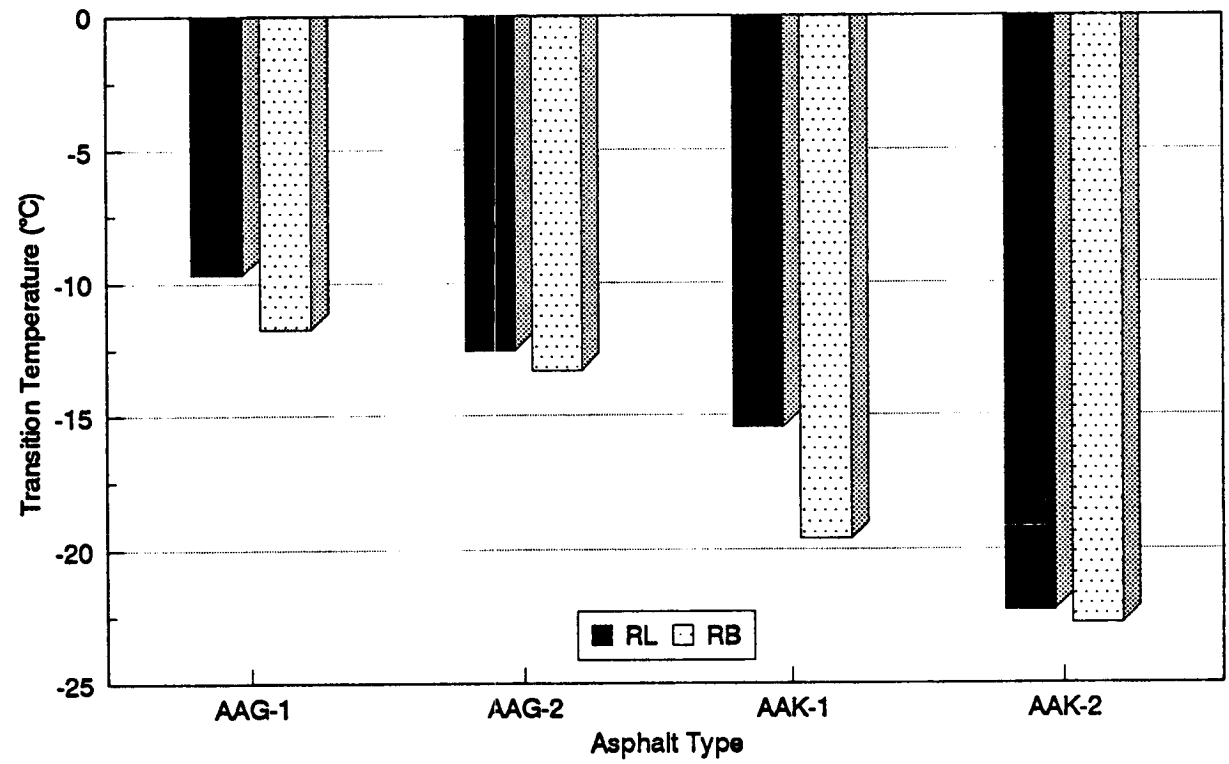


**Figure 6.6. Effect of aggregate type on transition temperature**

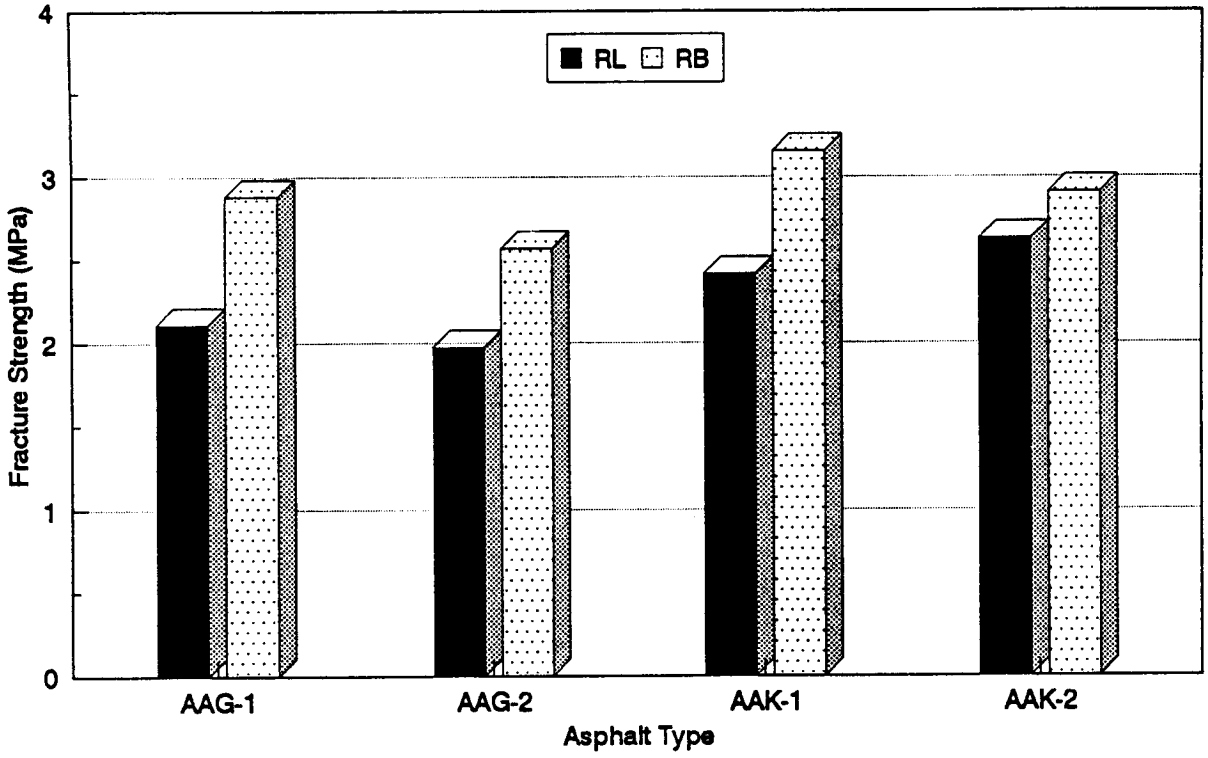


**Figure 6.7. Effect of aggregate type on fracture strength**

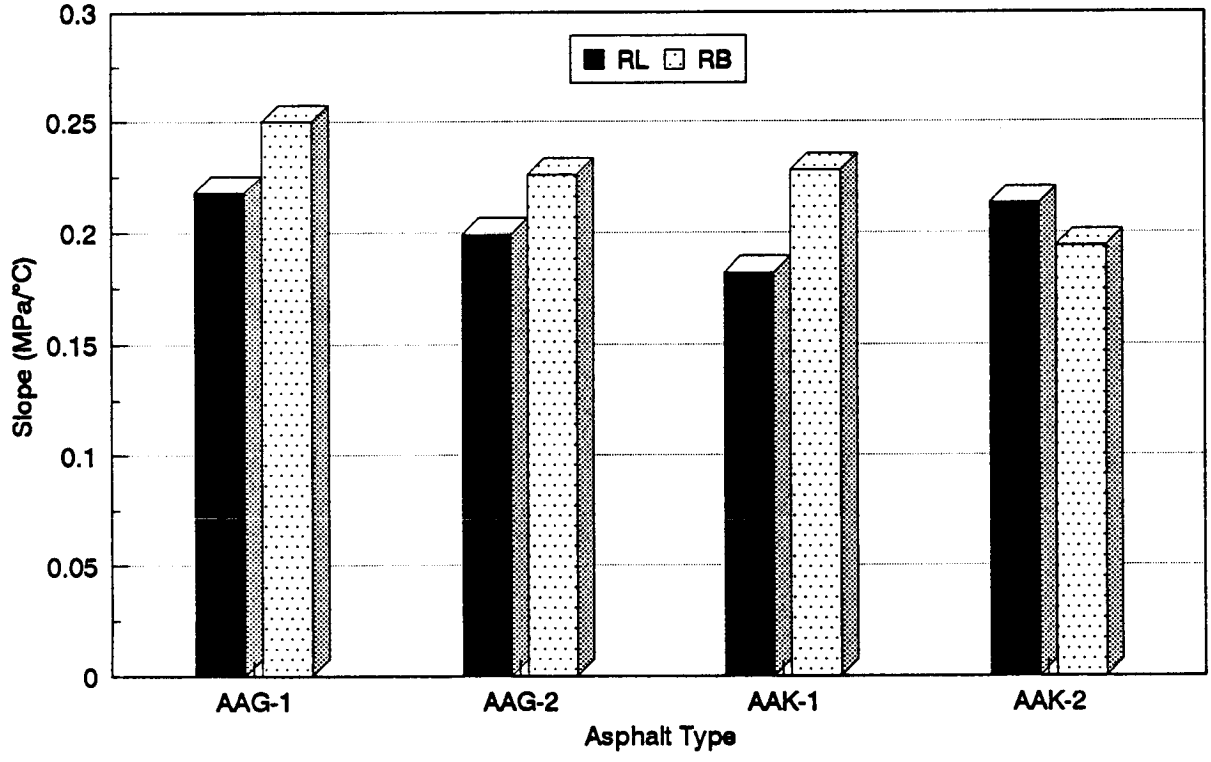


**Figure 6.8. Effect of aggregate type on slope (dS/dT)**

**Table 6.4. Summary of the results from the statistical analysis of test results depending on asphalt type and stress relaxation**

| | Fracture Temperature (°C) | | Fracture Strength (MPa) | |
|---|---|---|---|---|
| Asphalt | Nonrelaxed | Relaxed | Nonrelaxed | Relaxed |
| AAG-1 | -17.88 | -19.53 | 2.950 | 2.516 |
| AAG-2 | -19.48 | -20.88 | 2.634 | 2.704 |
| AAK-1 | -26.40 | -27.10 | 3.198 | 2.678 |
| AAK-2 | -32.20 | -30.85 | 2.993 | 2.251 |
| Range (max. - min.) | 14.32 | 11.32 | 0.564 | 0.453 |

| | Overall Fracture Temperature (°C) | Overall Fracture Strength (MPa) |
|---|---|---|
| Nonrelaxed | -23.99 | 2.944 |
| Relaxed | -24.59 | 2.537 |
| Range (max. - min.) | 0.60 | 0.407 |

| Variables | Fracture Temperature | Fracture Strength | Slope | Transition Temperature |
|---|---|---|---|---|
| Asphalt type | HS | NS | N/A | N/A |
| Relaxation | S | S | N/A | N/A |
| Void | NS | HS | N/A | N/A |
| Interaction between asphalt and relaxation | S | NS | N/A | N/A |

HS = highly significant (Type III $P_r > F$ value is less than 0.05 and Type III mean square is significant).
S = significant (Type III $P_r > F$ value is less than 0.05 but Type III mean square is not significant).
NS = not significant (Type III $P_r > F$ value is greater than 0.05 and Type III mean square is not significant).

The Type III $P_r > F$ values indicate that asphalt type, stress relaxation, and the interaction between asphalt type and stress relaxation are significant factors in fracture temperature. The Type III mean squares indicates that fracture temperature is most affected by asphalt type followed by stress relaxation and the interaction between asphalt type and stress relaxation. Variations of fracture temperature depending on asphalt type are much greater than those caused by stress relaxation. LSMEAN of fracture temperature for relaxed and nonrelaxed specimens are compared as a function of asphalt type in Figure 6.9. The decrease in fracture temperatures caused by stress relaxation is greater for specimens with asphalts AAG-1 and AAG-2. In the case of specimens with asphalts AAK-1 and AAK-2, no significant difference in fracture temperature between relaxed and nonrelaxed specimens can be seen. Thus, the overall fracture temperature for relaxed specimens is slightly colder than for nonrelaxed specimens.

The Type III $P_r > F$ values indicate that air voids content and stress relaxation are significant factors of fracture strength. The Type III mean squares indicate that fracture strength is most affected by air voids content followed by stress relaxation. Stress relaxation tends to decrease the fracture strength of the specimen. Figure 6.10 shows LSMEAN of fracture strengths for relaxed and nonrelaxed specimens depending on asphalt type. Fracture strengths for relaxed specimens with AAG-1, AAK-1, and AAK-2 are 0.4 to 0.7 MPa lower than for nonrelaxed specimens. But in the case of specimens with AAG-2, no significant difference in fracture strength between relaxed and nonrelaxed specimens was observed. The overall fracture strength for relaxed specimens is approximately 0.4 MPa lower than for nonrelaxed specimens.

## 6.5 Effect of Various Cooling Rates

Test results with cooling rates of 1°, 2°, and 5°C/hr were analyzed together with test results with a cooling rate of 10°C/hr. LSMEAN of the test results are compared in Figures 6.11 through 6.14.

As shown in Figure 6.11, fracture temperature tends to become warmer as cooling rate increases up to 5°C/hr. Beyond 5°C/hr, fracture temperature decreases slightly. Transition temperature consistently becomes warmer as cooling rate increases, as shown in Figure 6.12. Fracture strength is also affected by cooling rate. Fracture strength tends to increase as cooling rate increases (Figure 6.13). (No consistent trend between fracture strength and cooling rate was observed for asphalt AAG-1.) As shown in Figure 6.14, slope (dS/dT) increases slightly with increasing cooling rate; however, no significant difference in slope was observed.

Cooling rate is also an important factor that affects test results in several ways. At a slower cooling rate (which means longer loading time), fracture and transition temperatures are colder and fracture strength tends to decrease. A slower cooling rate allows a greater amount of stress relaxation and results in a colder fracture temperature and lower fracture strength. Typically, fracture temperature was coldest and fracture strength was lowest at 1°C/hr. For mixtures with AAK-2 asphalt, fracture temperature at a cooling rate of 1°C/hr

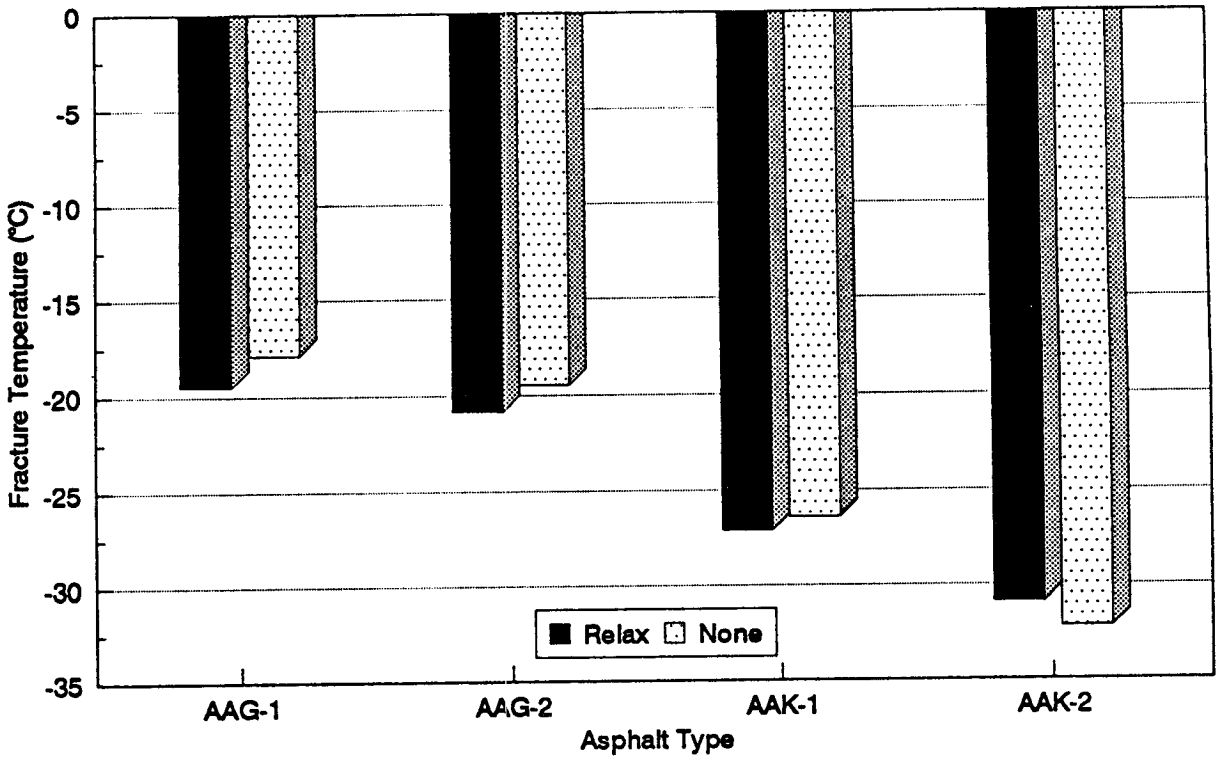


**Figure 6.9. Effect of stress relaxation on fracture temperature**

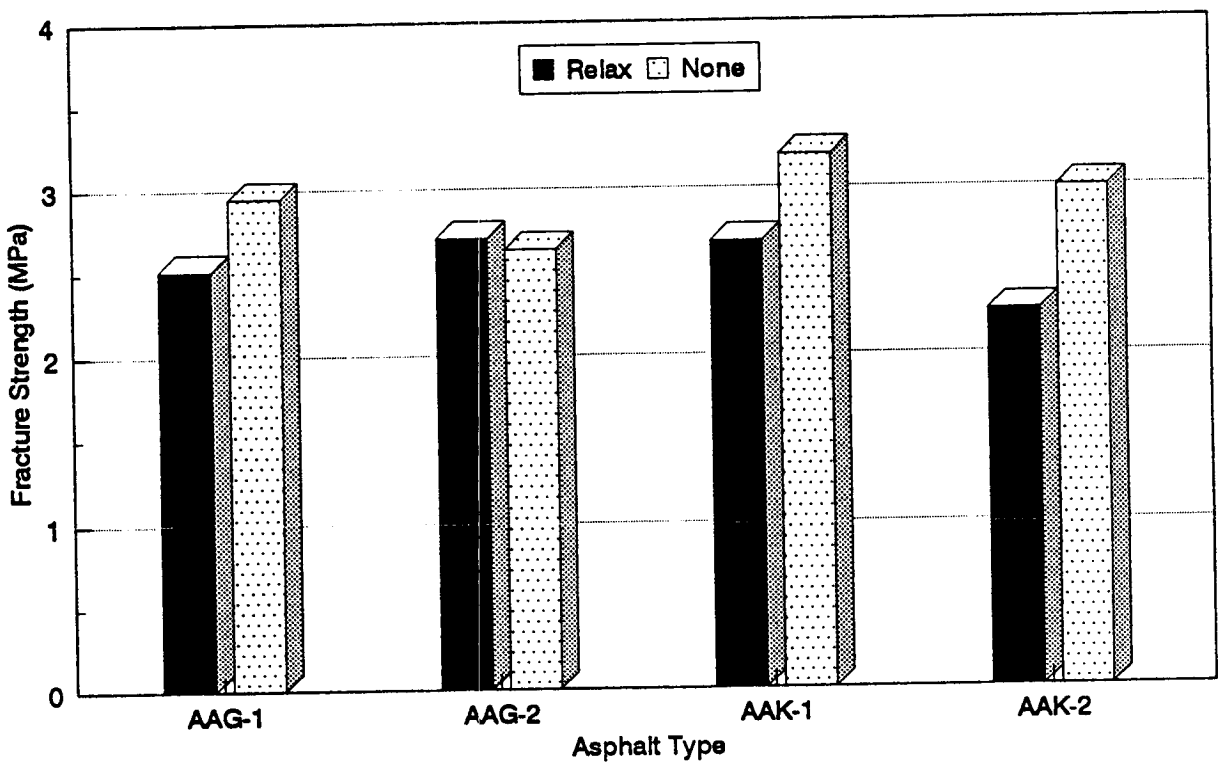


**Figure 6.10. Effect of stress relaxation on fracture strength**

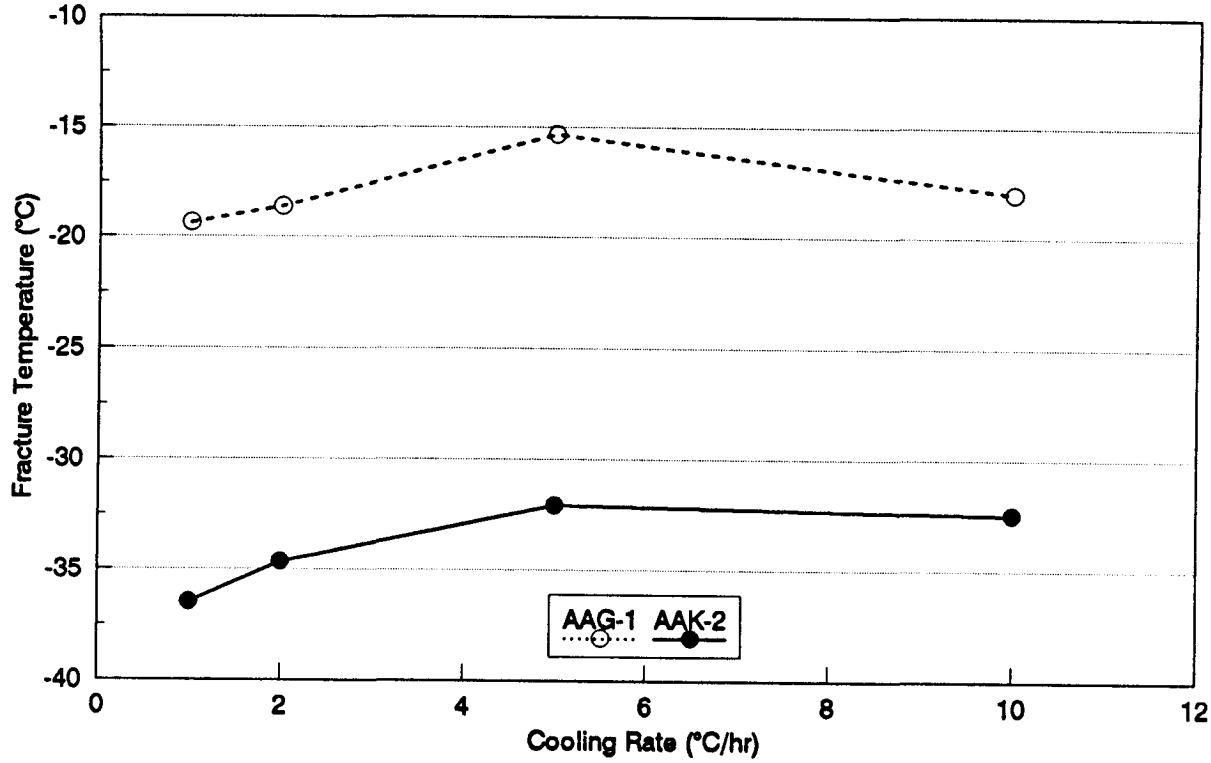


**Figure 6.11. Effect of cooling rate on fracture temperature**

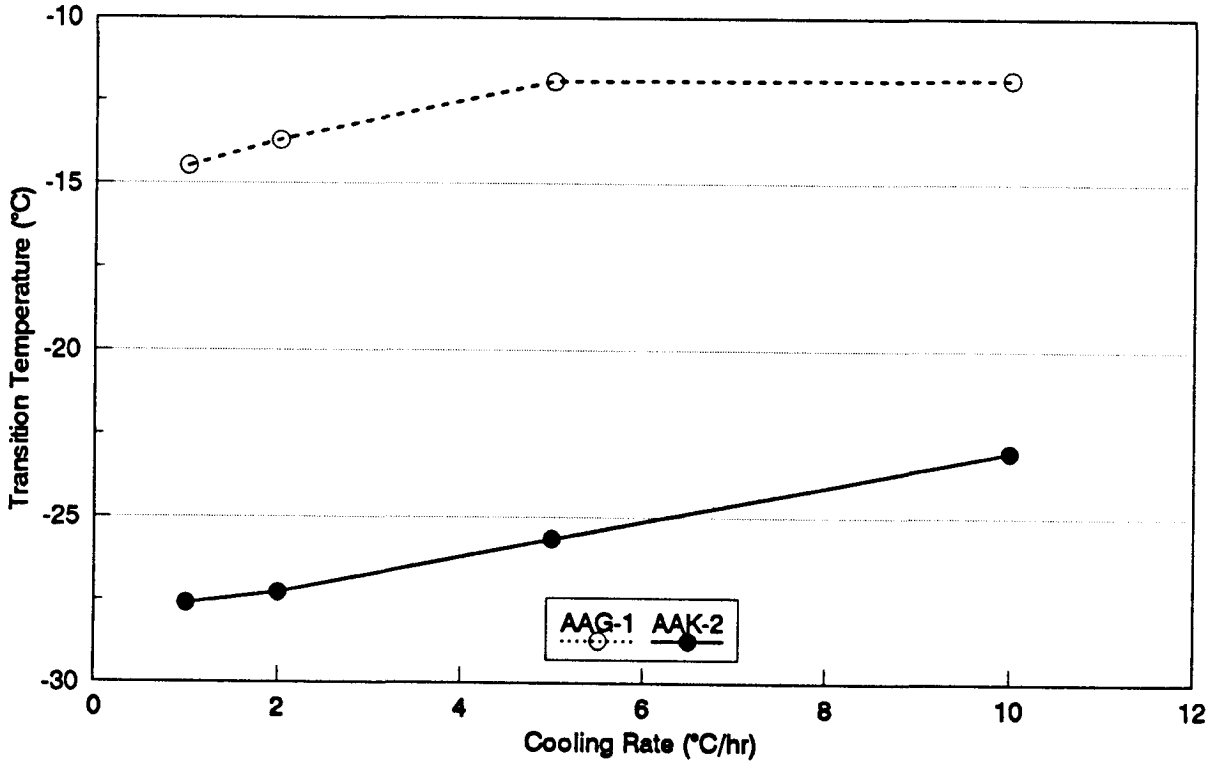


**Figure 6.12. Effect of cooling rate on transition temperature**

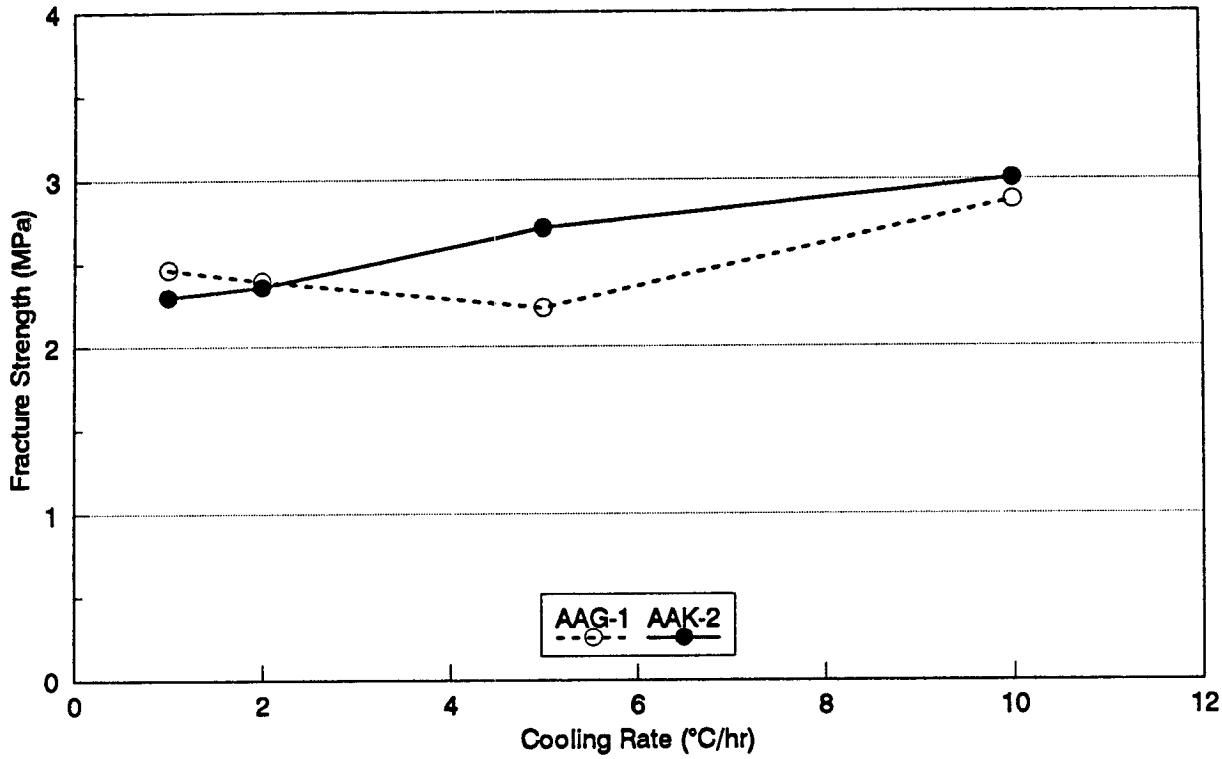


**Figure 6.13. Effect of cooling rate on fracture strength**

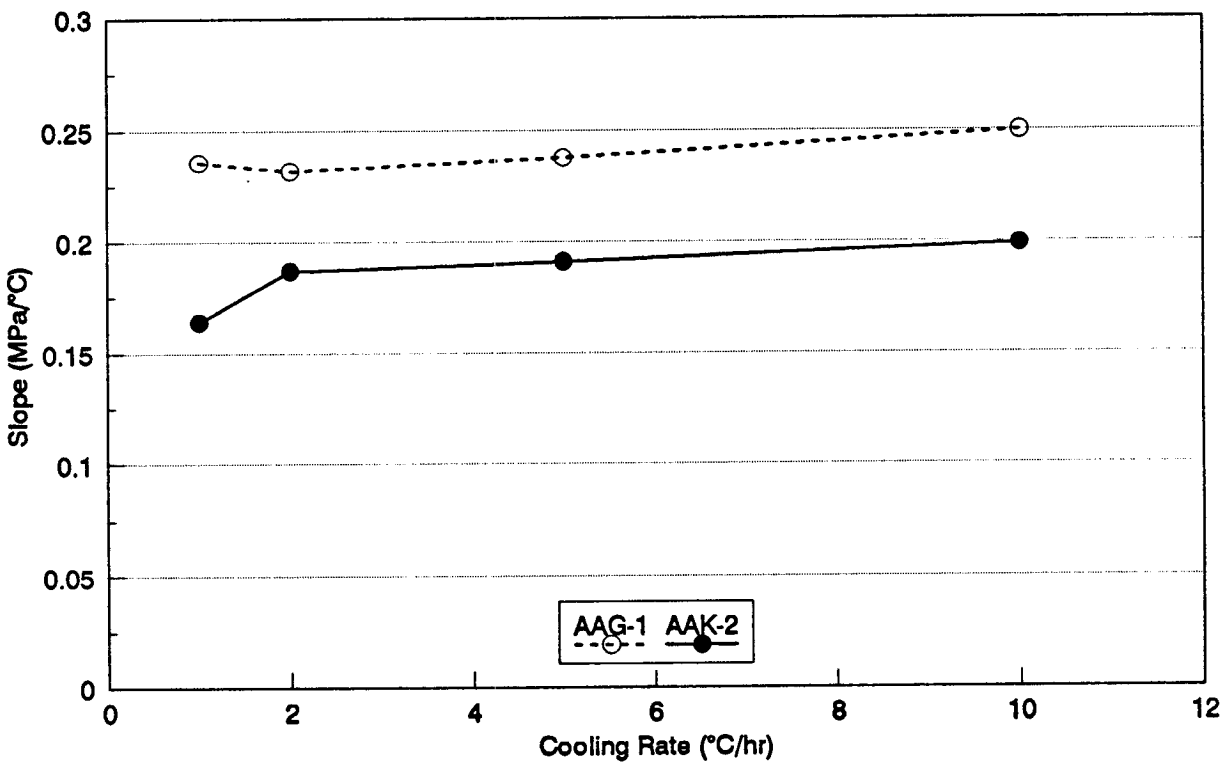


**Figure 6.14. Effect of cooling rate on slope (dS/dT)**

was approximately 5°C colder than the fracture temperature at 10°C/hr, and fracture strength at 1°C/hr was approximately 0.7 MPa lower than the fracture strength at 10°C/hr.

As discussed in the previous section, the field cooling rates observed in North America do not exceed 1°C/hr. Thus, a cooling rate of 1°C/hr is required to better evaluate the low-temperature cracking resistance of asphalt concrete pavements in the field. Notwithstanding this fact, a test at 10°C/hr can still provide valuable information regarding the low-temperature cracking characteristics of asphalt concrete mixtures.

## 6.6 Effect of Aging

Fracture and transition temperatures are significantly affected by degree of aging. Figures 6.15 and 6.16 show LSMEAN of fracture and transition temperatures for two different aging conditions. Fracture and transition temperatures are considerably warmer for aged specimens than for unaged specimens.

Fracture strengths of aged specimens are compared with those of unaged specimens in Figure 6.17. Fracture strengths are lower for aged specimens than for unaged specimens. The fracture strength of a specimen aged at 135°C is much lower than the fracture strength of a specimen aged at 110°C. LSMEAN of slope are also lower for aged specimens (Figure 6.18).

All properties measured by TSRST were significantly affected by aging. Fracture and transition temperatures increased and fracture strength and slope decreased with aging. Increase in fracture and transition temperatures and decrease in fracture strength and slope were greater for specimens aged at 135°C than for specimens aged at 110°C. As the mixture is subjected to aging, the viscosity of the asphalt cement in the mixture increases and the asphalt cement becomes stiffer. The mixture becomes more resistant to deformation, and additional stresses will develop during cooling. Thus, the mixture becomes more susceptible to cracking.

The degree of influence of aging depends on the asphalt type. Specimens with asphalt AAK-2 are affected by aging to a greater extent. Fracture temperature of aged (at 135°C) specimens with AAG-1 was approximately 5°C warmer than for unaged specimens. For aged (135°C) specimens with asphalt AAK-2, fracture temperature was approximately 10°C warmer. This situation may be due to the chemical composition of asphalt cement. It is understood that the degree of increase in viscosity caused by aging depends on the amount of asphaltenes in the asphalt cement (Petersen 1990). The increase in the viscosity of asphalt cement caused by aging is greater for asphalt cement containing more asphaltenes. The asphaltene content (n-heptane + iso-octane) of the asphalt cements used in this study is 21.7 percent in asphalt AAK-2 and 9.1 percent in asphalt AAG-1. It follows that when evaluating the low-temperature cracking characteristics of asphalt concrete mixtures, long-term aging of the mixtures is required.

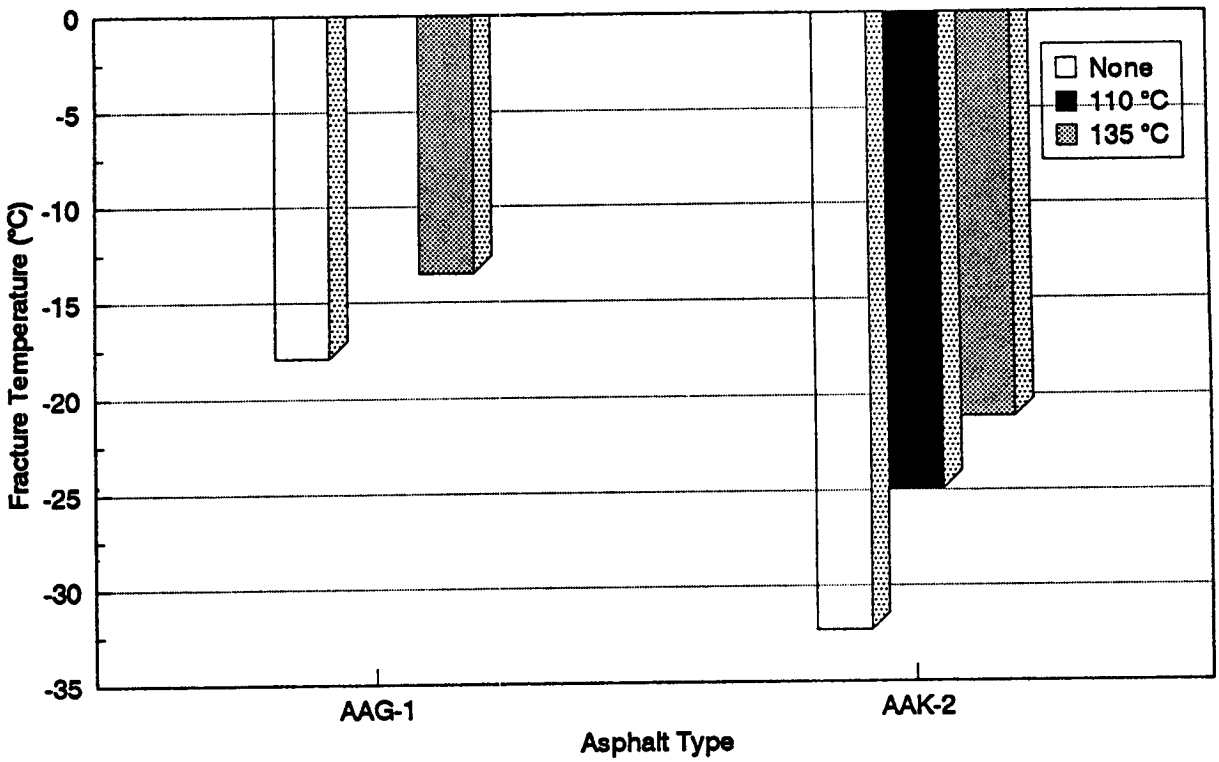


**Figure 6.15. Effect of aging on fracture temperature**

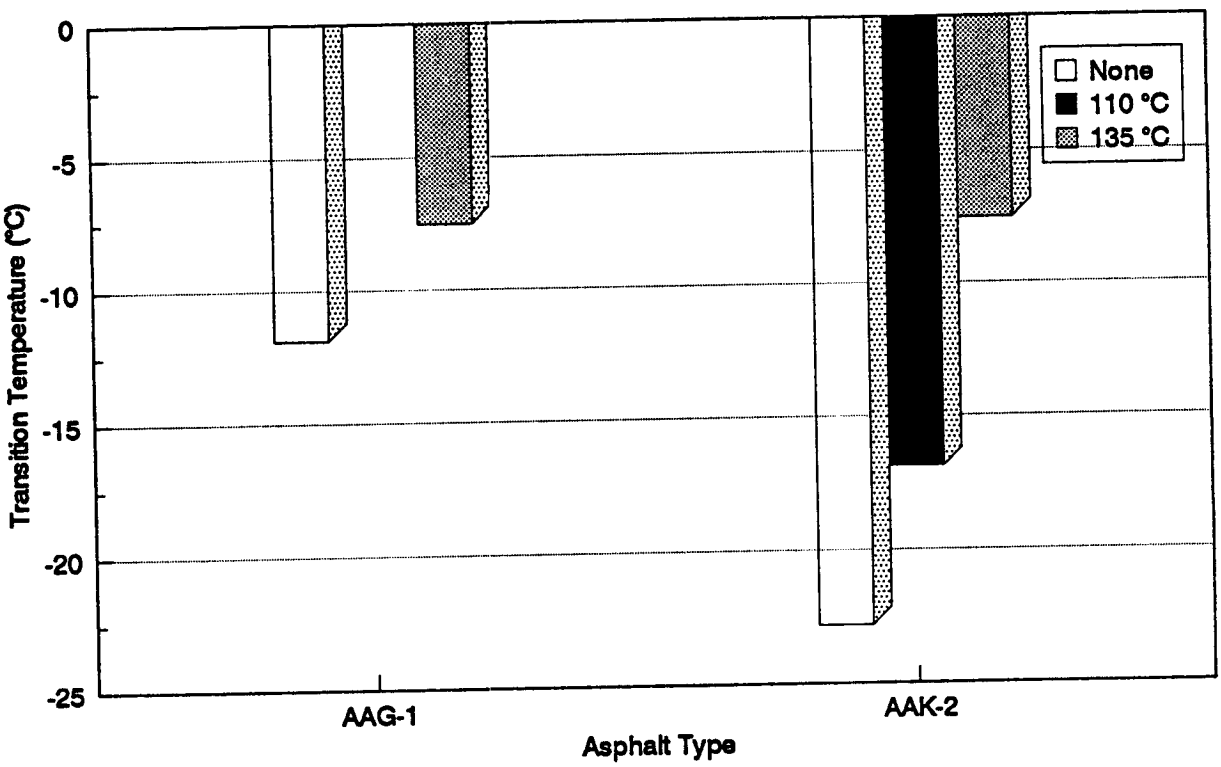


**Figure 6.16. Effect of aging on transition temperature**

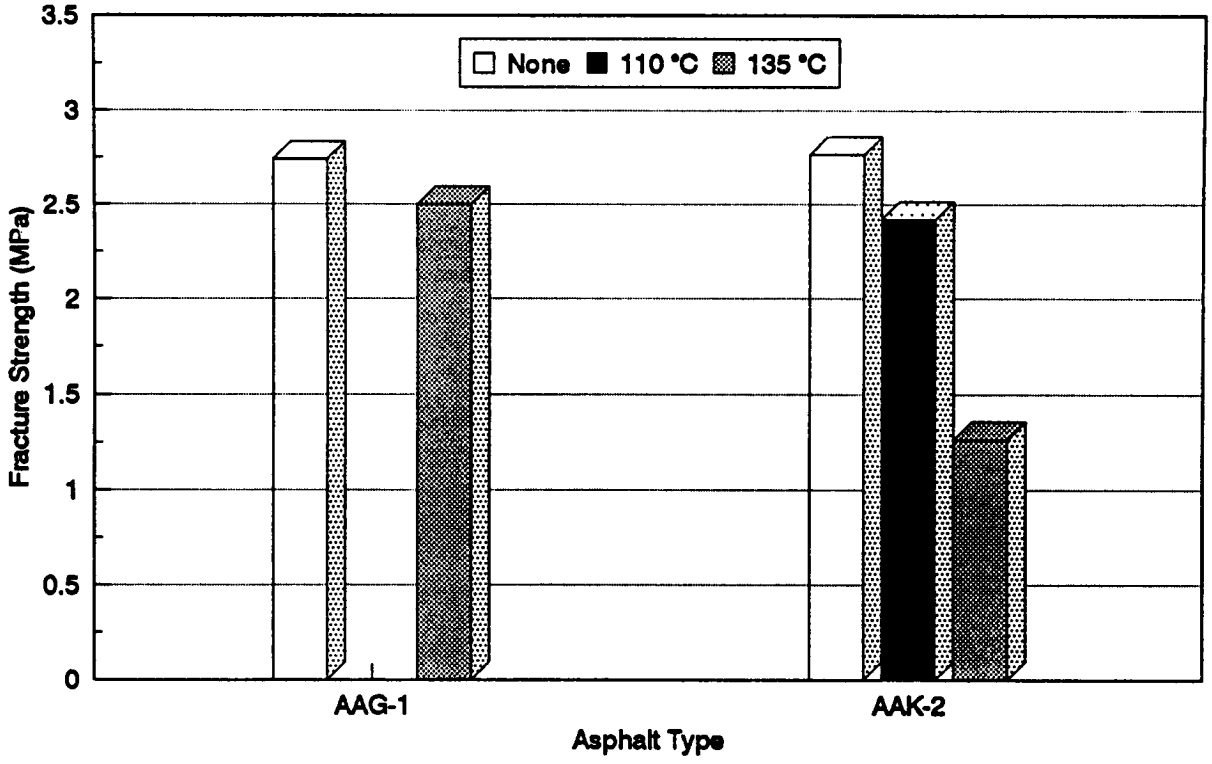


**Figure 6.17. Effect of aging on fracture strength**

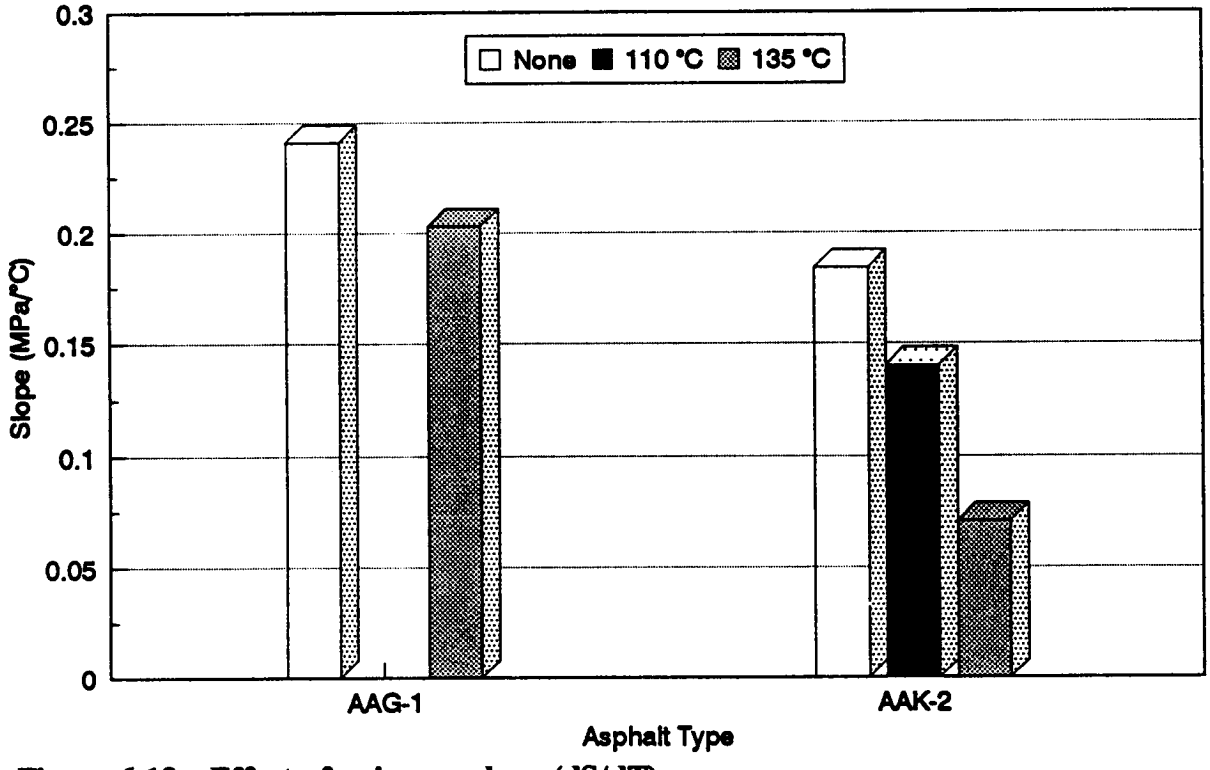


**Figure 6.18. Effect of aging on slope (dS/dT)**

## 6.7 Discussion

The repeatability of TSRST was evaluated based on the coefficient of variation for fracture and transition temperature, fracture strength, and slope. The repeatability of TSRST is excellent for fracture and transition temperatures, and reasonable for fracture strength and slope. The coefficients of variation for fracture and transition temperatures were below 10 percent. For fracture strength and slope, the coefficients of variation were generally below 20 percent.

From the statistical analysis of TSRST results over a range of condition, all the variables considered in the experiment designs are identified as significant factors of test results. These include asphalt type, aggregate type, air voids content, specimen size, degree of aging, stress relaxation, and cooling rate. Fracture and transition temperatures are most affected by asphalt type. They are affected to a lesser extent by aggregate type, specimen size, degree of aging, and cooling rate. Fracture strength and slope are most affected by air voids content and aggregate type. They are also affected by asphalt type, stress relaxation, and cooling rate to a lesser extent.

The low-temperature cracking resistance performance ranking of asphalts based on fracture temperature is AAK-2> AAK-1> AAG-2> AAG-1 for all variables considered. The ranking of asphalts identified from TSRST is in excellent agreement with the ranking based on the physical properties of the asphalt cements. Fracture strength is not considered to be sensitive to asphalt type.

The RB aggregate showed better resistance to low-temperature cracking than the RL aggregate. The fracture temperature of specimens with RB aggregate was colder than specimens with RL aggregate. Fracture strength was greater for specimens with RB aggregate than for specimens with RL aggregate. The better performance of the RB aggregate may be attributed to its rough surface texture and angular shape. Aggregate with a rough surface texture and angular shape can provide more bonding and interlocking between aggregate and asphalt cement, thereby leading to a higher fracture strength and a colder fracture temperature.

Considering the effect of specimen size, fracture temperature was colder for larger specimens. This situation may be due to the fact that it takes a larger specimen longer to reach thermal equilibrium. The fracture strength of a smaller specimen was slightly greater. This result is somewhat surprising because the aspect ratio (length/width) of the smaller specimen (5.3) was a little larger than that of the larger specimen (5.0).

The decrease in fracture temperature caused by stress relaxation was significant for specimens with stiffer asphalts (AAG-1 and AAG-2). But no significant decrease in fracture temperature was observed for specimens with softer asphalts (AAK-1 and AAK-2). Fracture strength was greater for nonrelaxed specimens. If stresses in the specimen are allowed to relax, the specimen will undergo less internal stress buildup with additional cooling. Thus, the time to reach fracture is delayed and the specimen will break at a colder temperature under a lower stress level.

As the cooling rate increases, fracture temperature becomes warmer and fracture strength tends to increase. At slower cooling rates (which result in longer loading time), stresses in the specimen will be relaxed and this fracture will occur at lower strength and colder temperature. Contrary to this hypothesis, fracture temperature was slightly colder at a cooling rate of 10°C/hr than at 5°C/hr.

As the specimen is aged, the asphalt cement becomes stiffer and the specimen is more resistant to deformation. That is, less stresses will be relaxed during cooling, which results in fracture at a warmer temperature. Fracture strengths were lower for aged specimens than for unaged specimens. This situation may be due to microcracks caused by aging. The effect of aging on fracture strength is inconclusive.

# 7

# Fundamental Properties of Asphalt Cement

As indicated by the statistical analyses, the fracture temperatures of asphalt concrete mixtures are most affected by asphalt type. Air voids content, specimen size, and aggregate type have much less influence on fracture temperature. Thus, an effort was made to relate fracture temperature to fundamental properties of asphalt cements. In addition, fracture temperature was related to two temperature susceptibility indices, namely, the penetration index and penetration viscosity number.

To evaluate the relationship between fracture temperatures and fundamental properties of asphalt cements, linear regression analyses were performed on test results for both 3.8 cm × 3.8 cm × 20.3 cm specimens with RB aggregate, 20.3/3.8 (RB), and 5.0 cm × 5.0 cm × 25.0 cm specimens with RB and RL aggregates, 25/5 (RB) and 25/5 (RL).

The fundamental properties of asphalt cements considered were penetration at 25°C, viscosity at 60°C, viscosity ratio at 60°C, and ring and ball (R&B) softening point. The penetration index (PI) and penetration viscosity number (PVN) were calculated using properties of asphalt cements.

## 7.1 Penetration

Figure 7.1 shows the relationship between least-square mean (LSMEAN) of fracture temperature and penetration at 25°C. The penetration of asphalt cement at 25°C is obviously related to the fracture temperature of asphalt concrete mixes. In general, fracture temperature tends to be colder for softer asphalt cement. A definitive linear relationship between penetration at 25°C and fracture temperature could not be established.

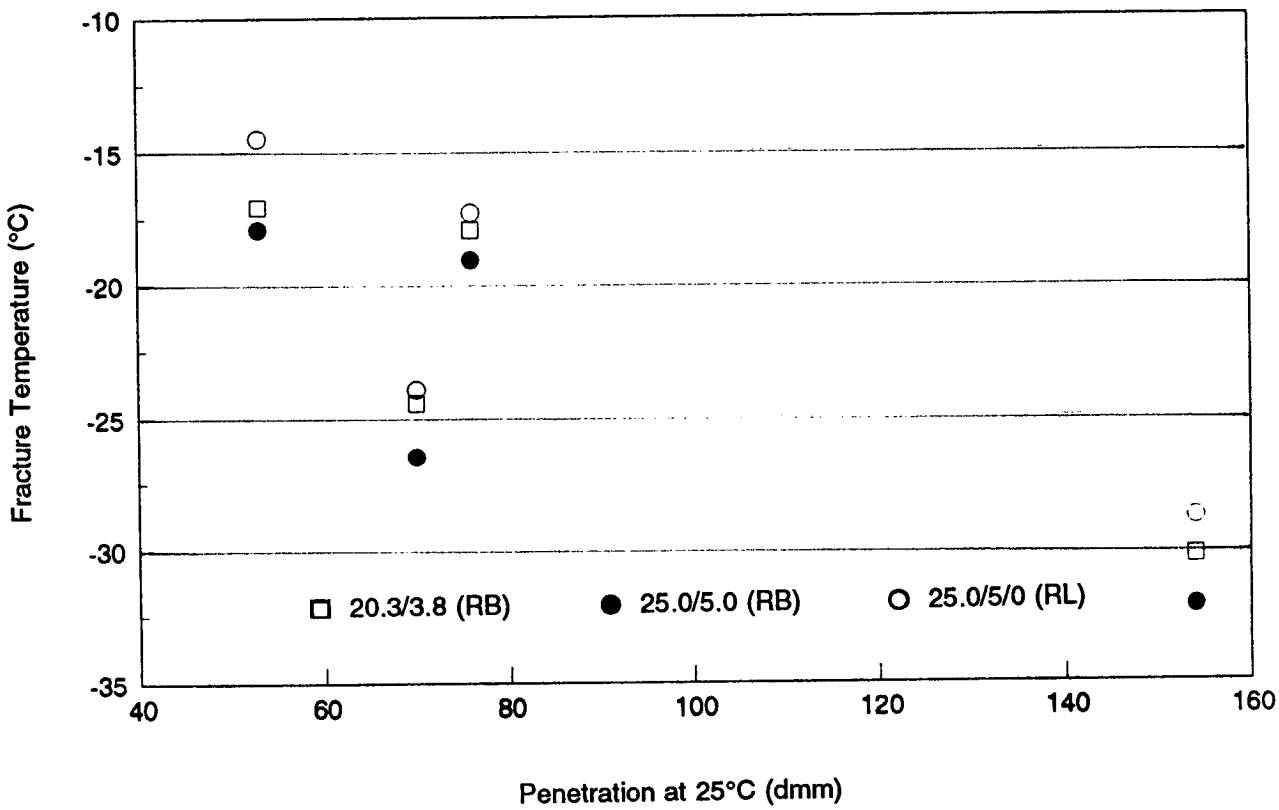


**Figure 7.1. Fracture temperature versus penetration at 25°C**

## 7.2 Viscosity Ratio

Fracture temperature can be related to the viscosity ratio of asphalt cement at 60°C. From the linear regression analysis, a regression model that relates viscosity ratio to fracture temperature was obtained for each data set. Summary statistics of the linear regression analysis are given in Table 7.1.

The R-squared value for each data set is over 0.80, and coefficients of variation are less than 10 percent. Figure 7.2 shows regression lines together with LSMEAN of observed fracture temperatures for 20.3/3.8 and 25/5 specimens with RB aggregate and for a 25/5 specimen with RL aggregate. Fracture temperature tends to be colder as viscosity ratio increases.

## 7.3 Temperature Susceptibility

As shown in Figure 7.3, there is no definite relationship between fracture temperature and PI. Fracture temperature tends to be colder as the PI increases.

Figure 7.4 shows the relationship between fracture temperature and PVN. Fracture temperature tends to be colder for asphalt concrete mixtures containing asphalt cements with greater PVNs. A definite relationship between fracture temperature and PVN could not be established.

## 7.4 Penetration and Viscosity

Fracture temperature can be correlated to penetration at 25°C combined with viscosity at 60°C. From the linear regression analysis, a regression model that combines penetration and viscosity to predict fracture temperature was obtained for each data set. Summary statistics of the linear regression analysis are presented in Table 7.2.

R-squared values for each case are above 0.94. The coefficients of variation for each data set are less than 5 percent. The first three graphs in Figure 7.5 show a regression line together with LSMEAN of the observed fracture temperatures. Observed fracture temperatures are highly correlated to predicted fracture temperature. The fourth graph in Figure 7.5 shows a regression line that considers all data sets together with observed fracture temperature. Although the root mean square error (MSE) for the overall regression model is higher than that for the individual models, observed fracture temperatures for cases of 20.3/3.8 (RB) and 25/5 (RB) are within or close to the 95 percent confidence interval. An excellent correlation between predicted and observed fracture temperature was obtained.

**Table 7.1. Summary statistics of linear regression analysis with viscosity ratio at 60°C**

| | Parameter Estimate | | | | |
|---|---|---|---|---|---|
| Data Set | Intercept | Viscosity Ratio | Root MSE | C.V. (%) | $R^2$ |
| 20.3/3.8 (RB) | -4.67784 | -7.50016 | 2.22053 | 9.78 | 0.84 |
| 25/5 (RB) | -4.69157 | -7.92638 | 2.09387 | 8.80 | 0.87 |
| 25/5 (RL) | -2.60896 | -7.83464 | 1.92207 | 9.03 | 0.89 |
| All | -4.19776 | -7.73321 | 2.23321 | 9.82 | 0.84 |

**Table 7.2. Summary statistics of linear regression analysis with penetration at 25°C and viscosity at 60°C**

| | Parameter Estimate | | | | | |
|---|---|---|---|---|---|---|
| Data Set | Intercept | Penetration | Viscosity | Root MSE | C.V. (%) | $R^2$ |
| 20.3/3.8 (RB) | -2.57138 | -0.15956 | -0.00328 | 1.09586 | 4.83 | 0.96 |
| 25/5 (RB) | -1.56132 | -0.17434 | -0.00386 | 0.99036 | 4.17 | 0.97 |
| 25/5 (RL) | -0.32668 | -0.16257 | -0.00368 | 0.99272 | 4.67 | 0.97 |
| All | -1.66551 | -0.16461 | -0.00364 | 1.42548 | 6.27 | 0.94 |

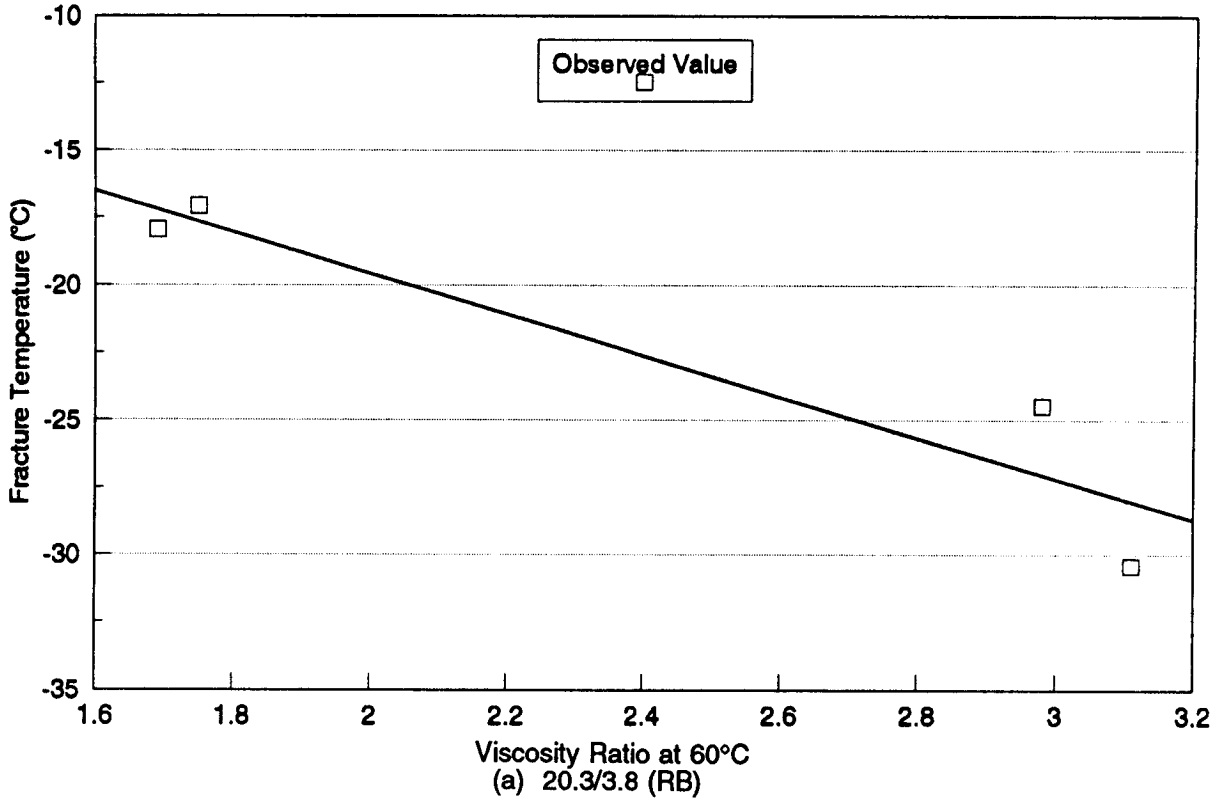


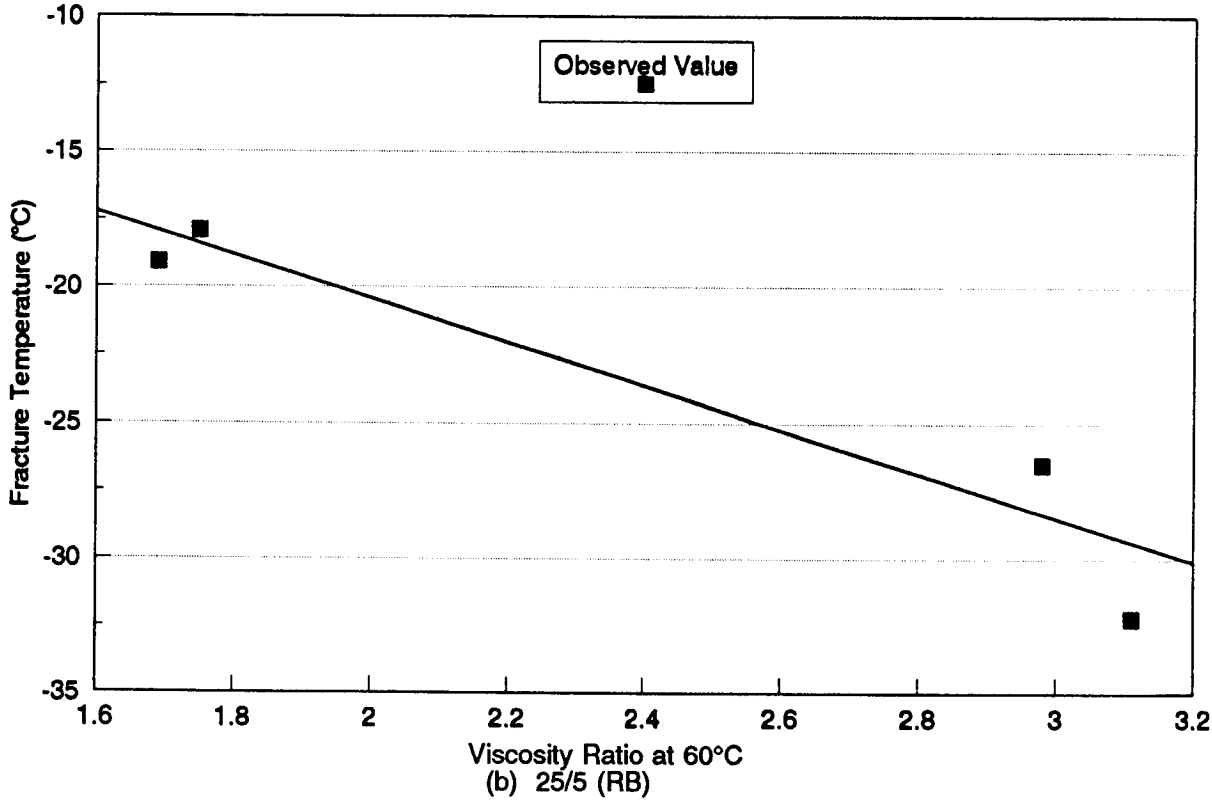


**Figure 7.2. Fracture temperature versus viscosity ratio at 60°C**

Continued on next page

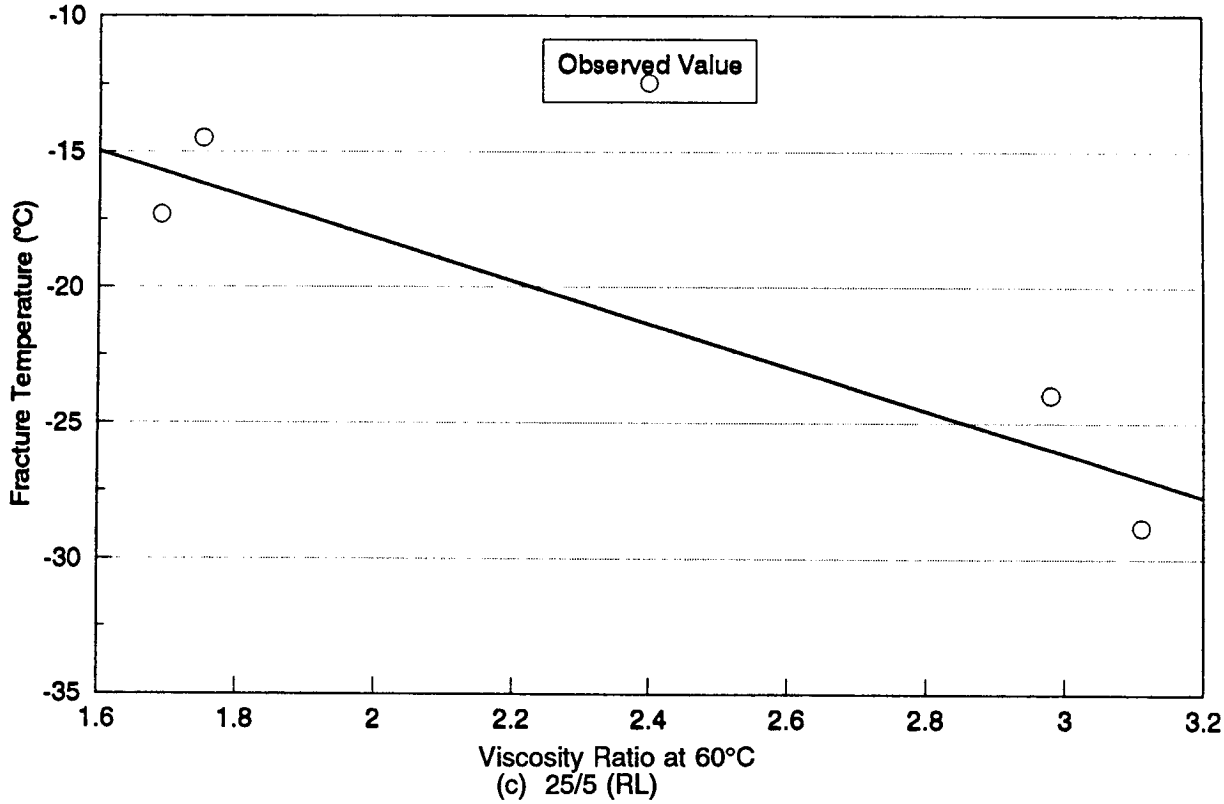


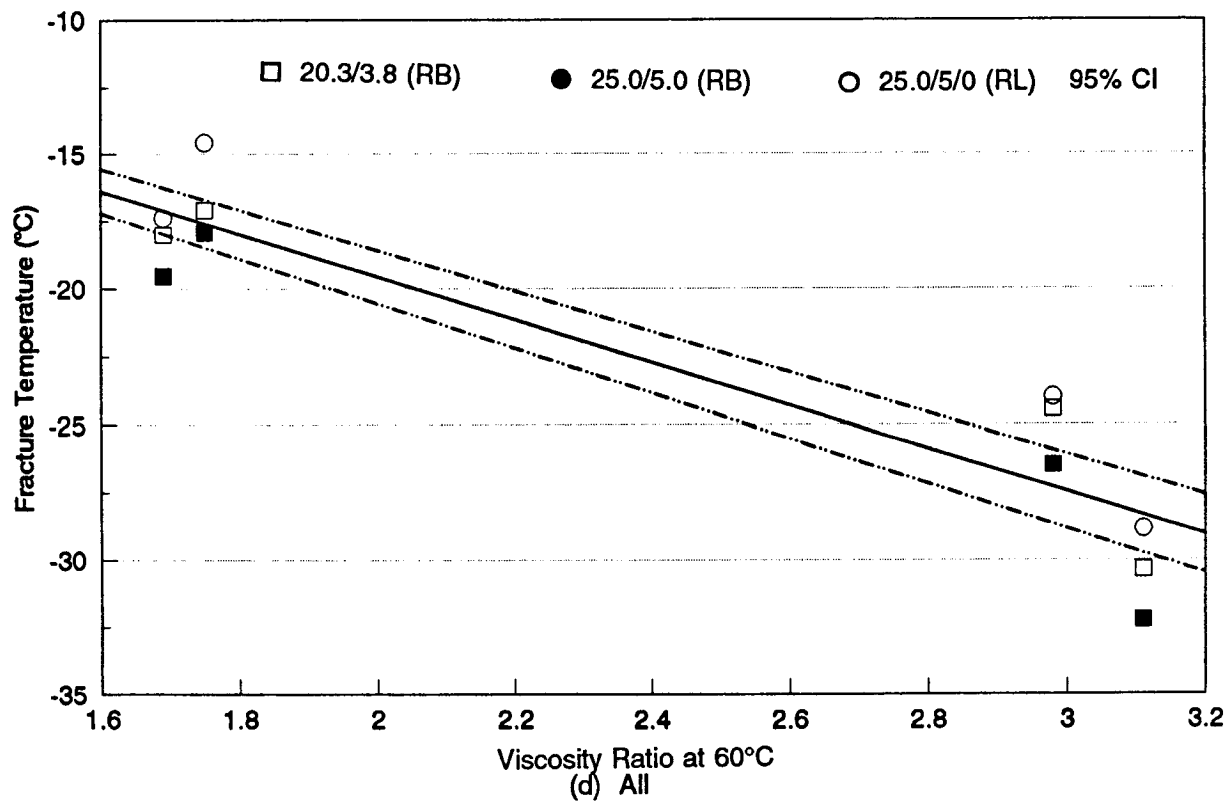


**Figure 7.2 (continued). Fracture temperature versus viscosity ratio at 60°C**

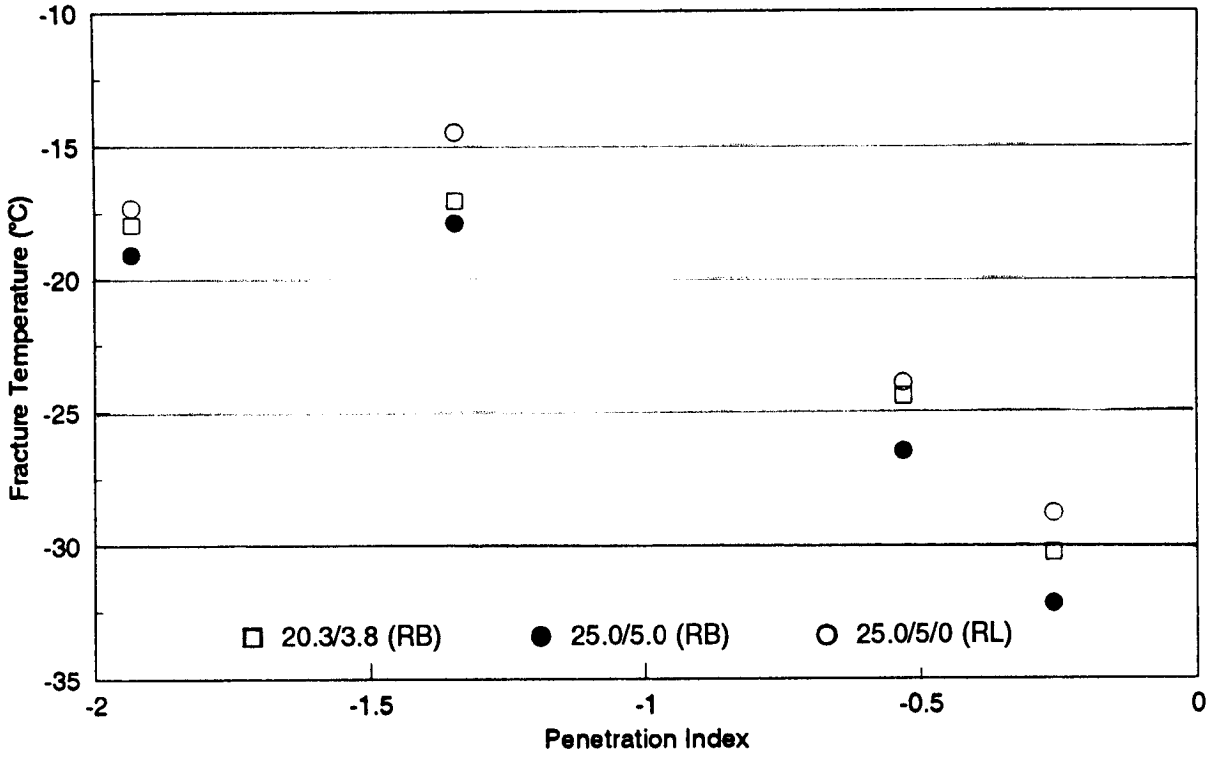


**Figure 7.3. Fracture temperature versus PI**

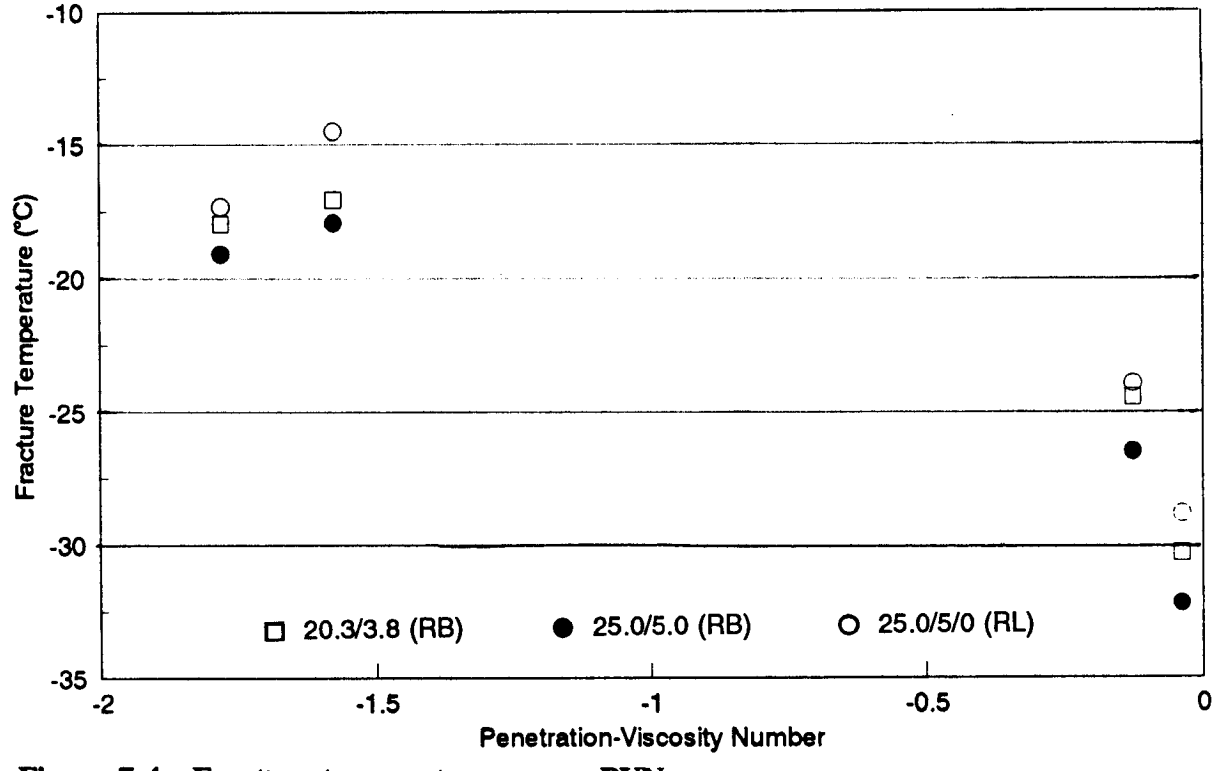


**Figure 7.4. Fracture temperature versus PVN**

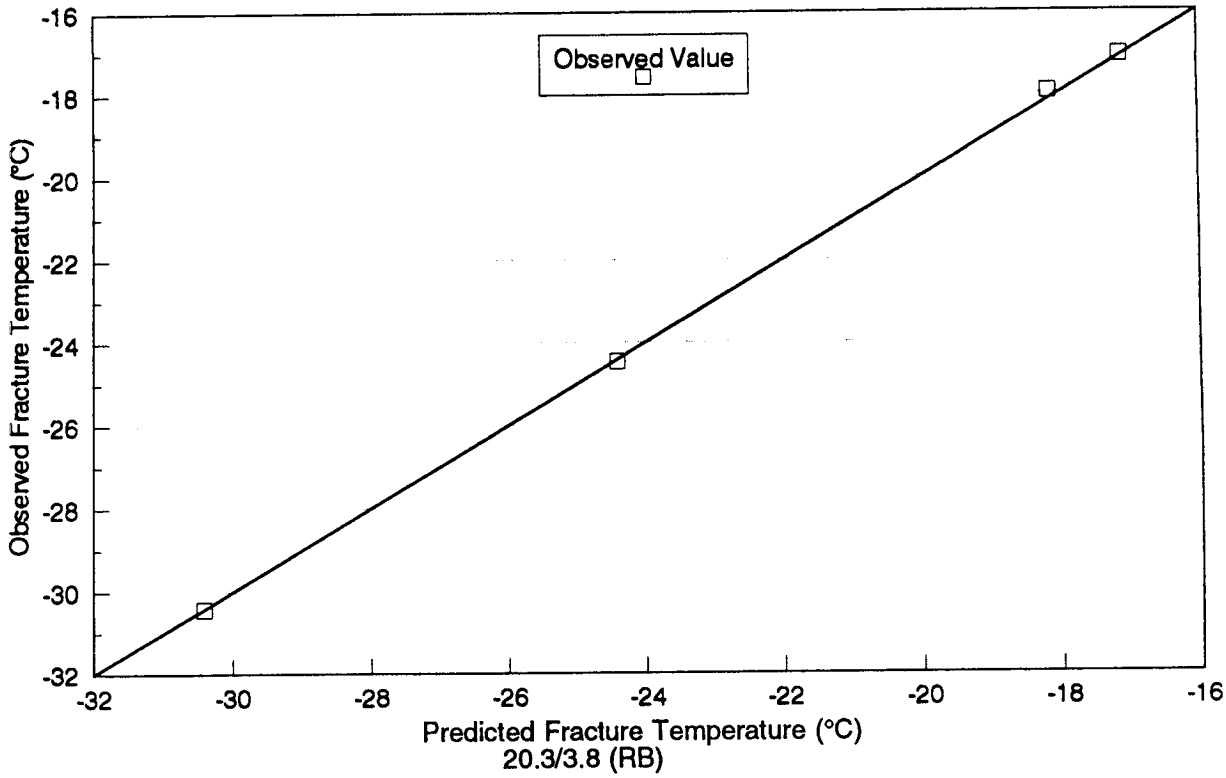


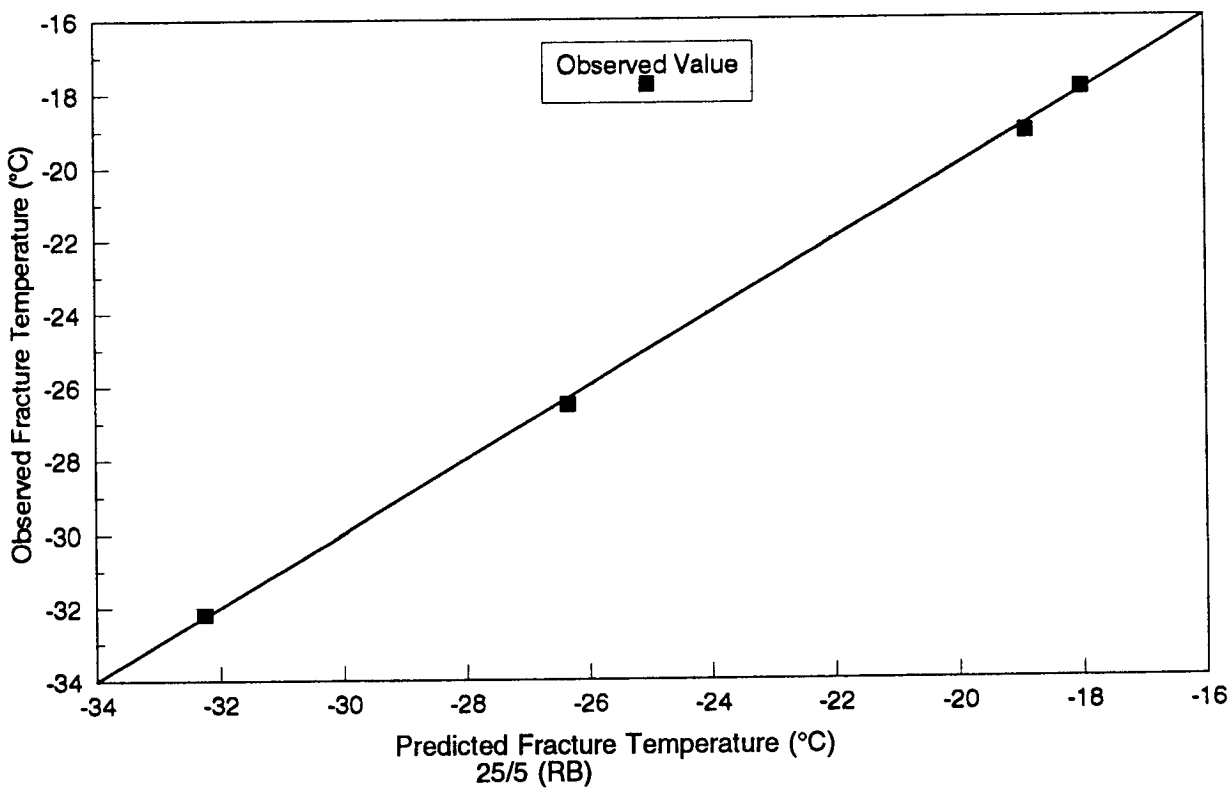


**Figure 7.5. Prediction of fracture temperature with penetration at 25°C and viscosity at 60°C**

Continued on next page

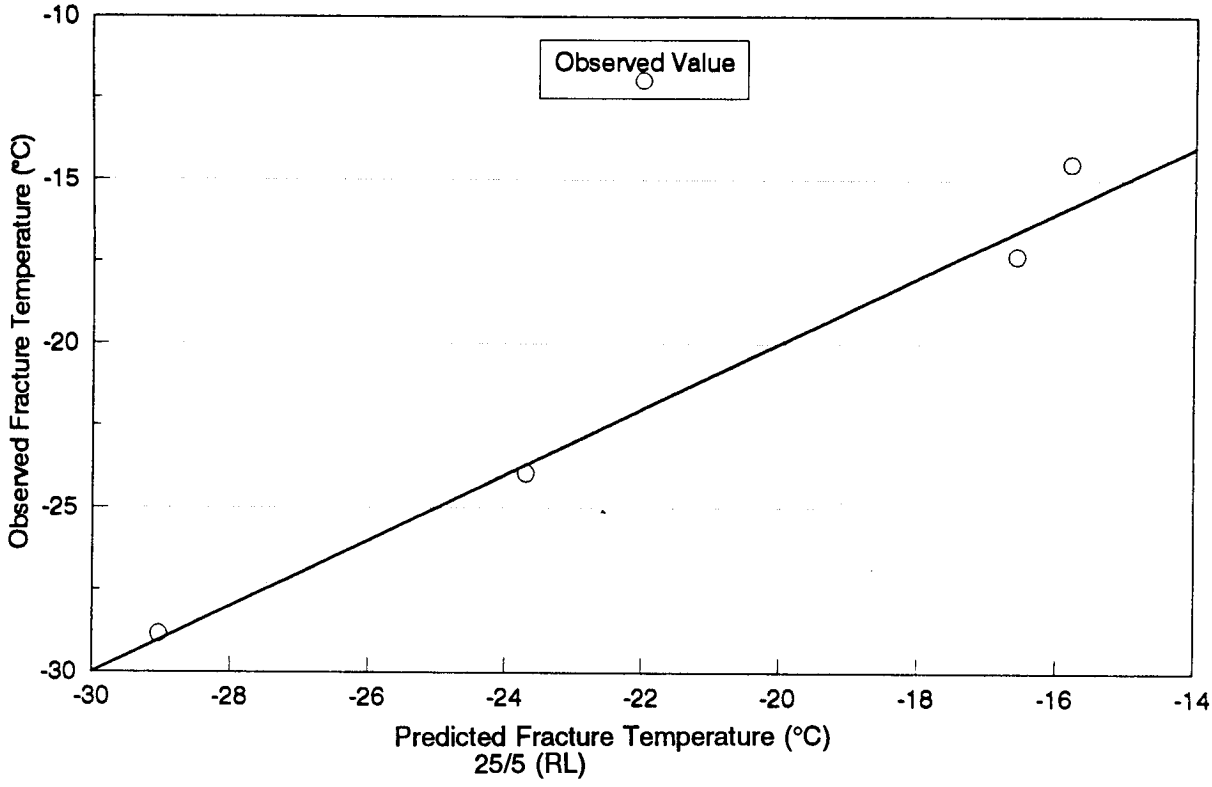


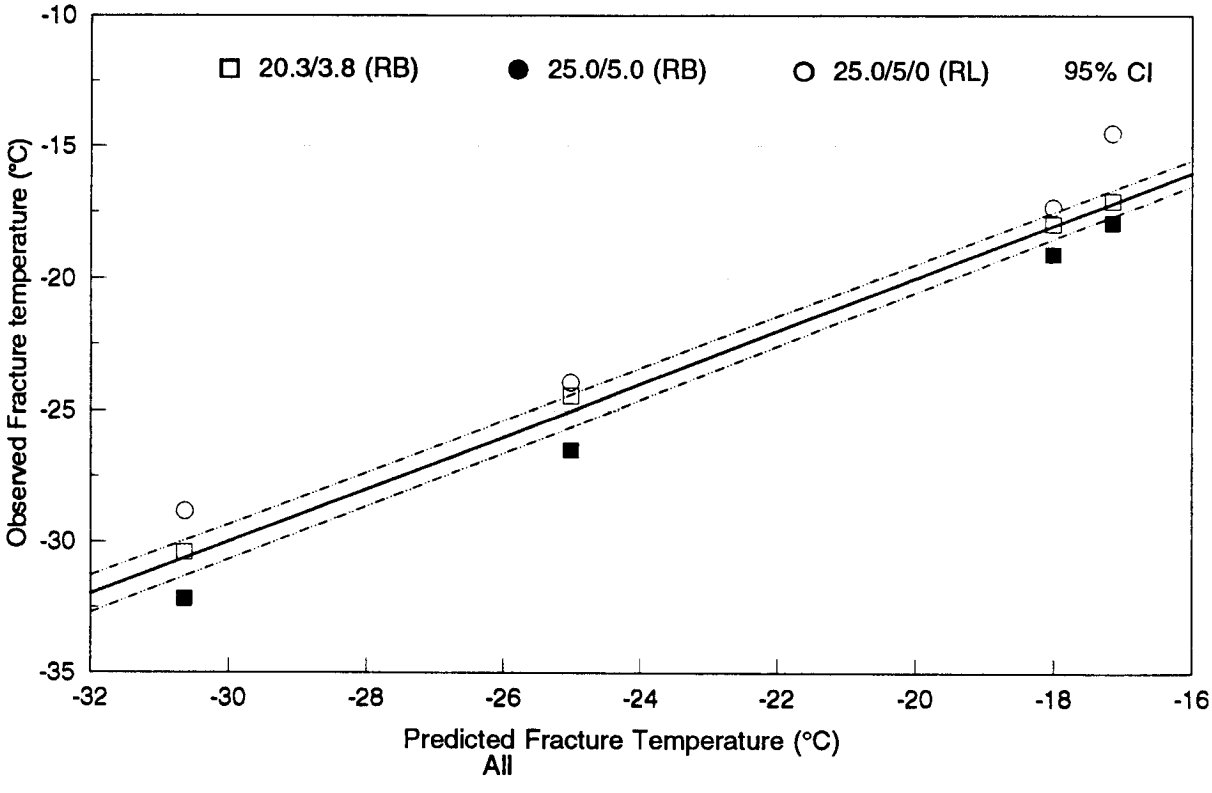


**Figure 7.5 (continued). Prediction of fracture temperature with penetration at 25°C and viscosity at 60°C**

## 7.5 Penetration and R&B Softening Point

Fracture temperature can also be correlated to penetration at 25°C combined with the R&B softening point. From the linear regression analysis with penetration at 25°C and the R&B softening point, a regression model that combines penetration and the R&B softening point was obtained for each data set (Table 7.3).

R-squared values for all cases are over 0.85. The coefficient of variation is greatest for the 5.0 cm × 5.0 cm × 25.0 cm specimens with RL aggregate. Figure 7.6 shows a regression line together with LSMEAN of observed fracture temperatures for each data set. There is a good correlation between predicted and observed fracture temperature. The fourth graph in Figure 7.6 shows a regression line that considers all data sets together with observed fracture temperature. Fracture temperatures for specimens with asphalt AAG-2 tend to be outside the 95 percent confidence interval.

## 7.6 Discussion

Penetration at 25°C, the penetration index, and the penetration viscosity number can only provide a general trend of fracture temperature of asphalt concrete mixtures.

The viscosity ratio at 60°C showed a possibility of good correlation with fracture temperature. However, at this time, it is not definite since the asphalts selected in the experiments had two extremes of viscosity ratio with no intermediate data.

The penetration at 25°C combined with the viscosity at 60°C or the R&B softening point showed good correlations with fracture temperature. Fracture temperatures predicted from the penetration at 25°C combined with the viscosity at 60°C are in excellent agreement with observed values. The R-squared values were over 0.95 and the coefficients of variation were below 5 percent. Fracture temperatures predicted from the penetration at 25°C combined with the R&B softening point are also in good agreement with observed values. The coefficients of variation and the root MSE are greater for the latter correlation than for the former correlation.

**Table 7.3. Summary statistics of linear regression analysis with penetration at 25°C and R&B softening point**

| | Parameter Estimate | | | | | |
|---|---|---|---|---|---|---|
| **Data Set** | **Intercept** | **Penetration** | **R&B** | **Root MSE** | **C.V. (%)** | **$R^2$** |
| 20.3/3.8 (RB) | 50.58555 | -0.19663 | -1.21082 | 1.70245 | 7.50 | 0.91 |
| 25/5 (RB) | 63.90138 | -0.22279 | -1.48065 | 1.94318 | 8.19 | 0.89 |
| 25/5 (RL) | 49.25994 | -0.19295 | -1.16067 | 2.34335 | 11.01 | 0.85 |
| All | 55.75106 | -0.20437 | -1.31248 | 2.14609 | 9.44 | 0.86 |

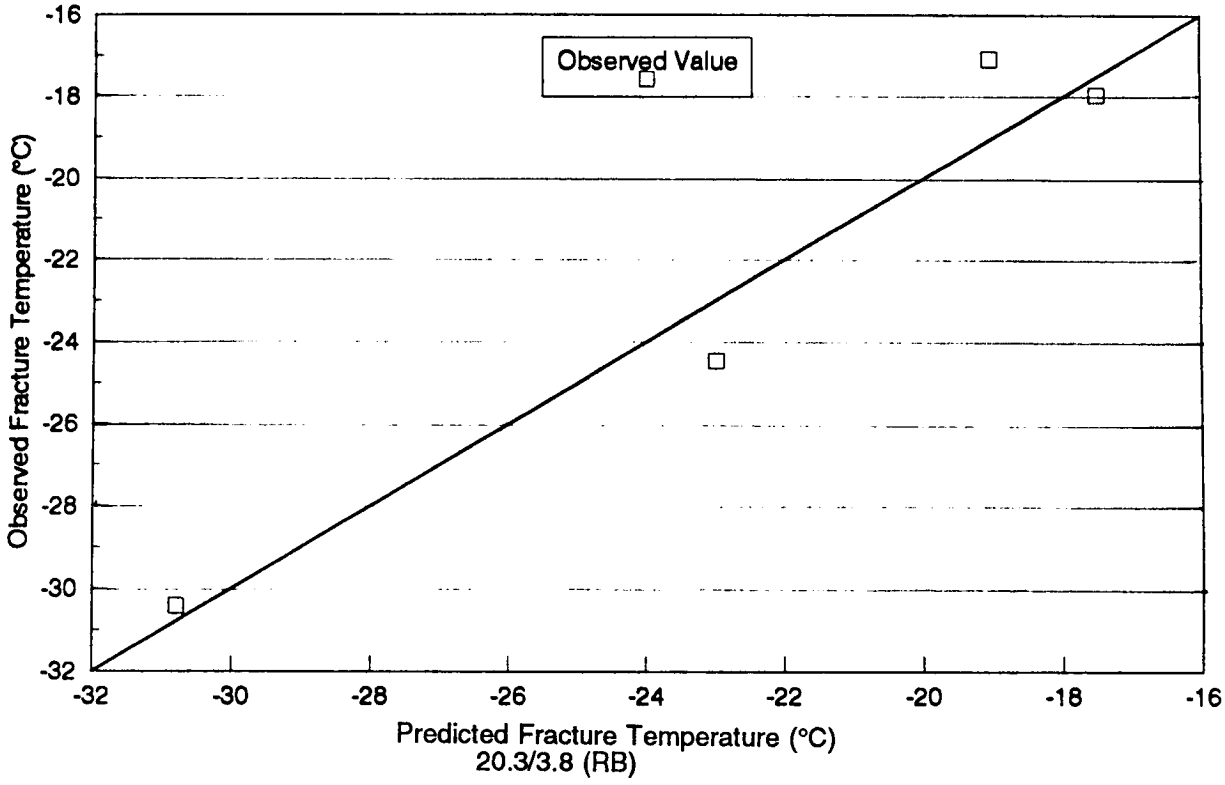


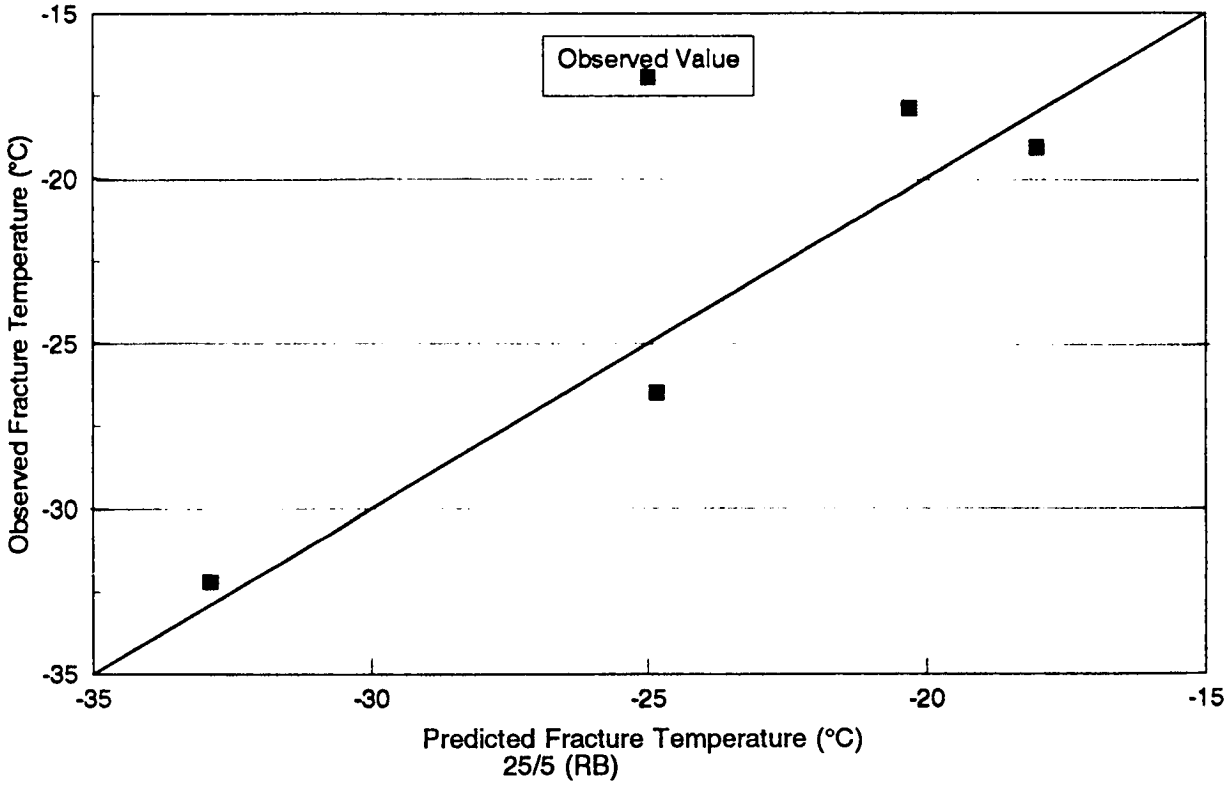


**Figure 7.6. Prediction of fracture temperature with penetration at 25°C and R&B softening point**

continued on next page

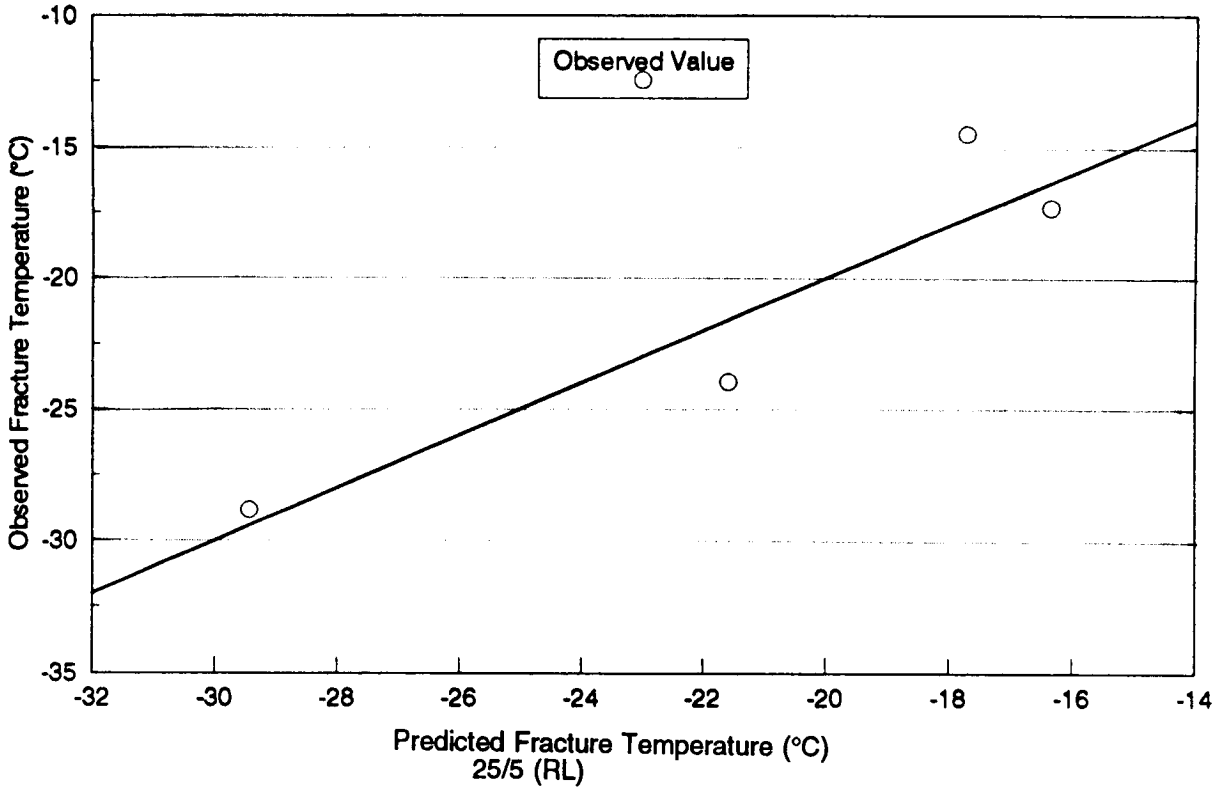


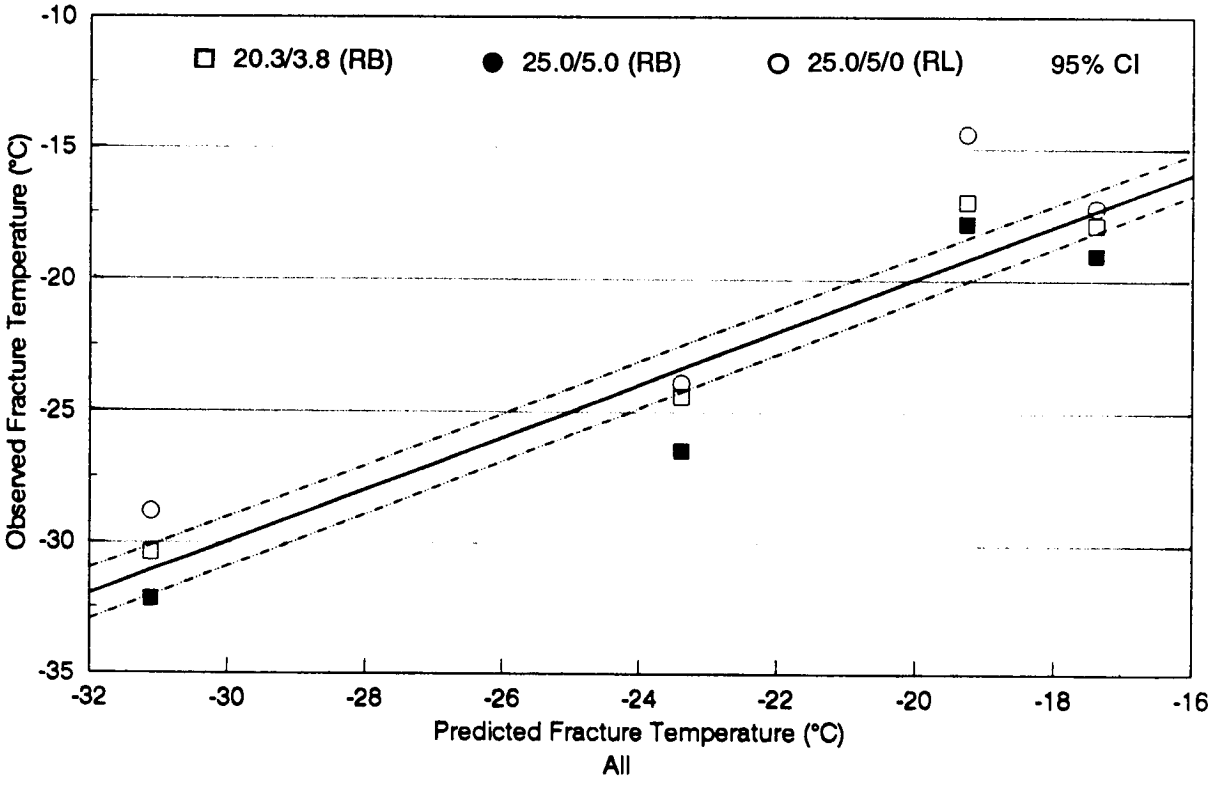


**Figure 7.6 (continued). Prediction of fracture temperature with penetration at 25°C and R&B softening point**

# 8

# Conclusions and Recommendations

## 8.1 Conclusions

Based on the results presented herein, the following conclusions can be made:

- The repeatability of TSRST based on the coefficient of variation is estimated as excellent for fracture and transition temperatures and good for fracture strength and slope.

- TSRST results provide an excellent indication of the low-temperature cracking resistance of asphalt concrete mixtures. A ranking of this resistance based on TSRST results is in good agreement with a ranking based on the physical properties of the asphalt cements used in the mixtures.

- All the variables considered in the experiment designs are identified as significant factors in the TSRST results. Variables include asphalt type, aggregate type, air voids content, specimen size, degree of aging, stress relaxation, and cooling rate. The interactions among variables are not significant except for the interaction between asphalt type and stress relaxation.

- Fracture and transition temperature are most sensitive to asphalt type but are also affected by aggregate type, specimen size, degree of aging, and cooling rate. Fracture strength and slope are most sensitive to air voids content followed by aggregate type. They are also affected by asphalt type, stress relaxation, and cooling rate.

- Aggregates with a rough surface texture and angular shape resist low-temperature cracking better, which leads to fracture at a higher stress level and colder temperature.

- Test results were affected by specimen size. Fracture temperature was colder for larger specimens. The fracture strength of smaller specimens was greater.

- Stress relaxation tends to lower fracture temperature and decrease fracture strength. The fracture temperature was colder for relaxed specimens than for nonrelaxed specimens. The decrease in fracture temperature caused by stress relaxation was significant for stiffer asphalts and not significant for softer asphalts. Fracture strength was lower for relaxed specimens.

- Cooling rate influences test results. A slower cooling rate allows more stress relaxation, thereby leading to fracture at a colder temperature and a lower stress level. As the cooling rate was increased, warmer fracture temperatures were observed and fracture strength tended to increase.

- The degree of aging affects the specimen's fracture temperature. As the specimen is aged, fracture temperature is warmer. At this time, the effect of aging on fracture strength is inconclusive.

- The penetration of asphalt cement at 25°C combined with the viscosity at 60°C or the ring and ball (R&B) softening point provide an excellent possibility for predicting the fracture temperature of asphalt concrete mixtures. The penetration index and penetration viscosity number did not provide a good definitive relationship with fracture temperature.

## 8.2 Recommendations

It is highly recommended that TSRST be used in routine mix designs and in expanded studies to evaluate the low-temperature cracking resistance of asphalt concrete mixtures. Based on the laboratory test results presented herein, TSRST convincingly demonstrates the effect of various mix and field variables on the low-temperature cracking resistance of such mixtures. The variables that significantly affect low-temperature cracking resistance in this study include asphalt cement type, aggregate type, aging, cooling rate (equivalent to loading rate), and stress relaxation. It is recommended that future studies with TSRST include the following:

1. An extensive range of asphalt types including modified asphalt cements.
2. A range of aggregate types to reflect differences in surface texture and particle shape.
3. Short-term and long-term age conditioning.
4. Slower cooling rates (1°C/hr).
5. Cylindrical and beam specimens.

In addition, it is also highly recommended that the following be tested in TSRST:

1. Modified asphalt cement concrete mixtures.
2. Large stone mixes.
3. Stone mastics.
4. Mixtures with asphalt cements that contain with different amounts of waxes and asphaltenes.

# 9

# References

American Standards of Testing Materials (1990). Road and paving materials; traveled surface characteristics. Annual Book of ASTM Standards, Vol. 04.03.

Anderson, D. A., D. W. Christenson, R. Dongre, M. G. Sharma, J. Runt, and P. Jordhal (1989). Asphalt behavior at low service temperatures. Report No. FHWA-RD-88-078, The Pennsylvania Transportation Institute, University Park, PA.

Anderson, K. O., and S. C. Leung (1987). Applications of a method for evaluation of low temperature tensile properties of asphalt concrete. Proceedings, Paving in Cold Areas Mini-Workshop, pp. 335-366.

Arand, W. (1987). Influence of bitumen hardness on the fatigue behavior of asphalt pavements of different thickness due to bearing capacity of subbase, traffic loading, and temperature. Proceedings, Sixth International Conference on Structural Behavior of Asphalt Pavements, University of Michigan, pp. 65-71.

Benson, P. E. (1976). Low temperature transverse cracking of asphalt concrete pavements in central and west Texas. Report No. TTI-2-9-72-175-2F. Texas Transportation Institute, Texas A&M University.

Busby, E. O., and L. F. Rader (1972). Flexural stiffness properties of asphalt concrete at low temperatures. Proceedings, Association of Asphalt Paving Technologists (AAPT), Vol. 41, pp. 163-187.

Carpenter, S. H (1983). Thermal cracking in asphalt pavements: an examination of models and input parameters. United States Army Corps of Engineers Cold Regions Research and Engineering Laboratory.

Carpenter, S. H., and T. VanDam (1985). Evaluation of low temperature performance of asphalt cements. United States Army Corps of Engineers Cold Regions Research and Engineering Laboratory.

Christison, J. T., D. W. Murray, and K. O. Anderson (1972). Stress prediction and low-temperature climatic environments. Proceedings, Third International Conference on the Structural Design of Pavements, London.

Committee on Characteristics of Bituminous Materials (1988). Low temperature properties of paving asphalt cements. State of the Art Report, Transportation Research Board.

Fabb, T. R. J. (1974). The influence of mix composition, binder properties and cooling rate on asphalt cracking at low temperature. Proceedings, AAPT, Vol. 43, pp. 285-331.

Finn, F. N., C. L. Saraf, R. Kulkarni, K. Nair, W. Smith, and A. Abdullah (1986). Development of pavement structural subsystems. National Cooperative Highway Research Program Report 291.

Fromm, H. J., and W. A. Phang (1972). A study of transverse cracking of bituminous pavements. Proceedings, AAPT, Vol. 41, pp. 383-423.

Haas, R. (1973). A method for designing asphalt pavements to minimize low-temperature shrinkage cracking. Research Report No. RR-73-1, Asphalt Institute.

Haas, R., F. Meyer, G. Assaf, and H. Lee (1987). A comprehensive study of cold climate asphalt pavement cracking. Proceedings, AAPT, Vol. 56, pp. 198-245.

Hadipour, K., and K. O. Anderson (1988). An evaluation of permanent deformation and low temperature characteristics of some recycled asphalt concrete mixtures. Proceedings, AAPT, Vol. 57, pp. 615-645.

Harrigan, E. T., R. B. Leahy, and J. S. Youtcheff, ed. (1994). *The SUPERPAVE™ Mix Design System Manual of Specifications, Test Methods, and Practices*. Report No. SHRP-A-379. SHRP, National Research Council, Washington, DC.

Janoo, V. (1989). Performance of soft asphalt pavements in cold regions. USA CRREL Special Report.

Janoo, V. C., J. Bayer Jr., T. S. Vinson, and R. Haas (1990). Test methods to characterize low temperature cracking. Proceedings of the Fourth Workshop in Paving in Cold Areas, Sapporo, Japan.

Jones, G. M., M. I. Darter, and G. Littlefield (1968). Thermal expansion-contraction of asphaltic concrete. Proceedings, AAPT, Vol. 37, pp. 56-100.

Kallas, B. F. (1982). Low-temperature mechanical properties of asphalt concrete. Research Report No. RR-82-3, Asphalt Institute.

Lytton, R. L., U. Shanmugham, and B. Garrett (1983). Design of flexible pavements for thermal fatigue cracking. Research Report No. 184-4, Texas Transportation Institute, Texas A&M University.

Monismith, C. L., G. A. Secor, and K. E. Secor (1965). Temperature induced stresses and deformations in asphalt concrete. Proceedings, AAPT, Vol. 34, pp. 248-285.

Osterkamp, T. E., G. C. Baker, B. T. Hamer, J. P. Gosink, J. K. Peterson, and V. Groul (1986). Low temperature transverse cracks in asphalt pavements in interior Alaska. Report No. AD-RD-86-26, Alaska Department of Transportation.

Petersen, J. C. (1990). Effects of physical and physiochemical factors on asphalt oxidative aging. Serviceability and Durability of Construction Materials, Proceedings, First Materials Engineering Congress, American Society of Civil Engineers , Denver, Colorado, pp. 244-254.

Ruth, B. E., L. L. Bloy, and A. A. Avital (1982). Prediction of pavement cracking at low temperatures. Proceedings, AAPT, Vol. 51, pp. 53-103.

SAS Institute Inc. (1991a). SAS language guide for personal computers. Release 6.03 edition, Cary, N.C.

SAS Institute Inc. (1991b). SAS/STAT user's guide for personal computers. Release 6.03 edition, Cary, N.C.

Shahin, M. Y., and B. F. McCullough (1972). Prediction of low-temperature and thermal-fatigue cracking in flexible pavements. Report No. 123-14, Center for Highway Research, University of Texas.

Sugawara, T., H. Kubo, and A. Moriyoshi (1982). Low temperature cracking of asphalt pavements. Proceedings, Workshop in Paving in Cold Areas, Vancouver, B.C., Vol. 1, pp. 1-42.

Sugawara, T., and A. Moriyoshi (1984). Thermal fracture of bituminous mixtures. Proceedings, Paving in Cold Areas Mini-Workshop, pp. 291-320.

Transportation Research Board (1989). Consistency, setting rate, and temperature susceptibility of asphalts: 1960-1987 annotated bibliography. Bibliography 64, National Research Council, Washington, D.C.

Vinson, T. S., V. C. Janoo, and R. C. G. Haas (1990). Summary report on low temperature and thermal fatigue cracking. SHRP-A/IR-90-001, National Research Council, Washington, D.C.

# Appendix A
# Results of TSRST

**Table A.1. Results of TSRST with 3.8 × 3.8 × 20.8 cm specimens**

Aggregate Type: RB (Granite) Cooling Rate: 10°C/hr

| Specimen ID | Asphalt Type | Air Voids (%) | Fracture Strength (psi) | Fracture Strength (MPa) | Fracture Temp. (°C) | Transition Temp. (°C) | dS/dT (psi/°C) |
|---|---|---|---|---|---|---|---|
| BK1H-21 | AAK-1 | 7.7 | 338 | 2.332 | -27.0 | -16.3 | 18.1 |
| BK1H-2 | | 9.4 | 277 | 1.911 | -24.75 | -15 | 18.9 |
| BK1H-3 | | 8.3 | 294 | 2.029 | -23.0 | -16 | 22.2 |
| BK1H-40 | | 6.3 | 407 | 2.808 | -26.0 | -16.6 | 28.5 |
| BK1L-21 | | 3.2 | 423 | 2.919 | -23.5 | -14.3 | 27.2 |
| BK1L-32 | | 3.3 | 380 | 2.622 | -22.4 | -13.4 | 24.3 |
| BK1L-30 | | 3.1 | 535 | 3.692 | -24.1 | -13.7 | 31.2 |
| BK1L-40 | | 4.5 | 413 | 2.850 | -24.6 | -13.8 | 27.3 |
| BK2H-20 | AAK-2 | 7.8 | 380 | 2.622 | -31.2 | N/A | 25.9 |
| BK2H-31 | | 7.8 | 354 | 2.443 | -30.5 | N/A | 24.7 |
| NBK2H-4 | | 7.5 | 342 | 2.360 | -31.1 | -21.7 | 25.5 |
| BK2H-30 | | 6.3 | 342 | 2.360 | -30.7 | -20.6 | 22 |
| BK2H-36 | | 8.7 | 313 | 2.160 | -30.75 | -21.8 | 22.3 |
| BK2L-20 | | 3.6 | 589 | 4.064 | -29 | -20.4 | 39.4 |
| BK2L-40 | | 4.2 | 598 | 4.126 | -30.2 | -21.5 | 38.4 |
| BK2L-35 | | 3.8 | 569 | 3.926 | -29.75 | -20.5 | 36 |

Continued on next page

**Table A.1 (continued). Results of TSRST with 3.8 × 3.8 × 20.8 cm specimens**

Aggregate Type: RB (Granite) Cooling Rate: 10°C/hr

| Specimen ID | Asphalt Type | Air Voids (%) | Fracture Strength (psi) | Fracture Strength (MPa) | Fracture Temp. (°C) | Transition Temp. (°C) | dS/dT (psi/°C) |
|---|---|---|---|---|---|---|---|
| BG1H-10 | AAG-1 | 8.1 | 378 | 2.608 | -17.7 | -9.5 | 33 |
| BG1H-23 | | 7.7 | 330 | 2.277 | -18.0 | -10.0 | 29.3 |
| BG1H-44 | | 8.8 | 367 | 2.532 | -17.8 | -10.6 | 32.6 |
| BG1L-40 | | 3.2 | 523 | 3.609 | -15.3 | -8.9 | 41.3 |
| BG1L-10 | | 4.9 | 461 | 3.181 | -15.9 | -9.1 | 37.2 |
| BG1L-30 | | 4.5 | 512 | 3.533 | -16.9 | -9.1 | 40.4 |
| BG1L-41 | | 4.5 | 484 | 3.340 | -18.1 | -9.1 | 34.4 |
| BG2H-10 | AAG-2 | 9.2 | 393 | 2.712 | -19.85 | -12.1 | 31.8 |
| BG2H-12 | | 7.0 | 380 | 2.622 | -19.2 | -12.7 | 34 |
| BG2H-22 | | 7.5 | 305 | 2.105 | -17.85 | -11.2 | 30.4 |
| BG2H-40 | | 9.8 | 360 | 2.484 | -18.35 | -12.2 | 34.5 |
| BG2H-20 | | 4.5 | 496 | 3.422 | -17.80 | -11.2 | 43.3 |
| BG2H-30 | | 5.7 | 438 | 3.022 | -17.75 | -11.1 | 41 |
| BG2L-30 | | 6.0 | 356 | 2.456 | -16.9 | -11.2 | 34.8 |
| BG2L-14 | | 4.6 | 456 | 3.146 | -17.75 | -11 | 39.6 |

## Table A.2. Results of TSRST with 5 × 5 × 25 cm specimens (RB)

Aggregate Type: RB (Granite) Cooling Rate: 10°C/hr

| Specimen ID | Asphalt Type | Air Voids (%) | Fracture Strength (psi) | Fracture Strength (MPa) | Fracture Temp. (°C) | dS/dT (psi/°C) | Transition Temp. (°C) |
|---|---|---|---|---|---|---|---|
| RBK1H5 | AAK-1 | 7.2 | 421 | 2.905 | -26.7 | 29.3 | -19.2 |
| RBK1H7 | | 7.5 | 398 | 2.746 | -25.9 | 30.9 | -19.4 |
| BK1H11 | | 7.8 | 377 | 2.601 | -26.1 | 27.4 | -19.7 |
| RBK1L1 | | 3.5 | 518 | 3.574 | -26.1 | 37.6 | -18.7 |
| RBK1L2 | | 3.8 | 547 | 3.774 | -27.6 | 38.6 | -20.4 |
| RBK1L3 | | 3.7 | 480 | 3.312 | -25.4 | 35.4 | -18.9 |
| RBK1L4 | | 4.3 | 592 | 4.085 | -26.9 | 43.2 | -21 |
| RBK1L5 | | 3.4 | 576 | 3.974 | -26.2 | 39.7 | -19.2 |
| RBK2H1 | AAK-2 | 7.4 | 404 | 2.788 | -32.8 | 26.4 | -23.3 |
| RBK2H2 | | 7.9 | 269 | 1.856 | -31.8 | 20.5 | -22.1 |
| RBK2H4 | | 7.6 | 322 | 2.222 | -33.3 | 21.4 | -23.6 |
| RBK2L1 | | 3.6 | 576 | 3.974 | -31.4 | 39.4 | -22.5 |
| RBK2L2 | | 3.9 | 526 | 3.629 | -31.8 | 31.8 | -22.3 |
| RBG1H1 | AAG-1 | 6.8 | 305 | 2.105 | -18.7 | 24.5 | -10 |
| RBG1H3 | | 7.4 | 422 | 2.912 | -18.5 | 38.8 | -13.1 |
| RBG1H4 | | 7.4 | 416 | 2.870 | -18.1 | 38.7 | -12.7 |
| RBG1L1 | | 4.0 | 423 | 2.919 | -16.9 | 37.9 | -11.9 |
| RBG1L2 | | 4.5 | 529 | 3.650 | -18.0 | 44.3 | -11 |
| RBG1L4 | | 4.5 | 464 | 3.202 | -17.1 | 36.8 | |
| RBG2H1 | AAG-2 | 7.6 | 318 | 2.194 | -20.8 | 25.4 | -12.9 |
| RBG2H2 | | 6.9 | 308 | 2.125 | -17.7 | 31.9 | -13 |
| RBG2H4 | | 7.0 | 307 | 2.118 | -19.6 | 26.9 | -12.8 |
| RBG2L1 | | 3.3 | 471 | 3.250 | -19.1 | 41.3 | -13.7 |
| RBG2L2 | | 3.6 | 308 | 2.125 | -16.5 | 30.8 | -11.5 |
| RBG2L4 | | 3.6 | 518 | 3.574 | -20.2 | 42.3 | -14 |

**Table A.3. Results of TSRST with 5 × 5 × 25 cm specimens (RL)**

Aggregate Type: RL (Chert) Cooling Rate: 10°C/hr

| Specimen ID | Asphalt Type | Air Voids (%) | Fracture Strength (psi) | Fracture Strength (MPa) | Fracture Temp. (°C) | dS/dT (psi/°C) | Transition Temp. (°C) |
|---|---|---|---|---|---|---|---|
| LK1H01 | AAK-1 | 7.2 | 330 | 2.277 | -24.4 | 24 | -15.3 |
| LK1H02 | | 7.3 | 322 | 2.222 | -23.4 | 24.6 | -15.5 |
| LK1L01 | | 5.5 | 345 | 2.381 | -24.1 | 26.2 | -15 |
| LK1L03 | | 6.4 | 319 | 2.201 | -24.4 | 24.7 | -16.1 |
| LK2H01 | AAK-2 | 6.8 | 340 | 2.346 | -28.3 | 29 | -22.3 |
| LK2H03 | | 6.9 | 401 | 2.767 | -29.4 | 33.9 | -23.1 |
| LK2L01 | | 4.2 | 490 | 3.381 | -28.4 | 40.1 | -23.1 |
| LK2L04 | | 3.9 | 375 | 2.588 | -28.9 | 26.6 | -20.5 |
| LG1H01 | AAG-1 | 9.7 | 216 | 1.490 | -15.2 | 22.9 | -9.8 |
| LG1H02 | | 9.2 | 214 | 1.477 | -15.4 | 21.6 | -9.6 |
| LG1L03 | | 5.5 | 330 | 2.277 | -14.5 | 35.2 | -9.2 |
| LG1L04 | | 5.2 | 264 | 1.822 | -13.9 | 32.6 | -10.4 |
| LG2H03 | AAG-2 | 7.4 | 256 | 1.766 | -17.2 | 28.5 | -13.4 |
| LG2H04 | | 7.8 | 214 | 1.477 | -18.4 | 22.3 | -12.9 |
| LG2L02 | | 6.5 | 235 | 1.622 | -17.2 | 24.1 | -12.1 |
| LG2L04 | | 6.7 | 284 | 1.960 | -17.3 | 29.4 | -12 |

**Table A.4. Results of TSRST with stress relaxation**

Aggregate Type: RB (Granite) Cooling Rate: 10°C/hr
Specimen Size: 5 × 5 × 25 cm

| Specimen ID | Asphalt Type | Air Voids (%) | Relax. at (°C) | Relax. for (hrs) | Fracture Strength (psi) | Fracture Strength (MPa) | Fracture Temp. (°C) |
|---|---|---|---|---|---|---|---|
| BK1H16 | AAK-1 | 8.2 | -22 | 6 | 267 | 1.842 | -27.5 |
| BK1H13 | | 8.7 | -22 | 6 | 277 | 1.911 | -26.8 |
| BK1L15 | | 4.5 | -22 | 6 | 428 | 2.953 | -27.5 |
| BK1L06 | | 3.3 | -22 | 6 | 507 | 3.498 | -26.7 |
| BK2H06 | AAK-2 | 7.3 | -22 | 6 | 298 | 2.056 | -31.8 |
| BK2H13 | | 7.0 | -22 | 6 | 288 | 1.987 | -30.03 |
| BK2L06 | | 3.1 | -22 | 6 | 475 | 3.278 | -30.9 |
| BK2L05 | | 3.1 | -22 | 6 | 349 | 2.408 | -30.5 |
| BG1H05 | AAG-1 | 8.4 | -14 | 6 | 185 | 1.277 | -19.0 |
| BG1H06 | | 8.4 | -14 | 6 | 243 | 1.677 | -19.9 |
| BG1L05 | | 4.9 | -14 | 6 | 431 | 2.974 | -18.3 |
| BG1L08 | | 3.8 | -14 | 6 | 492 | 3.395 | -21.1 |
| BG2H08 | AAG-2 | 7.3 | -14 | 6 | 347 | 2.394 | -22.4 |
| BG2H13 | | 8.9 | -14 | 6 | 268 | 1.849 | -20.4 |
| BG2L07 | | 4.8 | -14 | 6 | 416 | 2.870 | -20.3 |
| BG2L03 | | 3.4 | -14 | 6 | 476 | 3.284 | -20.5 |

**Table A.5. Results of TSRST with various cooling rates**

Aggregate Type: RB (Granite) Specimen Size: 5 × 5 × 25 cm

(a) Asphalt Type: AAK-2

| Specimen ID | Air Voids (%) | Cooling Rate (°C/hr) | Fracture Strength (psi) | Fracture Strength (MPa) | Fracture Temp. (°C) | dS/dT (psi/°C) | Transition Temp. (°C) |
|---|---|---|---|---|---|---|---|
| BK2H01 | 7.4 | 10 | 404 | 2.788 | -32.8 | 26.4 | -23.3 |
| BK2H02 | 7.9 | 10 | 269 | 1.856 | -31.8 | 20.5 | -22.1 |
| BK2H04 | 7.6 | 10 | 322 | 2.222 | -33.3 | 21.4 | -23.6 |
| BK2L01 | 3.6 | 10 | 576 | 3.794 | -31.4 | 39.4 | -22.5 |
| BK2L02 | 3.9 | 10 | 526 | 3.629 | -31.8 | 31.8 | -22.3 |
| BK2602 | 5.1 | 5 | 418 | 2.884 | -32.0 | 28 | -25 |
| BK2601 | 5.7 | 5 | 413 | 2.850 | -30.7 | 35.7 | -26 |
| BK2608 | 5.5 | 2 | 380 | 2.622 | -34.8 | 28.1 | -27.6 |
| BK2607 | 5.5 | 2 | 342 | 2.360 | -34.1 | 28.5 | -26.7 |
| BK2604 | 5.9 | 1 | 356 | 2.456 | -37.0 | 22.2 | -27.2 |
| BK2606 | 6.5 | 1 | 297 | 2.049 | -36.1 | 24.7 | -28.1 |

Continued on next page

**Table A.5 (continued). Results of TSRST with various cooling rates**

Aggregate Type: RB (Granite) Specimen Size: 5 × 5 × 25 cm

(b) Asphalt Type: AAG-1

| Specimen ID | Air Voids (%) | Cooling Rate (°C/hr) | Fracture Strength (psi) | Fracture Strength (MPa) | Fracture Temp. (°C) | dS/dT (psi/°C) | Transition Temp. (°C) |
|---|---|---|---|---|---|---|---|
| BG1H01 | 6.8 | 10 | 305 | 2.105 | -18.7 | 24.5 | -10 |
| BG1H03 | 7.4 | 10 | 422 | 2.912 | -18.5 | 38.8 | -13.1 |
| BG1H04 | 7.4 | 10 | 416 | 2.870 | -18.1 | 38.7 | -12.7 |
| BG1L01 | 4.0 | 10 | 423 | 2.919 | -16.9 | 37.9 | -11.9 |
| BG1L02 | 4.5 | 10 | 529 | 3.650 | -18.0 | 44.3 | -11 |
| BG1L04 | 4.5 | 10 | 464 | 3.202 | -17.1 | 36.8 | |
| BG1601 | 6.7 | 5 | 267 | 1.842 | -15.6 | 28.3 | -12 |
| BG1603 | 6.9 | 5 | 323 | 2.229 | -15.6 | 37.3 | -12.2 |
| BG1602 | 7.0 | 2 | 357 | 2.463 | -18.7 | 38.6 | -15 |
| BG1607 | 6.7 | 2 | 277 | 1.911 | -19.1 | 25.1 | -12.8 |
| BG1605 | 7.3 | 1 | 296 | 2.042 | -19.7 | 29.2 | -13.6 |
| BG1606 | 6.7 | 1 | 347 | 2.394 | -19.7 | 35 | -15.8 |

## Table A.6. Results of TSRST with aged specimens

Aggregate Type: RB (Granite) Cooling Rate: 10°C/hr
Specimen Size: 5 × 5 × 25 cm

| Specimen ID | Asphalt Type | Air Voids (%) | Aging Temp. (°C) | Fracture Strength (psi) | Fracture Strength (MPa) | Fracture Temp. (°C) | dS/dT (psi/°C) | Transition Temp. (°C) |
|---|---|---|---|---|---|---|---|---|
| BK2H01 | AAK-2 | 7.4 | No | 404 | 2.7876 | -32.8 | 26.4 | -23.3 |
| BK2H02 | | 7.9 | No | 269 | 1.8561 | -31.8 | 20.5 | -22.1 |
| BK2H04 | | 7.6 | No | 322 | 2.2218 | -33.3 | 21.4 | -23.6 |
| BK2L01 | | 3.6 | No | 576 | 3.9744 | -31.4 | 39.4 | -22.5 |
| BK2L02 | | 3.9 | No | 526 | 3.6294 | -31.8 | 31.8 | -22.3 |
| BK2HL1 | | 7.8 | 110 | 351 | 2.4219 | -26 | 23 | -19.6 |
| BK2HL2 | | 7.8 | 110 | 310 | 2.139 | -25.5 | 13.7 | -16.7 |
| BK2HL3 | | 8.5 | 110 | 208 | 1.4352 | -24 | 14.1 | -15.7 |
| BK2LL2 | | 6.7 | 110 | 382 | 2.6358 | -25.3 | N/A | N/A |
| BK2LL5 | | 5.1 | 135 | 240 | 1.656 | -20.1 | 14.2 | -8.0 |
| BK2LL6 | | 4.2 | 135 | 183 | 1.2627 | -21 | 12.0 | -6.0 |
| BK2LL8 | | 4.9 | 135 | 32 | 2.2218 | -21.1 | 17.7 | -8.1 |
| BG1H01 | AAG-1 | 6.8 | No | 305 | 2.1045 | -18.7 | 24.5 | -10.0 |
| BG1H03 | | 7.4 | No | 422 | 2.9118 | -18.5 | 38.8 | -13.1 |
| BG1H04 | | 7.4 | No | 416 | 2.8704 | -18.1 | 38.7 | -12.7 |
| BG1L01 | | 4.0 | No | 423 | 2.9187 | -16.9 | 37.9 | -11.9 |
| BG1L02 | | 4.5 | No | 529 | 3.6501 | -17.1 | 44.3 | -11.0 |
| BG1L04 | | 4.5 | No | 464 | 3.2016 | -17.1 | 36.8 | N/A |
| BG1HL1 | | 10.6 | 135 | 285 | 1.9665 | -14.7 | 22.8 | -7.7 |
| BG1HL2 | | 10.6 | 135 | 219 | 1.5111 | -14.6 | 19.4 | -8.1 |
| BG1HL3 | | 8.5 | 135 | 310 | 2.139 | -13.6 | 24.7 | -7.5 |
| BG1HL4 | | 8.1 | 135 | 291 | 2.0079 | -13.0 | 23.9 | -7.3 |
| BG1LL1 | | 5.0 | 135 | 373 | 2.5737 | -13.4 | 33.1 | -7.8 |
| BG1LL2 | | 5.9 | 135 | 417 | 2.8773 | -14.8 | 33.5 | -7.8 |
| BG1LL3 | | 6.9 | 135 | 385 | 2.6565 | -14.0 | 30.1 | -7.4 |
| BG1LL4 | | 6.1 | 135 | 309 | 2.1321 | -12.1 | 26.8 | -7.6 |